博士学位論文

Study on plane magnetic abrasive finishing combined with electrolytic process

電解を複合した平面磁気研磨法に関する研究

平成 30 年 8 月

宇都宮大学大学院
博士後期課程　システム創成工学専攻

孫　旭

Contents

Contents

Contents

Contents

Chapter 1 Introduction

1.1 Introduction

1.1.1 Introduction of SUS304 stainless steel materials

In this research, the SUS304 stainless steel plane as workpiece was used to be polished. Firstly, the basic characteristic of SUS304 stainless steel materials will be investigated and introduced in this chapter. The SUS304 stainless steel as a kind of 18-8 series austenitic stainless steel is a common stainless steel material. The crystal structure (metallography) of austenite is shown in Figure 1.1[1-4]. The physical property and chemical composition of SUS304 stainless steel is respectively shown in Table 1.1 and Table 1.2. Because of good corrosion resistance, heat resistance, low temperature strength and mechanical properties, stamping, bending and other good hot workability, no heat treatment hardening phenomenon, and other outstanding advantages [5]. The SUS304 stainless steel material has been widely used in tableware, building materials, automobile parts, medical instruments, chemical products, semiconductor industry, ship components, atomic force, aero-space industry and so on.

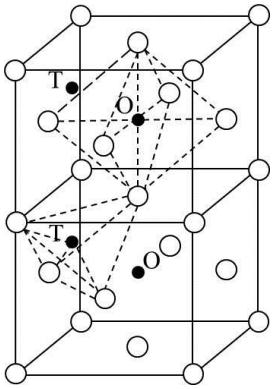

Fig. 1.1 The crystal structure (metallography) of austenite

Table 1.1 The physical property of SUS304 stainless steel

Tensile strength	$\sigma_b \geq 520$ Mpa
Conditional yield strength	$\sigma_{0.2} \geq 205$ MPa
Elongation	$\delta_5 = 40\%$
Reduction in area	ψ (%) ≥ 60
Hardness	HB ≤ 187, HRB ≤ 90, HV ≤ 200
Density (20 ° C, g / cm ^{3})	7.93
Melting point (° C)	1398 ～ 1454
Specific heat capacity (0 to 100 ° C, KJ · kg^{-1}K^{-1})	0.502
Thermal Conductivity (W · m^{-1} · K^{-1})	(100° C) 16.3; (500° C) 21.5
Linear expansion coefficient (10^{-6} · K^{-1})	(0～100° C) 16.3; (100～500° C) 21.5
Resistivity (20C, 10^{-6}Ω·M)	0.73
Longitudinal elastic modulus (20 ° C, KN / mm 2)	193
Young's modulus	E = 194020 MPa
Hardening index	n = 0.193

Table 1.2 The chemical composition of SUS304 stainless steel

Fe (%)	Cr (%)	Ni (%)	Mn (%)	Si (%)	C (%)	P (%)	S (%)
67～72	17～19	8～11	≤ 2.00	≤ 1.00	≤ 0.07	≤ 0.035	≤ 0.03

1.1.2 Summary of available SUS304 stainless steel machining processes

Generally, there are six kinds of polishing methods for SUS304 stainless steel machining processes. There are respectively mechanical polishing, chemical polishing, electrolytic polishing, ultrasonic polishing, fluid polishing and magnetic abrasive polishing. (a) Through cutting the plastic deformation of surface material to remove the protrusions of polished surface to obtain smooth surface, which is called mechanical polishing method. Employing this method, the surface roughness can reach 0.008 μm. (b) The principle of chemical polishing is that since the protruding portions are closer to cathode than the concave portions of workpiece, the current density of protruding portions is larger and eluted rate is also relatively faster. Thereby, these protruding portions of workpiece are preferentially leveled during electrolytic process, and the surface precision polishing can be completed by elution. The main advantage of this method is that the shape of the complex parts can be polished and a lot of workpieces simultaneously efficiently can be polished without complex finishing equipment. Generally, the surface roughness of polished workpiece can reach to several tens μm by chemical polishing. (c) The basic principle of electrolytic polishing is as same as chemical polishing. Compared with the chemical polishing, the electrolytic polishing can eliminate the impact of the cathode reaction and the effect of chemical polishing is better. (d) Ultrasonic polishing is to place the workpiece in the abrasive suspension and place it in the ultrasonic field together, the surface of workpiece is polished by the oscillating effect of the ultrasonic wave. Since the ultrasonic machining macroscopic force is small, it does not cause deformation of the workpiece. However, the fabrication and installation of machining tool is difficult. (e) Fluid polishing is to rely on high-speed flow of liquid and abrasive particles to polish the surface of workpiece. Common methods are: abrasive jet processing, liquid jet processing,

hydro-dynamic grinding and so on. (f) Magnetic abrasive polishing is using magnetic abrasive under the action of magnetic field to form magnetic brush to polish the surface of workpiece. This processing method is high efficiency, good quality, easy to control the processing conditions, good working conditions. With a suitable abrasive, the surface roughness can reach R_a 0.1 μ m.

As the method of electrolytic polishing, fluid polishing and other methods are difficult to accurately control the geometric accuracy of workpiece. In addition, polished surface quality can satisfy the requirements of surface quality through chemical polishing, ultrasonic polishing, magnetic polishing and other methods. Thus, the mirror processing is still based on mechanical polishing.

Table 1.3 Polishing methods and polishing effects of SUS304 stainless steel material

Polishing methods of SUS304 stainless steel material	Polishing effects
a. Mechanical polishing	R_a: 0.008 μm
b. Chemical polishing	R_a: 10 μm
c. Electrolytic polishing	R_a < 1μm
d. Ultrasonic polishing	------
e. Fluid polishing	------
f. Magnetic abrasive polishing	R_a: 0.1μm

1.2 Developing history of magnetic abrasive finishing

Magnetic abrasive finishing technology was initially proposed from by the former Soviet Union engineer Kargolow in 1938. Since the 1960s, the MAF research and application technology have been researched and conducted by many researchers from the former Soviet Union such as Knoovalov, Hulev, Baron and Saluievich, etc.. As the basis of magnetic processing is magnetic abrasive, a lot of experimental work has been conducted for the preparation of magnetic abrasive in the former Soviet Union. The former Soviet Union researchers have obtained many invention patents through the research of magnetic abrasive composition, ratio and structure. The popularity has expanded to Germany, Poland and the USA, Bulgaria and so on since 1960's [6]. The research journal about magnetic abrasive finishing process or magnetic abrasive machining process was found earliest in the USSR in 1974. However, according to the report the method was developed in USSR during the Soviet Union era. The research paper was regarding the finishing of cylinder bar external diameter and flat surface finishing. There was also research paper regarding deburr for hydraulic pumps gears and edges deburr finishing method. Bulgaria researchers have been developing the MAF technology since the mid-1970s and have been conducting the research of composite magnetic abrasive since the late 1980s. It was reported that during the 1980's many researches regarding magnetic slurry and magnetic abrasive finishing machine was conducted in Bulgaria and Soviet. Applications regarding MAF for the purpose of edge finishing were mostly conducted in Germany. The researchers of Japan have carried out the MAF research since the early 1980s, and a lot of magnetic abrasive finishing equipments have been developed by them. Representative researchers are Takeo Shinmura, Toshio Aizawa from Japan Utsunomiya University; Masahiro Anzai, Koichi Masaki from Japan's Tokyo University and so on. Anong them, Takeo Shinmura developed

a variety of magnetic abrasive finishing equipments which can process ferromagnetic workpiece and non-ferromagnetic workpiece, such as plane magnetic abrasive finishing device, cylindrical inner and outer surfaces magnetic abrasive finishing device, spherical magnetic abrasive finishing device, and so on [7-10]. Then, Takeo Shinmura respectively researched these finishing characteristics [11-13]. Some of these processing equipments adopted permanent magnets to produce a constant magnetic field; some of these processing equipments used the electromagnets to form the intensity to control the magnetic field; some of these processing equipments exerted a certain amplitude and frequency of vibration for the moving workpiece to achieve magnetic abrasive finishing; some of these processing equipments utilized the method of producing a rotating magnetic field to achieve magnetic abrasive finishing. Takeo Shinmura not only developed a variety of magnetic abrasive finishing equipments, but also conducted more in-depth theoretical analysis and experimental research in a variety of processing conditions, such as magnetic field strength, machining gap, relative velocity of abrasive and workpiece, composition of magnetic abrasive and particle size and other factors effect on the quality and efficiency of processing. Masahiro Anzai has conducted the research for the preparation technology of magnetic abrasive, and them successfully researched and developed several valuable magnetic abrasives [14]. The used magnetic abrasive preparation methods include: plasma powder melting method (PPM), ferromagnetic metal materials and abrasive fiber mixing method, liquid magnetic abrasive. Compared with the high temperature sintering method, the characteristics of these magnetic abrasive preparation methods are simple, low cost and high using value.

Since the 1990s, Japan and abroad have emerged Hitomi Yamaguchi, Kiyoshi Suzuki, Vijay Kumar Jain, Suhas S. Joshi, Shaohui Yin, Yanhua Zou and other outstanding

researchers for magnetic abrasive finishing technology. Yamaguchi has developed method for polishing the internal surface of non-ferromagnetic pipes through the application of magnetic fields [15-17]. She has developed three methods finishing internal surface of pipes: 1) using static magnetic pole polished rotating long pipe; 2) using rotating magnetic pole polished long non rotatable pipe; 3) using magnet abrasive finishing polished diameter less 20 mm small pipe along linear travel. Kiyoshi Suzuki et al. developed metal short fiber mixed magnetic grains and proposed MAF process using centrifugal force [18]. Kim et al. proposed magnetic polishing of free from surface using two types of magnetic polishing tool [19]. Jain et al. have studied the MAF process on non-magnetic stainless steel workpiece and concluded that the working gap and circumferential speed are the parameters which significantly influence the surface roughness value, proved force and change in surface roughness (ΔR) increase with increase in current to the electromangnet and decrease in the working gap [20, 21]. Joshi et al. ananlyzed the polished plane surface by MAF, and concluded that the surface finishing may improve significantly with an increase in the grain size, feeding rate and current [22]. Shaohui Yin et al. developed three modes (horizontal vibration, vertical vibration and compound vibration) of vibration-assisted MAF process for polishing flat surface and 3D micro-surved surface [23-25]. Pandey et al. have studied the mechanism of surface finishing in UAMAF (Ultrasonic-Assisted Magnetic Abrasive Finishing) process and verified that the polishing effectiveness of MAF can be improved significantly by add ultrasonic vibrations [26, 27]. Yanhua Zou et al. proposed a plane MAF process using a constant-pressure magnetic brush, studied on internal surface of tubes and plane magnetic abrasive trajectory and elevated the surface precision and homogeneity [28-30].

In recent years, the research and popularity of magnetic abrasive finishing technology

have expanded in various universities and research institutions around the world in countries, such as China, India, South Korea, Egypt, Taiwan, Brazil, Canada, and Iran.

1.3 Developing trend of magnetic abrasive finishing

Currently, the study of magnetic abrasive finishing is mainly reflected in the field of magnetic abrasive finishing process and theory, processing equipments and magnetic abrasives and other fields, some unsolved problems still need to be studied in the future.

(1) The development of new magnetic abrasives is very necessary. At present, the domestic and foreign produced magnetic abrasive is high cost, short service life and low finishing efficiency. The fundamental reason is that the magnetic susceptibility of magnetic material is low. However, if the solubility and magnetic susceptibility are improved by some means, the production costs will be significantly improved. Therefore, the new magnetic abrasives should to be developed and the cost of produced magnetic abrasive should be reduced. Moreover, the service life of magnetic abrasive should be improved and the cutting capacity should be enhanced.

(2) Magnetic grinding is not only affected by the workpiece material and the size of the workpiece, but also by the constraints of the shape. The removal effect is different for different position, different angles and different curvature of the surface. In order to obtain the same surface roughness for the whole surface, the processing parameters should be deeply researched.

(3) In recent years, due to the introduction of CNC machine tools and CAD/CAM technology, making the majority of mold manufacturing to achieve automation. Thus, the research of magnetic abrasive automation has very important significance.

(4) Magnetic grinding devices with alternating magnetic fields are very reliable due to the absence of moving parts, but the magnetic abrasives with strong magnetic properties are required to use in alternating magnetic fields finishing.

(5) As the electrochemical processing and magnetic abrasive finishing processing have a role for the material removal, and the mechanical action of pure magnetic abrasive finishing does not destroy the original accuracy of the workpiece. Therefore, it is possible to consider increasing the capability of mechanical action in the composite processing, so that the magnetic abrasive finishing not limited to scratch the oxide film but also at the same time directly involved in finishing. Thereby, the processing quality and efficiency can be improved. However, there is little report for regarding electrochemical processing combined with magnetic abrasive finishing processing method. Zou et al. have proposed that magnetic abrasive finishing combined with electrolytic process for SUS304 stainless plane polishing & A6063 aluminum pipe [31-33]. The finishing efficiency of alloy materials can be improved through this novel composite processing method from their reports. Chen et al. have proposed that using electrolytic-magnetic abrasive finishing polished the nickel-based superalloy GH4169 [34]. Both finishing efficiency and surface quality can be improved through this composite processing method. Pandey et al. have reported that using chemo assisted magnetic abrasive finishing polished tungsten plane workpiece in 12th global conference on sustainable manufacturing [35]. Through a series of experimental investigations, it can be found that the surface finish is improved by 79.52%. Guo et al. have reported that processing Al 6061 with electrochemical magnetic abrasive finishing [36, 37]. In addition to proving that this method was effective, they also found the limit of surface quality through researching the removal depth. Through the reports from these researchers, it can be considered the finishing efficiency of metal material can be improved by EMAF process.

1.4 Research objective

With the rapid development of science and technology, the various fields such as semiconductor related industries, bio-related industries and aerospace-related industries, various new products are becoming smaller and more multifunctional are rapidly developing. Therefore, for the accuracy requirement of the products is gradually getting higher. In addition, the small part consists of a number of fine parts and complex shapes. The surface accuracy of fine parts and complex parts is also required to leads up to a mirror finish. Magnetic abrasive finishing (MAF) as a type of super precision processing is applied in various occasions such as surface finishing of complex shape parts, inner and outside polishing of elongated tubes and burr removal. Furthermore, the plane magnetic abrasive finishing method is using magnetic brush formed by magnetic particles to process workpiece. However, the processing power of the magnetic brush is limited, which is a problem for the ultra-precision processing. Since high efficiency and high precision surface finishing can't be realized at the same time with a single processing method in many cases, it is important to develop a processing method to combine traditional machining with other polishing methods. In this research, we developed electrolytic magnetic abrasive finishing method (EMAF) aiming at realizing ultra-precise machining in short time by combining magnetic abrasive finishing with electrolytic action.

1.5 Thesis strategy and structure

In order to investigate the finishing mechanical and mechanism for achieving stainless steel plane mirror processing, almost all of the factors for affecting the processing characteristics have been surveyed through the book titled “Ultra precision processing by electrolytic composite polishing method” [38]. Firstly, the selection of finished workpiece material, finished surface roughness and shape accuracy are important for the electrolytic composite mirror processing. Except for the selected workpiece before machining, there are many processing factors during the electrolytic magnetic abrasive finishing (EMAF) process, such as diameter of electrode, rotational speed of machining tool, pressing pressure of abrasive grains, diameter of abrasive grains, density of abrasive grains, feeding speed of X-Y stage, working voltage, concentration of electrolyte etc. The detailed machining conditions have been shown in the Figure 1.2 which is cited from the book titled “Ultra precision processing by electrolytic composite polishing method”.

In this research, we emphatically selected some processing influencing factors from aforementioned processing factors to study and analyze. The rotational speed of machining tool, working voltage, diameter of abrasive grains, feeding speed of X-Y stage, concentration of electrolyte and working voltage have been studied and analyzed. In addition, we have researched the finishing time of the composite processing stage combined with the finishing time of the magnetic grinding stage. According to this research, we described the system model of electrolytic magnetic abrasive finishing shown in Figure 1.3.

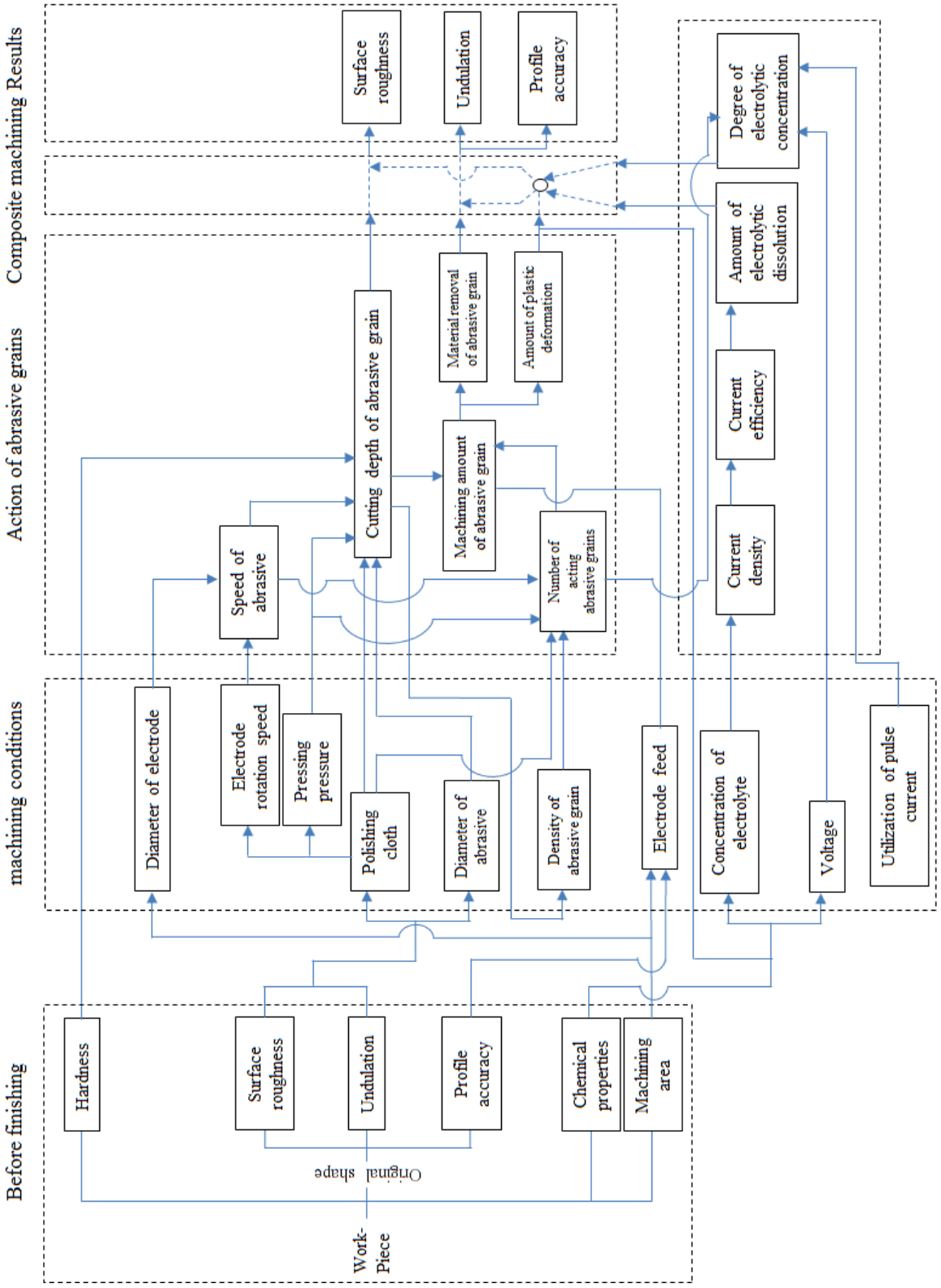

Fig. 1.2 System model of electrolytic combined processing

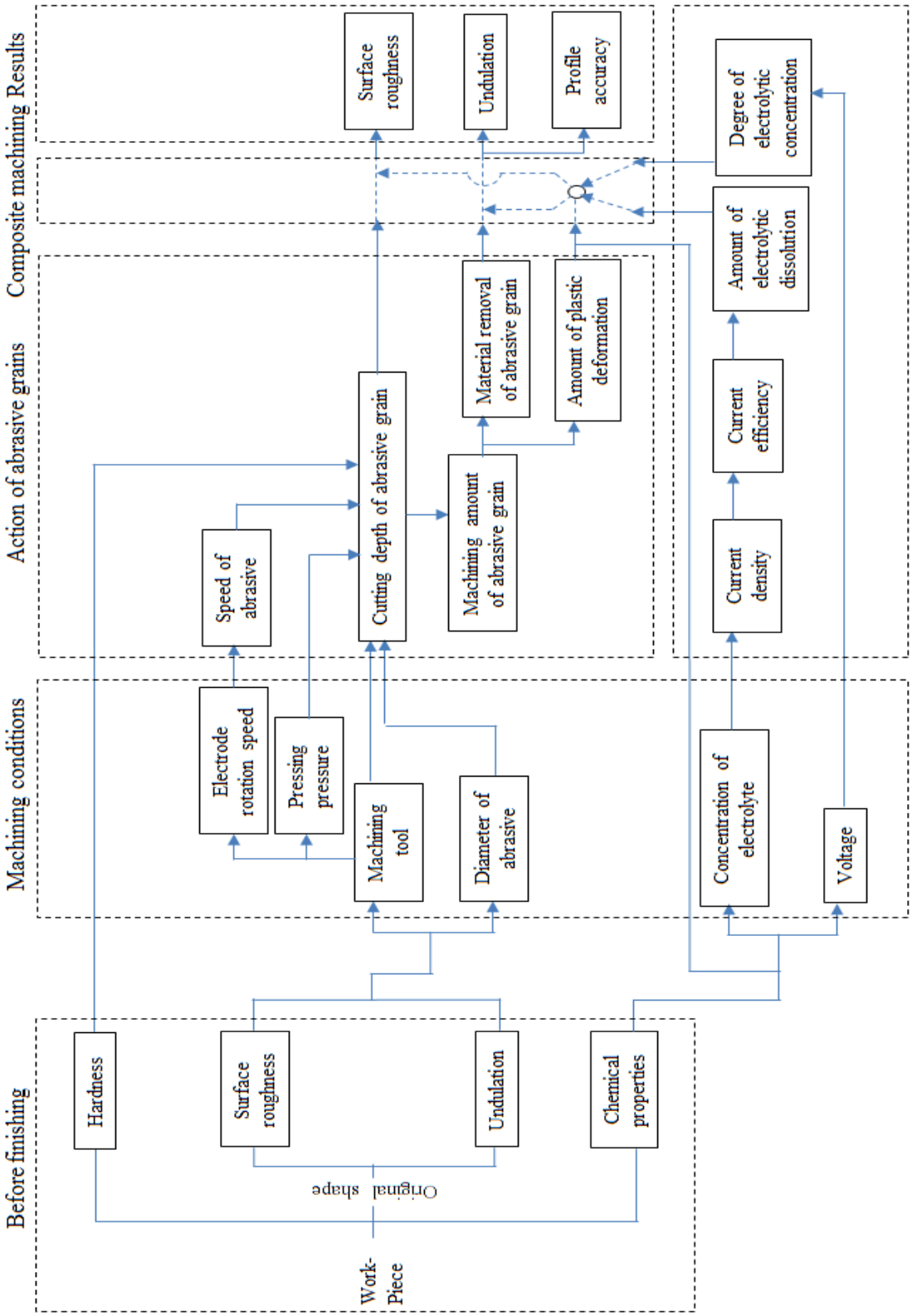

Fig. 1.3 System model of electrolytic magnetic abrasive finishing

1.6 The composition of this paper

The contents of each chapter for the thesis were generalized as follows:

(1) The characteristics of the material SUS304, the processing method of the processing material SUS304, and the magnetic grinding method have been introducted in the first chapter. Furthermore, the research objective and research content have been generalized.

(2) In the second chapter, we have respectively introduced basic processing principle of magnetic abrasive finishing, electrolytic machining and electrolytic magnetic abrasive finishing. Moreover, experimental setup, electrolytic magnetic compound machining tools and measuring instruments have been described and introduced in the third chapter.

(3) The feasibility of electrolytic magnetic abrasive finishing (EMAF process) was preliminarily verified through a series of comparative experiments in the third chapter. Since the machining efficiency of EMAF process can be improved by about 50% than the machining efficiency of traditional MAF process, we will focus on researching the optimal finishing parameters in the next few chapters.

(4) The experimental conditions and experimental results of traditional magnetic abrasive finishing have been reported in the forth chapter. Through comparing experimental results, we have basically achieved to explord the mechanical finishing characteristics of electrolytic magnetic compound machining tool, and selected the optimization of mechanical finishing parameters for electrolytic magnetic abrasive finishing.

(5) The experimental conditions and experimental results about electrolytic machining have been reported in the fifth chapter. Through comparing experimental results, the work for explording the electrolytic machining characteristics of electrolytic magnetic compound machining tool has been done, and selected the optimization of electrolytic

machining parameters for electrolytic magnetic abrasive finishing. Furthermore, we also analyzed changes in surface morphology, composition, and hardness through observing and measuring.

(6) The experimental conditions and experimental results by electrolytic magnetic abrasive finishing have been reported in the sixth chapter. According to the optimal finishing conditions from magnetic abrasive finishing experiment and electrolytic machining experiment, electrolytic magnetic abrasive finishing experiments have been conducted. We focused on researching the combinations of first finishing step (EMAF step) time and second finishing step (MAF step) time. The optimal combination of EMAF step time and MAF step time has been determined through comparing experimental results. Additionally, it is proved that EMAF process method ebable to significantly improve surface finishing efficiency of metal materials.

(7) Finally, the research results of this thesis have been summeried in the last chapter.

Chapter 2 Development of magnetic abrasive finishing combined with electrolytic finishing for processing SUS304 plane

The developed new compound finishing method includes two kinds of finishing process which is respectively magnetic abrasive finishing and electrolytic process. Therefore, the two different processes are achieved through a novel compound machining tool which has been designed by us. The principle of magnetic abrasive finishing, electrolytic process and magnetic abrasive finishing combined with electrolytic finishing will be introduced in this chapter.

2.1 Traditional plane magnetic abrasive finishing

Figure 2.1 shows the schematic of traditional “plane magnetic abrasive finishing process” using static magnetic field which is proposed by Shinmura [1, 2]. The magnetic poles are disposed on the top of the workpiece plane. The iron particles are mixed with magnetic abrasive particles and attracted along the magnetic force lines. Then, the magnetic brush is formed on the bottom of the magnetic poles. The relative rotation of magnetic pole combines with reciprocating feeding movement of workpiece, a relative friction is produced between surface of workpiece and magnetic brush. The friction is combined with fluctuating magnetic force produced by magnetic brush. Thus, the material removal and surface accuracy of mirror-polishing can be effectively realized.

Normally, magnetic brush is used to finishing workpiece in traditional plane magnetic abrasive finishing process. Then, in order to obtain high accuracy surface, the micro magnetic abrasive particles need to be used in ultra-precision finishing process. However,

there is a serious problem that the hardness of magnetic abrasive particles is softer than the hardness of SUS304 stainless steel. Moreover, the service life of magnetic abrasive particles is short, if the magnetic abrasive particles cannot promptly be replaced during MAF process, the finishing ability of MAF process will be rather limited. Thus, it is difficult for traditional MAF process to achieve both high accuracy surface and machining efficiency.

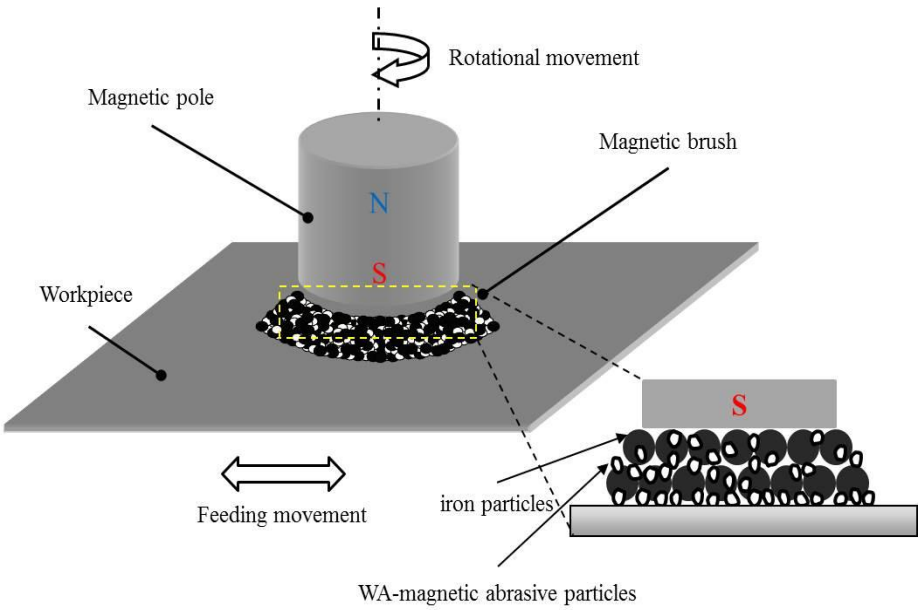

Fig. 2.1.1 Schematic of traditional "plane MAF polishing process"

Figure 2.1.2 shows finishing force analysis of magnetic particles in the magnetic field. The magnetic particles along magnetic equipotential line direction generate a force F_x and along magnetic force line direction generate a force F_y [3]. The force F_x and force F_y can be calculated through the following formula (1) and (2):

$$F_x = KD^3\chi\mu_0 H(\partial H/\partial x) \quad (1)$$

$$F_y = KD^3\chi\mu_0 H(\partial H/\partial y) \quad (2)$$

Where "K" is the correction coefficient of volume, "D" is the diameter of magnetic particle,

"χ" is the susceptibility of magnetic particle, "μ_0" is the permeability of vacuum, "H" is the magnetic field intensity, $\partial H/\partial x$ and $\partial H/\partial y$ are respectively gradients of magnetic field intensity in x and y directions.

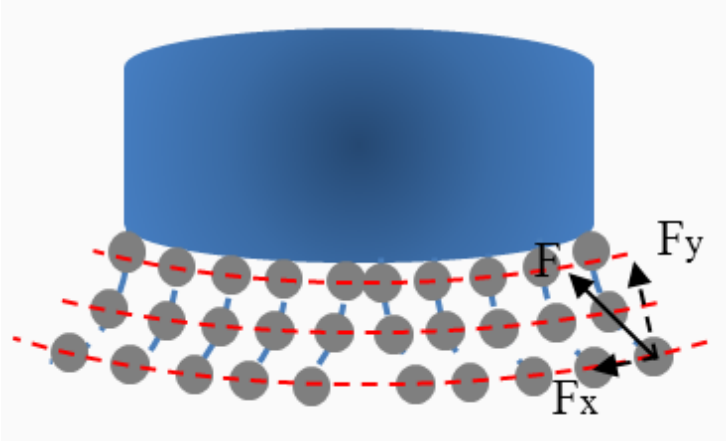

Fig. 2.1.2 Finishing force analysis of magnetic particles in the magnetic field

2.2 Electrolytic machining

Since the electrolytic process is an important part of EMAF process, principle of electrolytic process will preferentially be introduced in the following. Figure 2.2.1 shows the machining principle of electrolytic process. The $NaNO_3$ solution is neutral which produces less pollution for environment. Thus, the $NaNO_3$ solution is adopted as the electrolyte in this study from the view of environmental protection. When turning on DC constant voltage power, aqueous solution of $NaNO_3$ will take place electrolytic reactions which are shown as equation (1) and (2).

$$NaNO_3 \rightarrow Na^+ + NO^{3-} \quad (1)$$

$$H_2O \rightarrow H^+ + OH^- \quad (2)$$

Ionization tendency order:

$Ag^+ > Cu^{2+} > H^+ > Pb^{2+} > Fe^{2+} > Zn^{2+} > Al^{3+} > Mg^{2+} > Na^+ > K^+$

Na^+ and H^+ move toward the cathode, NO^{3-} and OH^- move toward the anode. Since ionization tendency of “Na” is stronger than ionization tendency of “H”, the reaction shown as equation (3) occurs at the cathode. The discharge of OH^- is easier than discharge of NO^{3-}, hence the reaction shown as equation (4) occurs at the anode. Through equation (3) and (4), it can be seen that H_2 is generated at the cathode and O_2 is generated at the anode [4].

$$2H^+ + 2e^- \rightarrow H_2 \uparrow \quad (3)$$

$$2OH^- \rightarrow H_2O + 1/2O_2 \uparrow + 2e^- \quad (4)$$

Discharge ease order: $SO_4^{2-} < NO_3^- < OH^- < Cl^-$

It is well known that the major composition of SUS304 is Fe (70%), Cr (20%) and Ni (10%). Generated oxygen at the anode has strong oxidizing. Hence, most of anode metal is oxidized under the action of oxygen. Moreover, a lot of mental ions such as Fe^{3+}, Cr^{6+}, Fe^{2+}, Cr^{3+} and Ni^{2+} etc. elements are eluted on the metal surface by the action of oxidation reaction [4]. Compared with the concave portions of workpiece, the protruding portions are closer to cathode. Thus, the current density of protruding portions is larger and eluted rate is also relatively faster. These protruding portions of workpiece are preferentially leveled during electrolytic process, and the surface precision polishing can be completed by elution [5, 6].

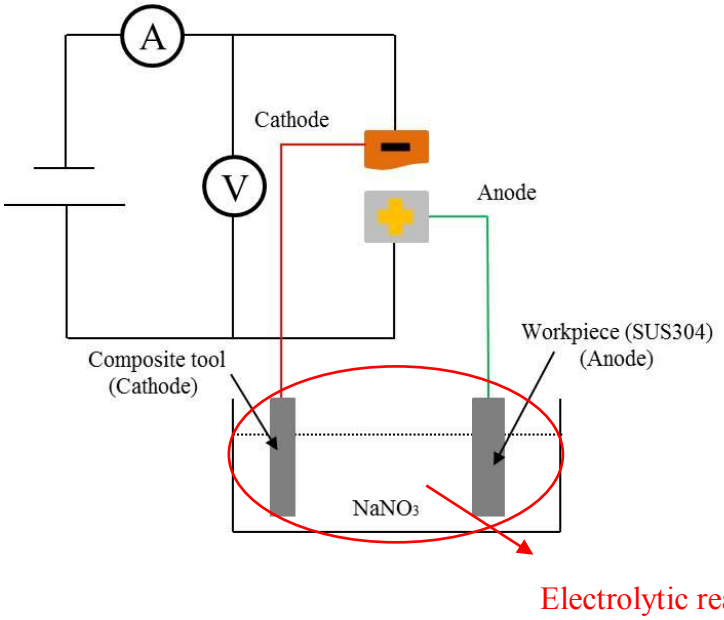

Fig. 2.2.1 Machining principle of electrolytic process

Since stainless steel SUS304 is an alloy material, a series of complex electrolysis reactions occur during electrolytic process. The schematic of electrolytic reactions is shown in Figure 2.2.2. The reactions of main metal ions which are described as equation

from (1) to (6) dissolved out from the metal surface.

$$Fe \rightarrow Fe^{2+} + 2e^{-} \quad (1)$$

$$Fe \rightarrow Fe^{3+} + 3e^{-} \quad (2)$$

$$Cr \rightarrow Cr^{3+} + 3e^{-} \quad (3)$$

$$Cr \rightarrow Cr^{6+} + 6e^{-} \quad (4)$$

$$Ni \rightarrow Ni^{2+} + 2e^{-} \quad (5)$$

$$3Fe^{2+} + Cr^{6+} \rightarrow 3Fe^{3+} + Cr^{3+} \quad (6)$$

Since H_2O molecular generates OH^- ions under the electrolytic action and generated OH^- ions move toward the anode, abovementioned metal ions combine with generated OH^- to form precipitates. The reactions of formed precipitates are described as equation from (7) to (11).

$$Fe^{2+} + 2OH^{-} \rightarrow Fe(OH)_2 \downarrow \quad (7)$$

$$Fe^{3+} + 3OH^{-} \rightarrow Fe(OH)_3 \downarrow \quad (8)$$

$$4Fe(OH)_2 + 2H_2O + O_2 \rightarrow 4Fe(OH)_3 \downarrow \quad (9)$$

$$Cr^{3+} + 3OH^{-} \rightarrow Cr(OH)_3 \downarrow \quad (10)$$

$$Ni^{2+} + 2OH^{-} \rightarrow Ni(OH)_2 \downarrow \quad (11)$$

With the reactions proceeding, a large amount of brown substance is produced in the transparent electrolyte. This phenomenon confirms the abovementioned chemical reactions. Simultaneously, passive film is also generated on the workpiece. However, the amount of dissolved out metal ions gradually decrease with a large number of passive film accumulate on the workpiece.

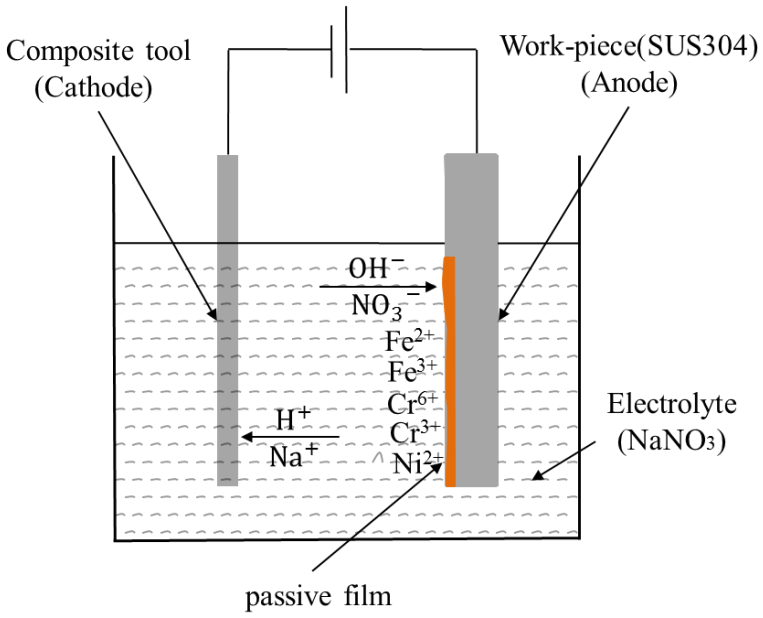

Fig. 2.2.2 Schematic of electrolytic reactions

2.3 Basic processing principle of EMAF

The main problem of using MAF process to polish the SUS304 plane is that pressing pressure of magnetic brush is deficiency. However, if the MAF process combines with the electrolytic process, passive films are generated under the action of electrolytic process. Since the hardness of passive films is far lower than that of SUS304 material, magnetic brush can effectively remove formed passive films from the electrolytic process. Thereby, above mentioned the main problem of using MAF process can be solved, and the machining efficiency can be improved by EMAF process. It is notable that EMAF process includes two finishing steps which are 1st finishing step (MAF process combines with electrolytic process step) and 2nd finishing step (MAF step). The schematic of stainless planar processing system is shown as Figure 2.3.1. The SUS304 workpiece as an anode is penetrated into electrolyte solution and connected to positive electrode of DC constant voltage power. The electrolytic magnetic compound machining tool as a cathode is located above the workpiece and connected to negative electrode of DC constant voltage power. There is a working gap between compound machining tool and workpiece plane. The magnetic brush is formed by mixed magnetic abrasive particles at the bottom of the magnetic poles. Then, magnetic brush conducts rotational movement. The electrolyte is injected by a pump and the flow rate of electrolyte is controlled through a flow meter. After turning on DC constant voltage power, the protruding portions will be preferentially leveled and the passive films will form on the surface of workpiece by electrolytic process. At the same time, using the magnetic abrasive particles of magnetic brush to exert friction on the surface of workpiece, the passive films can be effectively removed. Thus, the efficient precision machining of workpiece surface can be realized through EMAF process. In addition, in order to avoid environmental pollution, the used electrolyte is collected into

a collecting container.

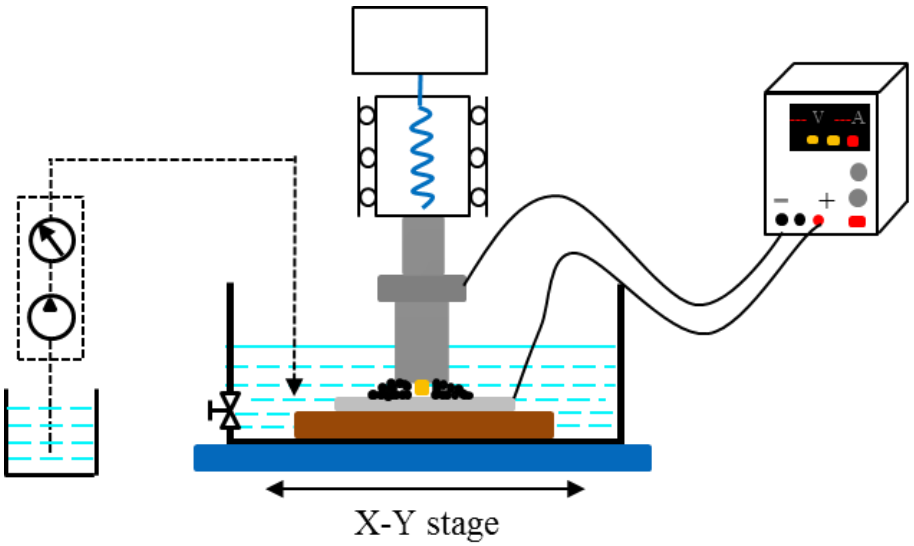

Fig 2.3.1 Schematic of stainless planar processing system

Figure 2.3.2 explains the basic machining principle of EMAF process. In this research, EMAF process includes two finishing steps which are respectively the 1st finishing step (EMAF step) and the 2nd finishing step (MAF step). Figure 2.3.2 (a) shows the original surface with a lot of initial hairlines before finishing. Figure 2.3.2 (b) shows the finished surface after EMAF step. When turning on DC constant voltage power, the protruding portions will be preferentially leveled and the passive films will form on the surface of workpiece by electrolytic process. Simultaneously, the magnetic abrasive particles of magnetic brush is used to exert friction on the surface of workpiece, the passive films can be effectively removed. By the way, the hardness of passive films is smaller than the hardness of SUS304 stainless material [4]. Thus, the efficiency of precision machining can be improved in the first finishing step through MAF process combines with electrolytic process. However, a few passive films generally still exist on the finished surface after EMAF step. The residual passive films will affect the surface accuracy. Hence, the MAF

step as a final process after EMAF step is used to completely remove passive films from in order to improve surface accuracy of workpiece. Figure 2 (c) shows the finished surface after MAF step.

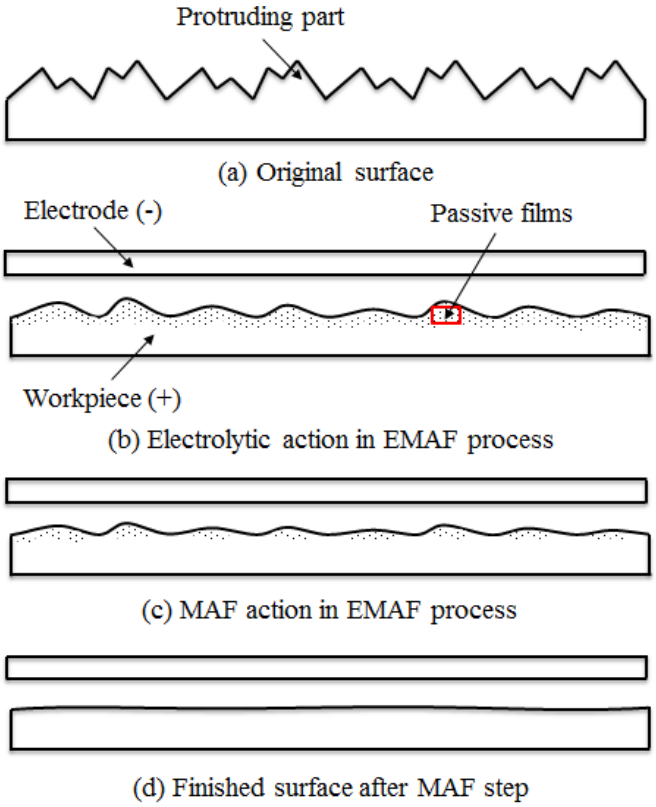

Fig 2.3.2 Schematic of EMAF process

2.4 Developed electrolytic magnetic compound machining tool

EMAF process method is usually divided into synchronous finishing and steps finishing. Synchronous EMAF process is realized by a special compound machining tool or a special separate machining tool [7, 8]; steps EMAF process is that passive films are formed by oxidizing agent before experiment, then passive films are removed by a dedicated magnetic machining tool [9].

Currently, the development of compound machining tools is very scarce for EMAF process of plane workpiece. A compound machining tool cited from "A study of processing Al 6061 with electrochemical magnetic abrasive finishing" [7, 10]. The working area of the compound machining tool is composed of two 90^0 diagonal fan-shaped electrodes and two 90^0 diagonal fan-shaped magnetic poles, and there is a height difference between magnetic poles and electrodes (The length of the magnetic pole is slightly shorter than the length of the electrode). A separate machining tool cited from "Research on the electrolytic-magnetic abrasive finishing of nickel-based superalloy GH4169" [8]. The magnetic machining tool and electrolytic machining are connected through a connecting rod.

In this study, in order to simplify finishing process, a novel electrolytic magnetic compound machining tool has been firstly developed and made [11]. The CAD drawing, three-dimensional images and external views of electrolytic magnetic compound machining tool is respectively shown in Figure 2.4.1. The electric current flows from the power supply to compound machining tool (cathode) through a copper piece contacting to a copper ring that is placed on the top of compound machining tool. The cathode is designed to be a cross-shape at the bottom of compound machining tool (two copper rods: 30 mm × 3 mm × 3 mm). The CAD drawing of the cathode is shown as Figure 2.4.2 (a).

The magnetic poles are constituted by four circular Nd-Fe-B permanent magnet (four magnetic poles: Φ 6 mm × 30 mm), and respectively distributed on four directions of the electrodes. In order to avoid short circuit which is caused by connection of magnetic brush and electrode, magnetic poles and electrodes are separated approximately 4 mm. The CAD drawing of the bottom of electrolytic magnetic compound machining tool is shown in Figure 2.4.2 (b). Figure 2.4.3 shows assembly drawing of electrolytic magnetic compound machining tool. Specific component names are recorded in the next to Table.

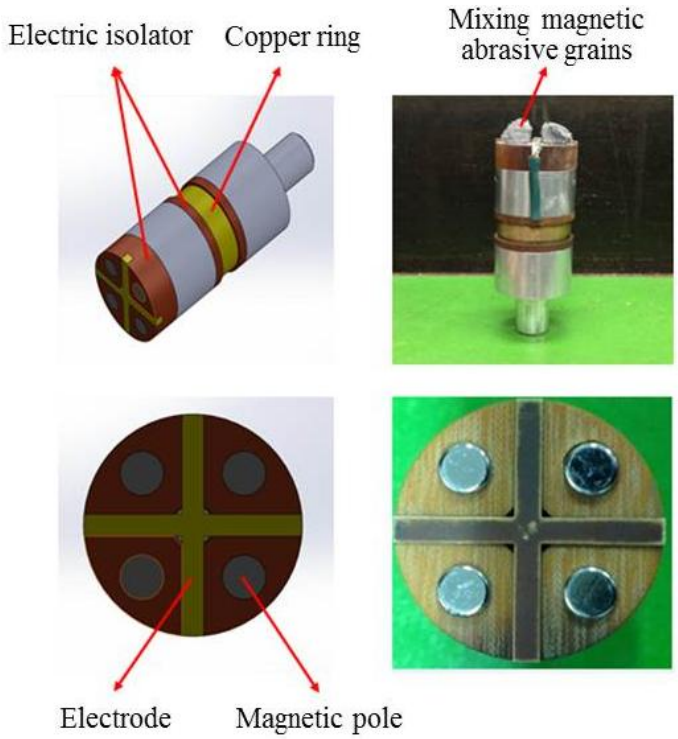

Fig. 2.4.1 Three-dimensional images and external views of electrolytic magnetic compound machining tool

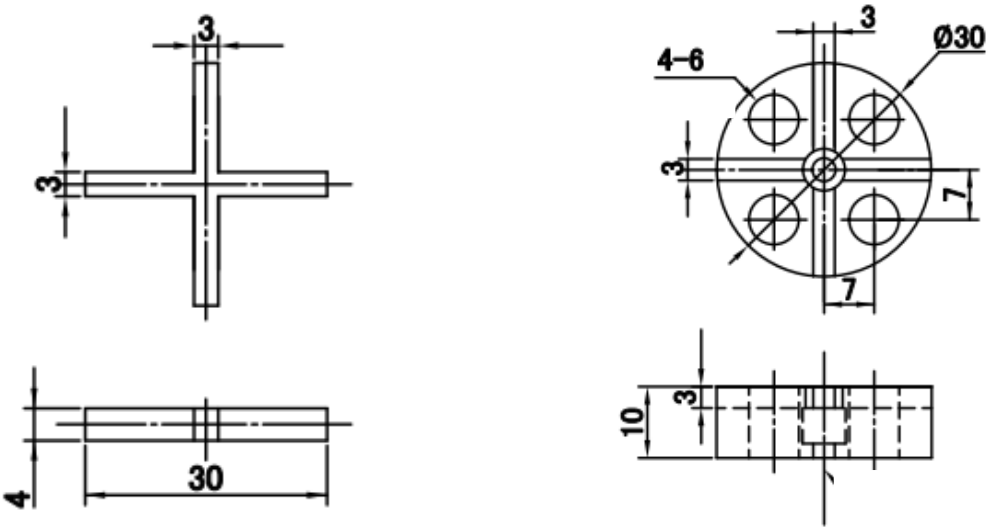

(a) Cathod (b) The bottom of compound machining tool

Fig. 2.4.2 Design drawings of the electrode (cathode) and the front of electrolytic magnetic compound machining tool

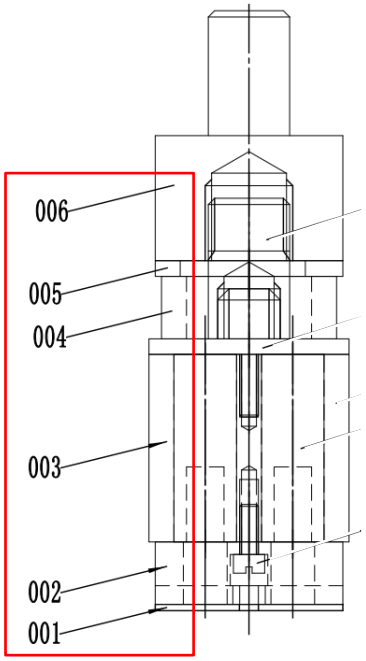

Component number	Component name
001	Electrode
002	Abduction plate
003	Torso of tool
004	Copper ring
005	Abduction plate
006	Tip of tool

Fig. 2.4.3 Assembly drawing of electrolytic magnetic compound machining tool

2.5 Experimental setup

Figure 2.5.1 shows the external photo of electrolytic magnetic abrasive finishing experimental setup. A SUS304 plane with 100 mm in length, 100 mm in width and 1 mm in thickness is used for the experiments. The SUS304 plane workpiece as an anode is located in the container and connects to the positive of DC constant voltage power. Electrolytic magnetic compound machining tool is fixed on the chuck of milling machine and placed on the top of SUS304 plane workpiece. The electrodes as a cathode are embedded into bottom of electrolytic magnetic compound machining tool and connected to the negative of DC constant voltage power through a carbon brush and connecting wires. A nozzle is placed near the carbon rod. The electrolyte ($NaNO_3$) is supplied from a nozzle by a pump, and the flow rate of electrolyte is controlled through a flow meter. The plane workpiece and container are laid on the X-Y stage. The feeding trajectory and velocity of X-Y stage are controlled by a numerical control (NC) program which has been compiled. When the experiments are performed, a certain working gap is adjusted between workpiece (anode) and compound machining tool (cathode). The magnetic brush is formed by mixing magnetic abrasive grains on the bottom of magnetic poles between magnetic poles and workpiece. Then, the electrolytic magnetic compound machining tool performs rotary motion. The rotational direction and velocity of compound machining tool are controlled by milling machine.

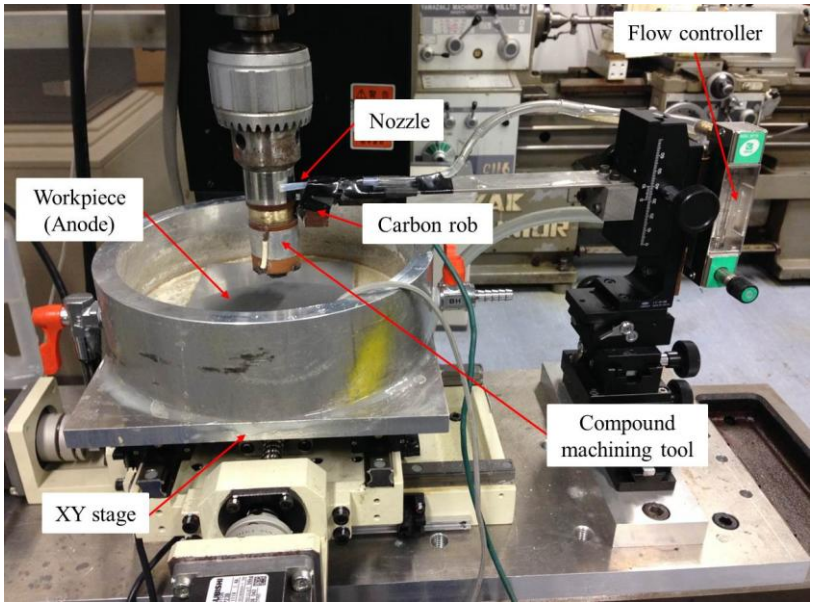

Fig. 2.5.1 External photo of experimental setup

2.6 Measuring instruments

In this research, there are many investigating factors for evaluating and investigating the finishing characteristics of magnetic abrasive finishing combined with electrochemical machining. For example: surface roughness R_a, material removal weight M, finished surface profile, surface composition of wprkpiece, surface hardness HV of workpiece and so on.

Before finishing and after each step of experiment, we respectively select 3 points in the central axis direction of the processing region, the surfaces of workpiece are observed at 3 locations as shown in Figure 2.6.1.

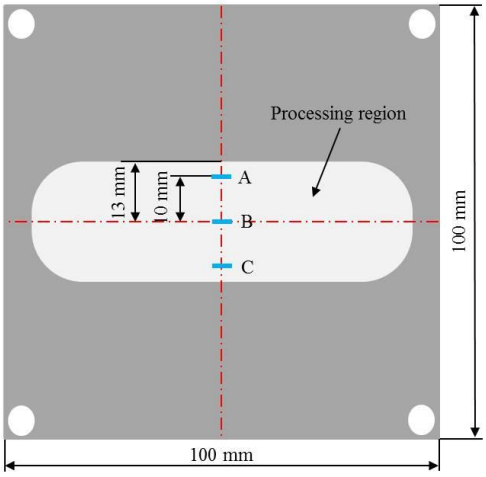

Fig. 2.6.1 Observed locations of surface specimen

The surface roughness of workpiece is measured through a contact surface roughness and profiling meter (Mitutoyo) which is shown as Figure 2.6.2. The length of straight line measurement is 4 mm, the measurement speed of the probe is 0.02 mm/s. The evaluation curve type is R-JIS. The contour arithmetic mean deviation R_a, microscopic roughness ten point height R_z and maximum height of the profile R_y can be measured through the contact surface roughness and profiling meter.

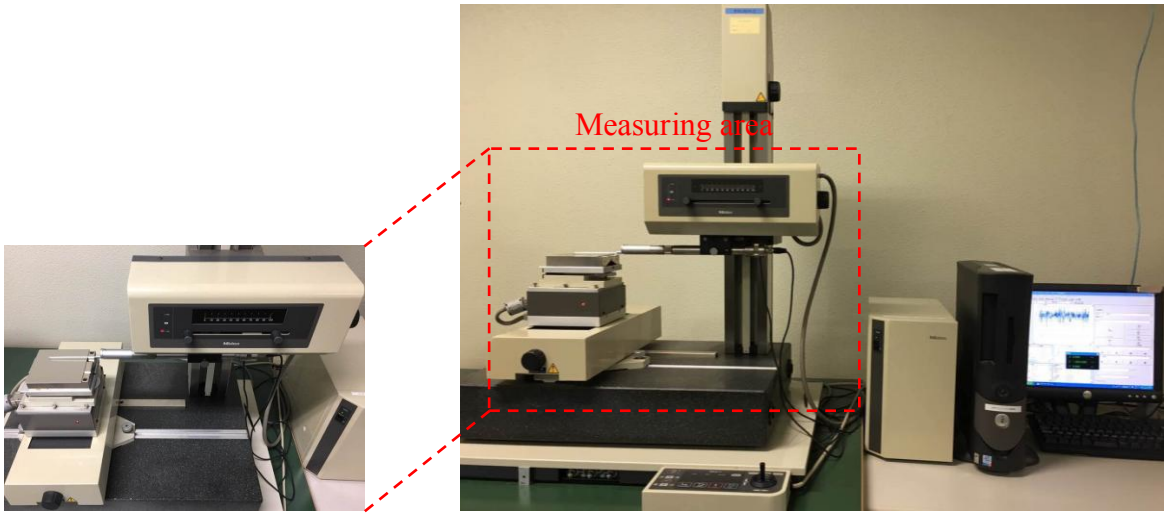

Fig 2.6.2 Contact surface roughness and profiling meter (Mitutoyo)

In order to compare the finishing effect of each processing stage, the profile of finished surface and before finishing can be observed and evaluated through the non-contact optical profiling microscope (Zygo New View 7300). Figure 2.6.3 shows the non-contact optical profiling microscope. In addition, the surface roughness R_a can be also measured through the non-contact optical profiling microscope.

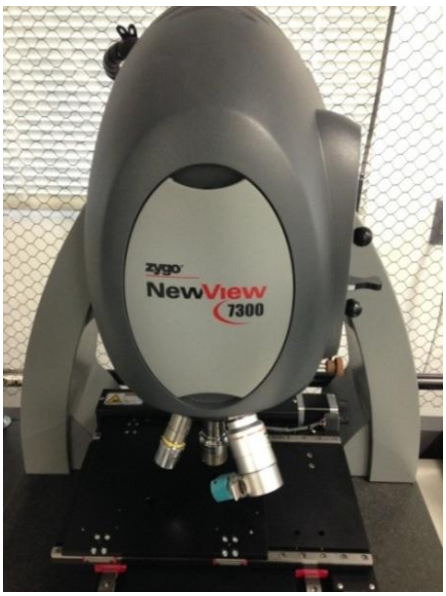

Fig 2.6.3 Non-contact optical profiling microscope (Zygo New View 7300)

Additionally, the profile and images of finished surface and before finishing are also observed and evaluated through the scanning electron microscope (SEM, HITACHI S4500). Figure 2.6.4 shows the scanning electron microscope. In electrolytic process and EMAF process, except for these above mentioned measurement parameters, the surface composition is needed to be investigated and analyzed since the passive films generated. Therefore, we should use the Energy Dispersive X-Ray (EDX) Spectroscopy to evaluate and obtain the change in elemental composition during different finishing processes. The above scanning electron microscope also has the function of Energy Dispersive X-Ray.

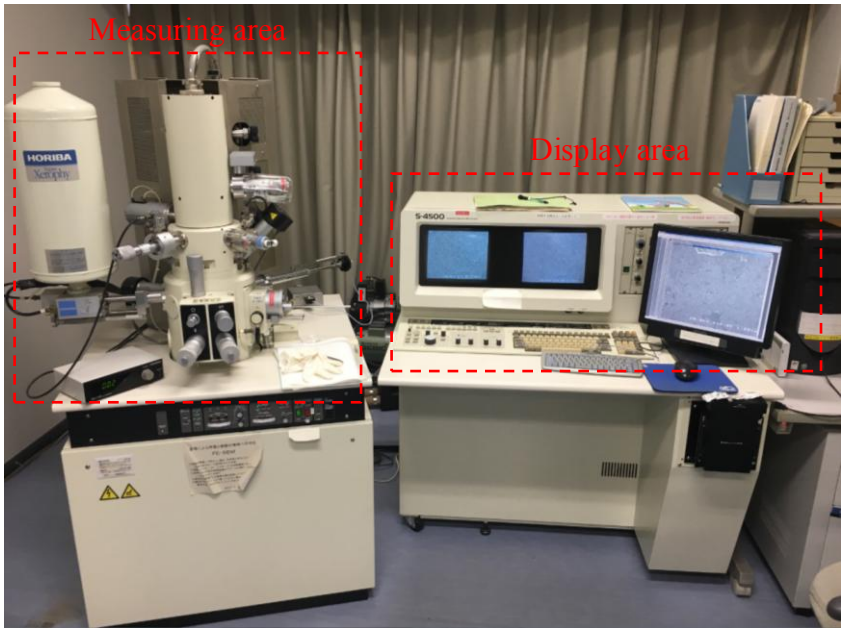

Fig 2.6.4 Scanning electron microscope, (SEM, HITACHI S4500)

The material removal weight *M* of before machining and after finishing is measured through a high-precision electronic scale which is shown in Figure 2.6.5. Through the Figure 2.6.5, it can be found that the accuracy of measured material removal weight *M* can reach 0.01 mg.

Fig 2.6.5 High-precision electronic scale

In order to prove surface hardness of generated passive films from electrolytic process is smaller than original hardness of SUS304 stainless steel material, the hardness of finished surface need to be measured through a hardness meter shown in Figure 2.6.6.

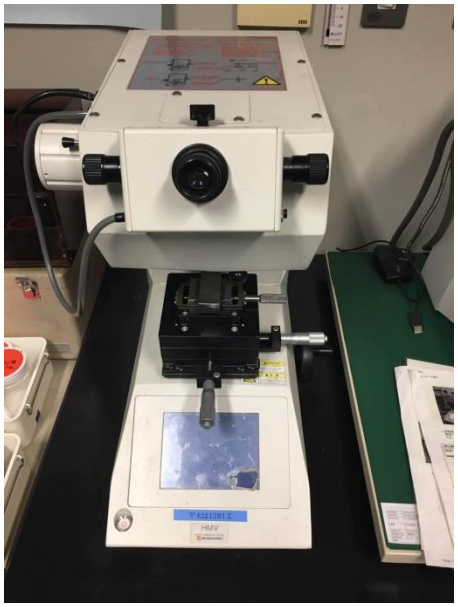

Fig. 2.6.6 Hardness meter

Finally, we will make a Table 2.1 to describe these measuring instruments which are used in different finishing processes.

Table 2.1 Measuring instruments are used in different finishing processes

Measuring instruments	**Finishing processes**
Contact surface roughness & profiling meter	MAF process, ECM process, EMAF process
Non-contact optical profiling microscope	MAF process, ECM process, EMAF process
Scanning electron microscope	MAF process, ECM process, EMAF process
High-precision electronic scale	MAF process, ECM process, EMAF process
Energy Dispersive X-Ray Spectroscopy	MAF process, ECM process, EMAF process
Hardness meter	MAF process, ECM process, EMAF process

2.7 Conclusion

The content of this chapter can be summarized as follows:

(1) Firstly, the processing principle of traditional plane magnetic abrasive finishing, electrolytic process and electrolytic magnetic abrasive finishing were respectively illustrated in this chapter.

(2) Then, the developed electrolytic magnetic compound machining tool and experimental setup were shown in this chapter.

(3) Finally, the specific measurement methods and measuring instruments were also introduced in this chapter.

Chapter 3 Preliminary verification experiments of EMAF process

In order to verify the feasibility of EMAF process, we firstly preformed a series of comparative experiments about MAF process, electrolytic process and EMAF process. The experimental results of three kinds of polishing methods were respectively reported in this chapter. In addition, the comparison of experimental results of MAF process and EMAF process was also reported in this chapter.

3.1 MAF experiments

3.1.1 Experimental conditions of MAF

In order to compare traditional MAF process with EMAF process, the traditional MAF process tests were firstly conducted at room temperature. The detailed experimental conditions of MAF process are shown in Table 3.1. Surface roughness of workpiece is measured at approximate 0.39 μm R_a as an original roughness before machining. The finishing time is selected as per 15 minutes (for 6 times) to measure and compare the finished surfaces difference. In order to ensure machining power to be adequate, the working gap is adjusted to 1 mm. For obtaining a higher surface accuracy and higher efficiency, the rotational speed of compound machining tool and feeding speed of X-Y stage are respectively adjusted to 450 rpm and 5 mm/s [1, 2]. After each step of tests, surfaces of workpiece are observed at 9 locations as shown in Fig. 3.1.1. The surface roughness of workpiece is measured through a non-contact optical profiling microscope (Wyko Vision NT1100) and the image of finished surface is observed by a scanning

electron microscope (HITACHI S4500).

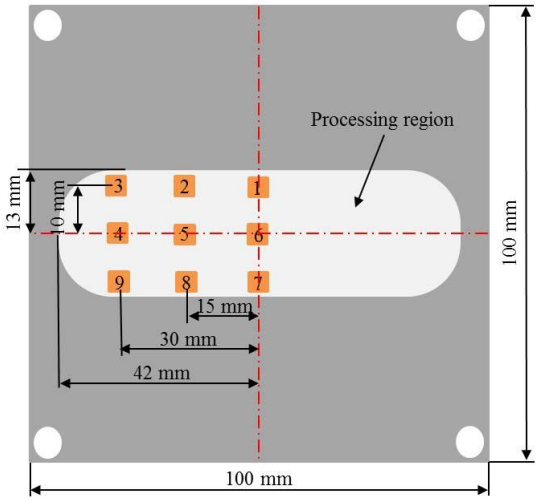

Fig. 3.1.1 Observed locations of surface specimen

Table 3.1 Experimental conditions of MAF process

Workpiece	SUS304 plane (100 × 100 × 1 mm)
Original roughness	0.39 μm R_a
Compound magnetic abrasives	Electrolytic iron powder (149 μm, 75 μm, 30 μm in mean diameter) WA particles: #800, #4000, #8000, #10000 Oily grinding fluid
Working gap	1 mm
Stage feeding speed	5 mm/s
Tool rotational speed	450 rpm
MAF test time	90 minutes

3.1.2 Experimental results and discussions of MAF process

Fig. 3.1.2 shows the non-contact 3D measurement of unfinished surface and finished surface at 75 min traditional MAF process test obtained through a non-contact optical profiling microscope. Compared with the surface profile of original workpiece, it can be clearly seen that the change in removal depth h_r at 75 min traditional MAF process, and the surface profile of workpiece almost tends to be planarized.

The SEM photograph of surface before MAF process is shown in Fig. 3.1.3 (a). The initial hairline of surface can be clearly seen through the SEM photograph. Fig. 3.1.3 (b) shows the SEM photograph of finished surface at 75 min traditional MAF process test obtained by a scanning electron microscope. Compared with the surface of original workpiece, it can be clearly found that the initial hairlines of surface have almost completely been removed. However, just a few concave portions still exist on the surface.

In order to quantitatively compare and estimate the difference of surface roughness R_a and material removal weight M under different finishing time of traditional MAF process (per 15 min). The maximum height roughness R_a in the captured field of 299 × 227 μm^2 is estimated using a non-contact optical profiling microscope. The change in material removal weight M is measured through a high-precision electronic scale. Fig. 3.1.4 shows the change in surface roughness R_a and material removal weight M as a function of MAF process time versus. The surface roughness R_a is an average surface roughness value of 9 observed locations. With finishing time increases, it is noted that the surface roughness remarkably descends from 390.98 nm R_a to 41.49 nm R_a at 75 min MAF process experiment, and then the surface roughness becomes stable after 75 min MAF process test; the material removal weight M continuously keeps increasing during 90 min MAF process test, but the rate of material removal weight M before 30 min MAF process test is more than the rate of material removal weight M after 30 min MAF process test. Since the service life of magnetic abrasive is short and the hardness of magnetic abrasive is relatively soft, it may be the main reason for that the surface roughness R_a becomes stable after 75 min MAF process test and the material removal weight rate before 30 min MAF process test is more than that after 30 min MAF process test.

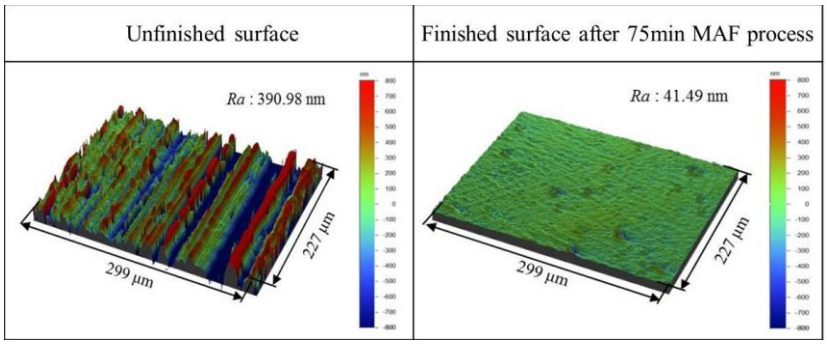

Fig. 3.1.2 Non-contact 3D measurement of unfinished surface and finished surface after 75 min MAF process

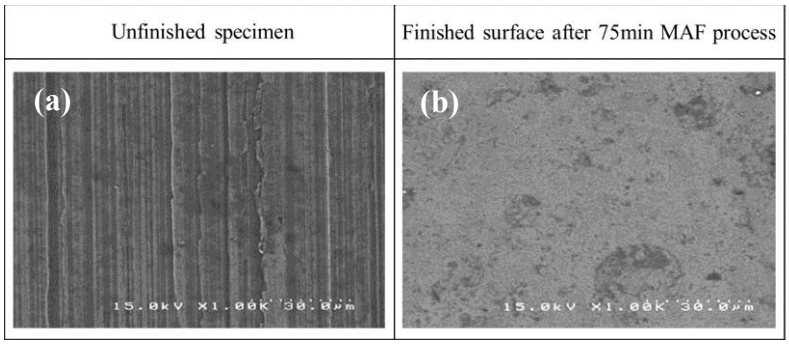

Fig. 3.1.3 SEM images of unfinished surface & finished surface after 75 min MAF process

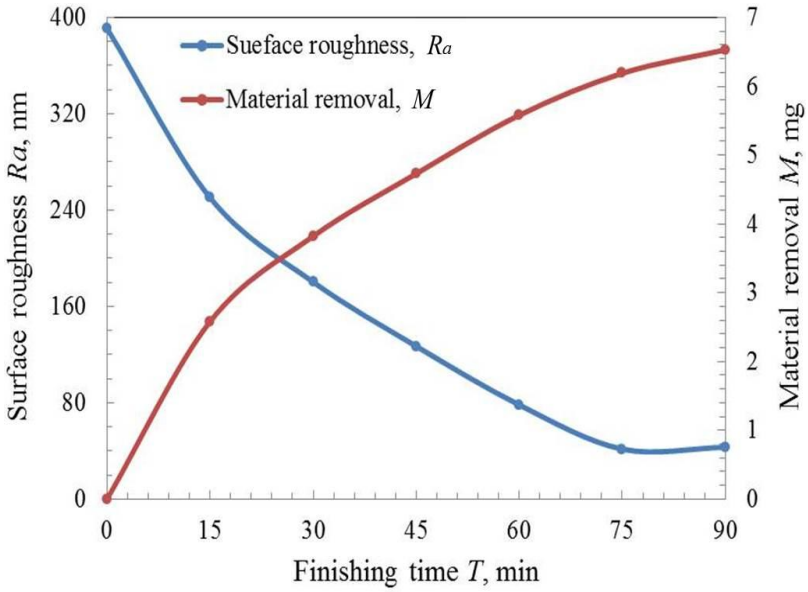

Fig. 3.1.4 Change in surface roughness R_a and material removal M as a function of MAF processing time

3.2 EMAF experiments

3.2.1 Experimental conditions of electrolytic process

By the foregoing narrative, it is easy to see that electrolytic process plays an extremely important role during EMAF process. Therefore, the investigation of electrolytic process is carried out before EMAF process. Table 3.2 describes experimental conditions of electrolytic process. Because finished surface roughness during electrolytic process generally can reach to below 0.2 μm R_a, the original surface roughness of workpiece is selected as approximate 0.39 μm R_a before machining. The working gap is adjusted to 1 mm in order to ensure processing effect. The rotational speed of compound machining tool and feeding speed of X-Y stage are respectively adjusted to 450 rpm and 5 mm/s. The main feature of electrolytic process is that processing speed can be accelerated. Thereby, the total finishing time is selected as 10 min, and the finished surface is measured at per 2 min. The 20wt% sodium nitrate is adopted as the electrolyte. The flow rate of electrolyte is adjusted to 300 ml/min. Electrical current is set as 2.5 A through an 8 V DC constant voltage. The value of working current can influence current density which can be calculated by equation (1). In other words, the current density can indirectly be controlled by voltage applied to electrodes.

$$J = I/A \tag{1}$$

Where "J" is current density; "I" is electrolytic current; "A" is area of cathode. Thus, it can be found that the current density "J" as an important parameter of electrolytic process is proportional to the electrolytic current "I" and inversely proportional to the area of cathode "A" through equation (1). After each step of electrolytic process experiment, the surface roughness of workpiece is measured through a non-contact optical profiling microscope;

the images of finished surface are observed by a scanning electron microscope.

Table 3.2 Experimental conditions of electrolytic process

Workpiece	SUS304 plane (100 × 100 × 1 mm)
Original roughness	0.39 μm R_a
Working gap	1 mm
Stage feeding speed	5 mm/s
Tool rotational speed	450 rpm
Working voltage	8 V
Electrolyte	$NaNO_3$ (20wt%)
Flow rate	300 ml/min
Electrolytic test time	10 minutes

3.2.2 Experimental results and discussions of electrolytic process

Fig. 3.2.1 shows a series of SEM photographs of surface before the electrolytic process and after the electrolytic process. The initial hairline of unfinished surface can be clearly seen through the SEM photograph (1000 times) of Fig. 3.2.1 (a). Fig. 3.2.1 (b) ～ (f) respectively shows the SEM photographs (1000 times) of finished surface at 2 min, 4 min, 6 min, 8 min and 10 min electrolytic process experiment obtained by a scanning electron microscope. Compared with the surface of workpiece before machining, it can be clearly found that the initial hairlines of surface have been almost completely removed. However, a lot of micro-porous generate on the surface of workpiece. Furthermore, under the action of electrolytic process, the number of micro-porous increases with the finishing time increases; the size of micro-porous becomes small with the finishing time increases, and the depth of microporous also deepens.

In order to investigate the optimal parameters of electrolytic process, the difference of surface roughness R_a and material removal weight M have been quantitatively compared and estimated at different finishing time of electrolytic process (per 2 min). Fig. 3.2.2

shows the change in surface roughness R_a and material removal weight M at different finishing time of electrolytic process. With the finishing time increases, it is noted that the surface roughness remarkably descends from 394.81 nm R_a to 160.03 nm R_a at 4 min finishing time of electrolytic process, and then the surface roughness R_a increases when the finishing time of electrolytic process is more than 4 min; the material removal weight M continuously keeps increasing during 10 min electrolytic process test, but the rate of material removal weight M before 4 min electrolytic process test is higher than that after 4 min electrolytic process test. Since the action of electrolytic process, the surface of SUS304 plane will accumulate a large number of passive films which can make the electrolytic current gradually to decrease, and then the eluting amount of metal ions will decrease. It may be the main reason for that the surface roughness R_a increases after 4 min electrolytic process test, and the rate of material removal weight M before 4 min electrolytic process test is higher than that after 4 min electrolytic process test.

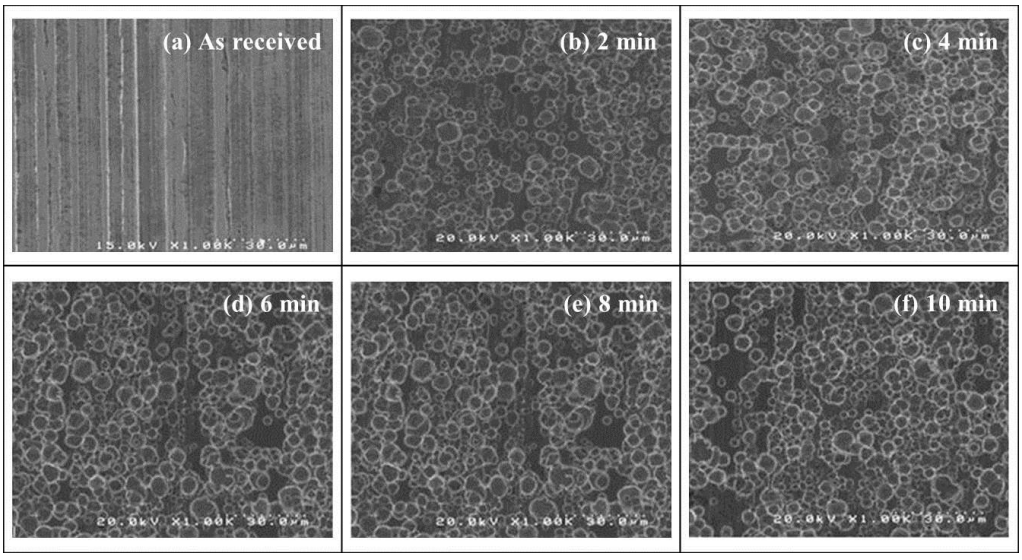

Fig. 3.2.1 Macroscopic confocal images of unfinished surface and finished surface in various conditions after 2 min, 4 min, 6 min, 8 min and 10 min experiments

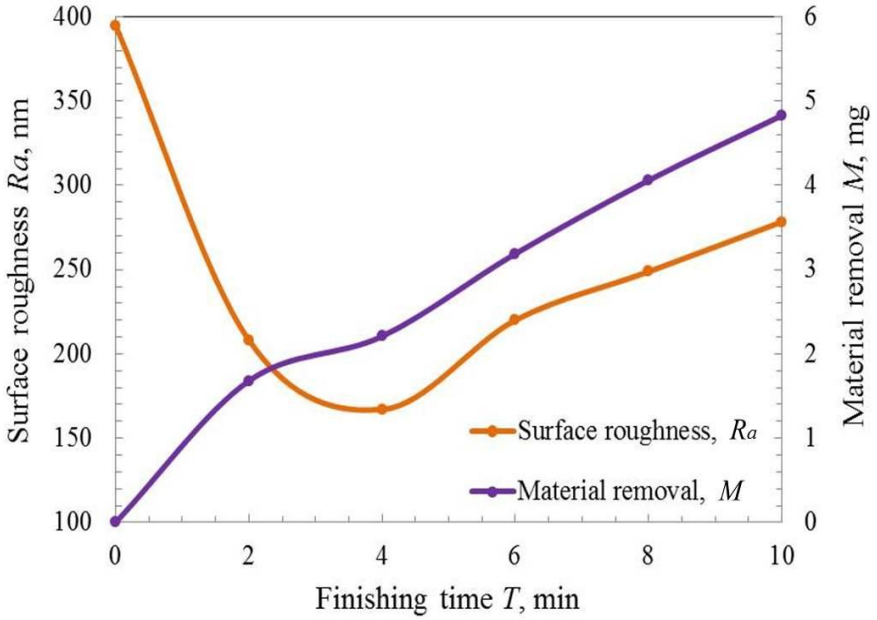

Fig. 3.2.2 Change in surface roughness R_a and material removal M as a function of electrolytic processing time

3.2.3 Experimental conditions of EMAF

The EMAF process step is conducted in one step simultaneously for combining electrolytic process and MAF process. Although the surface can be leveled through electrolytic process, generated passive films by the action of electrolytic process will affect the accuracy of surface. Thus, in order to completely remove passive films, electrolytic process has to be stopped before MAF process. Since over a long period electrolytic process can lead to the formed passive films thicken, the finishing time of EMAF process step is selected as 4 min. After EMAF process, electrolytic process is stopped and MAF process continues to be conducted for 41 min. The total EMAF finishing time is selected as 4 min, 15 min, 25 min, 35 min, 40 min and 45 min to observe and compare the difference of polishing surfaces during different steps of MAF process. The detailed experimental conditions of EMAF are shown as Table 3.3. The sodium nitrate 20wt% is used as electrolyte and flows at 300 ml/min. Electrolytic current is set as 2.5 A through an 8 V DC

constant voltage. According to equation (1), the current density can be indirectly controlled by voltage applied to electrodes. After each step of EMAF process tests, surface roughness R_a of workpiece is measured through a non-contact optical profiling microscope; the image of finished surface is observed by a scanning electron microscope.

Table 3.3 Experimental conditions of EMAF process

Workpiece	SUS304 plane (100 × 100 × 1 mm)
Original roughness	0.39 μm R_a
Compound magnetic abrasives	Electrolytic iron powder (149 μm, 75 μm, 30 μm in mean diameter) WA particles #800, #4000, #8000, #10000 Oily grinding fluid
Working gap	1 mm
Stage feeding speed	5 mm/s
Tool rotational speed	450 rpm
Working voltage	8 V
Electrolyte	$NaNO_3$ (20wt%)
Flow rate	300 ml/min
EMAF test time	4 min (EMAF) + 41 min (MAF)

3.2.4 Experimental results and discussions of EMAF process

Fig. 3.2.3 shows the non-contact 3D measurement of finished surface at 45 min EMAF process experiment (it includes 4 min EMAF process & 41 min MAF process) obtained through a non-contact optical profiling microscope. Compared with the surface profile of workpiece before machining, it can be clearly seen that the change in removal depth h_r at 45 min EMAF process, and the surface profile of workpiece tends to be planarized. Furthermore, compared with the surface profile of workpiece during traditional MAF process, it can be obviously found that the surface roughness R_a of EMAF process is a little better than the surface roughness R_a of traditional MAF process.

The SEM photograph of original surface before EMAF process is shown in Fig. 3.2.4 (a).

The initial hairline of unfinished surface can be clearly seen through the SEM photograph. Fig. 3.2.4 (b) shows the SEM photograph of finished surface after the first finishing step (4 min EMAF process). It can be seen that a small amount of micro-porous still exists on the finished surface through the SEM photograph. Moreover, it also indicates that when two kinds of finishing processes simultaneously are executed, the action of MAF process can not completely remove the generated passive films from electrolytic process. The SEM photograph of finished surface after the second finishing step (41 min MAF process) is shown in Fig. 3.2.4 (c). Compared with the original surface of workpiece, it can be clearly found that the initial hairline of surface has been almost completely removed. Furthermore, it also can be confirmed that MAF process plays an essential role during the EMAF process.

Fig. 3.2.5 shows the change in surface roughness R_a and material removal weight M under different finishing time of EMAF process. The measurement of change in surface roughness R_a is operated through a non-contact optical profiling microscope. With the finishing time increases, the surface roughness descends from original surface roughness 393.08 nm R_a to 268.44 nm R_a after the first finishing step (EMAF process), and then the surface roughness continues to descend from 268.44 nm R_a to 31.58 nm R_a after the second finishing step (single MAF process). It is noted that the surface roughness firstly descends from 393.08 nm R_a to 30.94 nm R_a at 40 min EMAF process test, and then the surface roughness R_a becomes stable after 40 min EMAF process test. The change in material removal weight M is measured through a high-precision electronic scale. The material removal weight M markedly continues to increase with the finishing time increases, but the rate of material removal weight M during the first finishing step (4 min EMAF process) is obviously higher than the rate of material removal weight M during the second finishing

step (41 min MAF process). Moreover, compared with the material removal rate of single MAF process, the material removal rate of EMAF process step is nearly 3 times than that of single MAF process step. Then, the change in surface roughness R_a is mainly caused by EMAF process itself. The removal depth h_r can be calculated by the following equation (2).

$$h_r = m/A_p\rho \tag{2}$$

Where "m" is mass of material removal, "A_p" is working area, and "ρ" is density of material. According to the result of material removal weight M shown in Fig. 3.2.5, the removal depth h_r is ranged from 0 to 2.4 μm. Yet, the surface roughness R_a has little change when finishing time is more than 40 min. It is probably because removal depth h_r is larger than the value of original roughness. Moreover, the effects of electrolytic process and magnetic abrasive have reached to finishing balance. Therefore, the surface roughness no longer declines. During the EMAF process, a large amount of metal ions dissociate from the surface of workpiece. Thus, the rate of material removal weight M before 4 min EMAF process (EMAF process step) is higher than the rate of material removal weight M after 4 min EMAF process test (single MAF process step).

Finally, the comparison of EMAF process and MAF process is shown in Fig. 3.2.6. It is recognized that the material removal efficiency of EMAF process is remarkably higher than that of traditional MAF process, and the surface quality of EMAF process is a little better than that of MAF process. Therefore, this new finishing process can be proven to more efficiently polish SUS304 plane than the traditional MAF process.

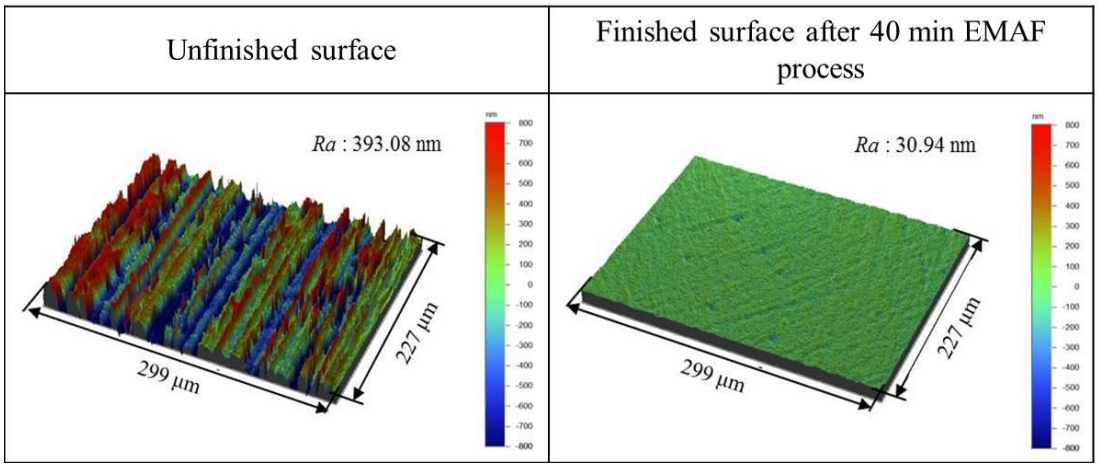

Fig. 3.2.3 Non-contact 3D measurement of unfinished surface and finished surface after 40 min EMAF process

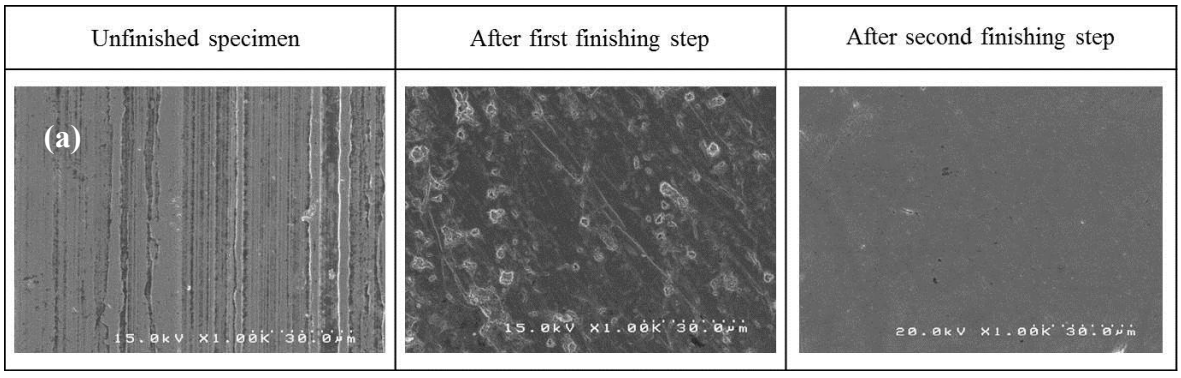

Fig. 3.2.4 Macroscopic confocal images of unfinished surface and finished surface in various conditions after first finishing step and second finishing step experiments

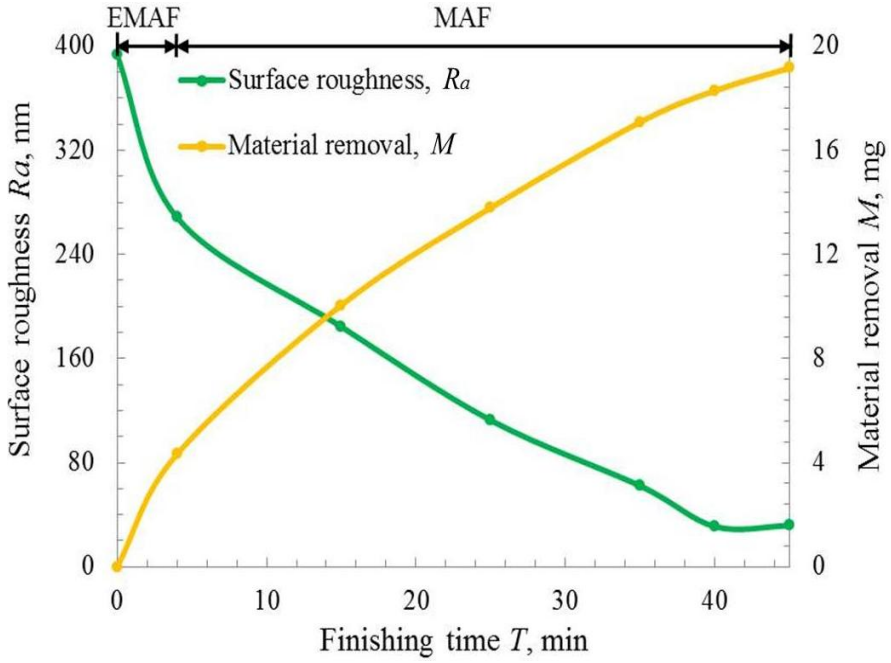

Fig. 3.2.5 Change in surface roughness R_a and material removal M as a function of EMAF processing time

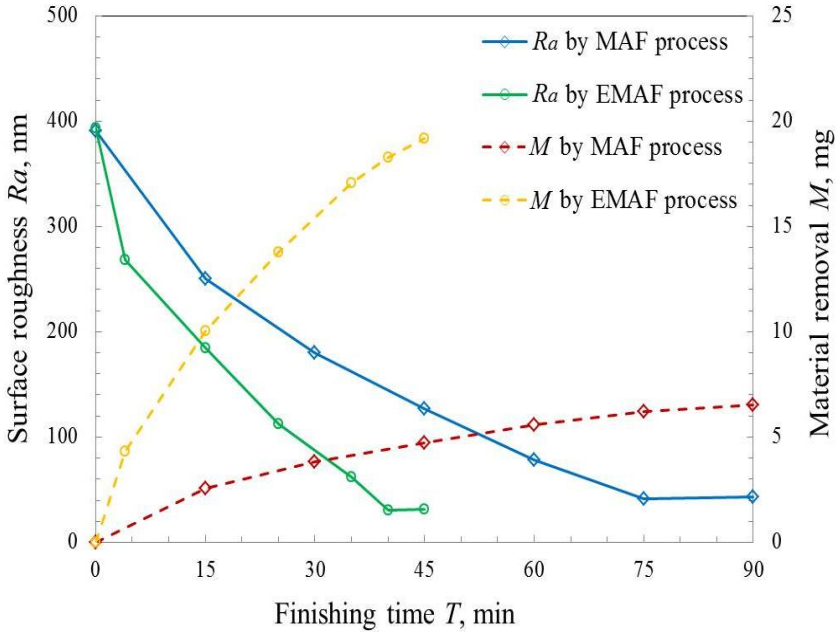

Fig. 3.2.6 The comparison of EMAF process and MAF process for surface roughness R_a and material removal M

3.3 Conclusions

In chapter 3, the experimental results of three kinds of polishing methods were respectively reported in this chapter. In addition, the comparison of experimental results of MAF process and EMAF process was also reported. The main conclusions are summarized as follows:

1. The results of experiments show that the surface roughness can reach to 41.49 nm R_a from 390.98 nm R_a by 75 min traditional MAF process; the surface roughness descends from 393.08 nm R_a to 30.94 nm R_a by 40 min EMAF process.

2. Since the electrolytic magnetic abrasive finishing can soften the surface of workpiece, the material removal weight M of total EMAF process is nearly 6 times than that of single traditional MAF process.

3. Through contrasting with traditional MAF process, it is confirmed that EMAF process can obtain a little higher quality surface, and machining efficiency is improved by about 50%. Therefore, this new finishing process can be proven to more efficiently polish SUS304 plane than the traditional MAF process.

Chapter 4 Stainless steel SUS304 plane workpiece finishing by using electrolytic magnetic compound machining tool in traditional magnetic abrasive finishing

MAF process as an important finishing part of EMAF process, the mechanical (MAF) finishing characteristics of electrolytic magnetic compound machining tool are necessary to be explored before EMAF process. Since their mechanical finishing characteristics are different for machining tools with different shapes of magnetic poles, we focused on investigating mechanical finishing characteristics for electrolytic magnetic compound machining tool through MAF process, such as amount of iron powder and WA abrasive grain, combinations of mixed magnetic abrasive, feeding speed of X-Y stage, rotational speed of compound machining tool and working gap.

4.1 Investigation of the amount of iron powder and WA abrasive grain

The amount of iron powder and WA abrasive grain has been firstly investigated in the traditional MAF process. Table 4.1.1 shows the experimental condition for investigating the amount of iron powder and WA abrasive grain. Surface roughness of workpiece is measured at approximate 160 ~ 220 nm R_a as an original roughness before machining. The finishing time is selected as per 10 min (for six times) to measure and compare the finished surface differences. In order to ensure machining power to be adequate, the working gap is adjusted to 1 mm. For obtaining a higher surface accuracy and higher efficiency, the rotational speed of compound machining tool and feeding speed of X-Y stage are respectively adjusted to 450 rpm and 5 mm/s [1, 2]. The amount ratio of electrolytic iron powder and abrasive grains is 4:1. The amount of electrolytic iron powder is respectively 0.8 g, 1.2 g and 1.6 g. The amount of WA abrasive grains is respectively 0.2 g, 0.3 g and 0.4 g. The amount of compound magnetic abrasives is respectively 1 g, 1.5 g and 2 g.

Chapter 4 Stainless steel SUS304 plane workpiece finishing by using electrolytic magnetic compound machining tool in traditional magnetic abrasive finishing

Table 4.1.1 Experimental condition for investigating amount of iron powder and WA abrasive grain

Workpiece	SUS304 plane (100 × 100 × 1 mm)
Original surface roughness	160 ~ 220 nm
Compound magnetic abrasives	Electrolytic iron powder (149 μm in mean diameter): 0.8 g, 1.2 g & 1.6 g Abrasive grains (# 8000): 0.2 g, 0.3 g & 0.4 g Compound magnetic abrasives: 1 g, 1.5 g & 2 g Oily grinding fluid: 2 ml
Workinge gap	1 mm
Feeding speed	5 mm/s
Rotational speed	450 rpm
MAF test time	60 min

Figure 4.1.1 shows the non-contact 3D measurement and SEM photographs of finished surface in various amounts of iron powder and WA abrasive grain conditions after 60 min MAF process obtained through a non-contact optical profiling microscope. Through comparing the finished surface profile in various amounts of iron powder and WA abrasive grain conditions, it is recognized that the surface roughness R_a in 1 g amount of iron powder and WA abrasive grain case is remarkably smaller than the surface roughness R_a in other amounts of iron powder and WA abrasive grain cases at 60 min tests. Through comparing the SEM photographs of finished surface in various amounts of iron powder and WA abrasive grain conditions, it also can be recognized that the finished surface accuracy in 1 g amount of iron powder and WA abrasive grain case is remarkably better than the finished surface accuracy in other amounts of iron powder and WA abrasive grain cases at 60 min tests. Furthermore, it can be clearly found that the initial hairlines of finished surface have almost completely been removed in 1 g amount of iron powder and WA abrasive grain condition through obtaining non-contact 3D measurement and SEM

photographs. However, a few concave portions still exist on the finished surface in other amounts of iron powder and WA abrasive grain conditions.

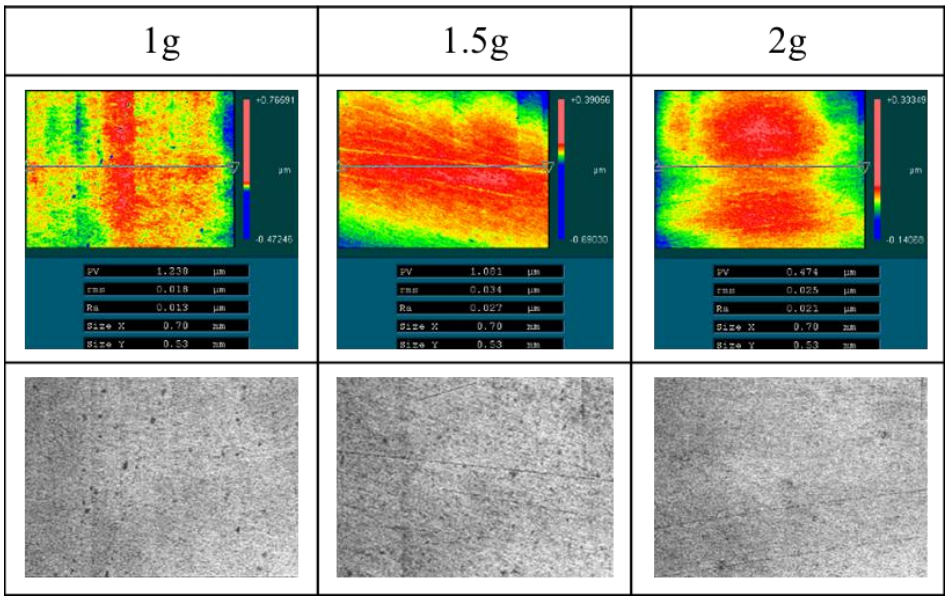

Fig. 4.1.1 Non-contact 3D measurement and SEM photographs of finished surface in various amounts of iron powder and WA abrasive grain conditions after 60 min MAF process

In order to quantitatively compare and estimate the difference of surface roughness R_a under different finishing times of traditional MAF process (per 10 min). The surface roughness R_a is estimated through using a contact optical profiling microscope. Figure 4.1.2 shows the change in surface roughness R_a as a function of MAF processing time under different amount of iron powder and WA abrasive grain conditions. The surface roughness R_a is an average surface roughness value of three observed locations. Through quantitatively compare under different amount of iron powder and WA abrasive grain conditions, it is noted that the surface roughness R_a in 1 g amount of iron powder and WA abrasive grain case is obviously smaller than the surface roughness R_a in other amounts of iron powder and WA abrasive grain cases.

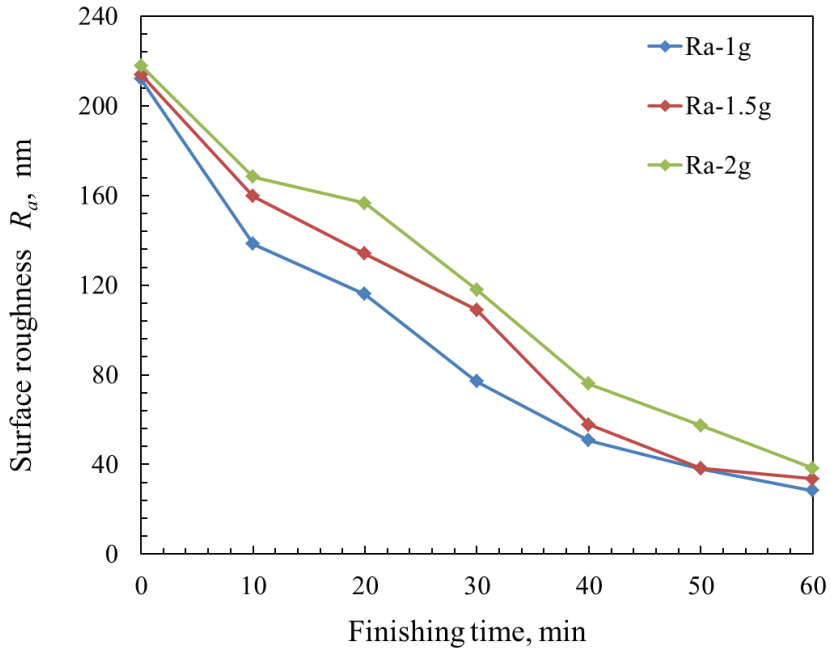

Fig. 4.1.2 Change in surface roughness R_a as a function of MAF processing time under different amount of iron powder and WA abrasive grain conditions

4.2 Investigation of the feeding speed of X-Y stage

According to previous experimental results, the amount of electrolytic iron powder is selected as 0.8 g, the amount of abrasive grains is selected as 0.2 g. Table 4.2.1 shows the experimental condition for investigating the feeding speed. Surface roughness of workpiece is measured at approximate 160 ~ 220 nm R_a as an original roughness before machining. The finishing time is selected as per 10 min (for six times) to measure and compare the finished surface differences. The working gap is adjusted to 1 mm. The rotational speed of compound machining tool is adjusted to 450 rpm. The feeding speed of X-Y stage is respectively set at 10 mm/s and 5 mm/s.

Table 4.2.1 Experimental condition for investigating the feeding speed of X-Y stage

Workpiece	SUS304 plane (100 × 100 × 1 mm)
Original surface roughness	160 ~ 220 nm
Compound magnetic abrasives	Electrolytic iron powder (149 μm in mean diameter): 0.8 g Abrasive grains (# 8000): 0.2 g Oily grinding fluid: 2 ml
Workinge gap	1 mm
Feeding speed	5 mm/s & 10 mm/s
Rotational speed	450 rpm
MAF test time	60 min

The non-contact 3D measurement and SEM photographs of finished surface in various feeding speed of X-Y stage conditions after 60 min MAF process obtained through a non-contact optical profiling microscope is shown in Figure 4.2.1. Through comparing the finished surface profile in various feeding speed cases, it is recognized that the surface roughness R_a at 10 mm/s feeding speed case is slightly smaller than the surface roughness R_a at 5 mm/s feeding speed case at 60 min tests. Through comparing the SEM photographs

of finished surface in various feeding speed cases, it also can be recognized that the finished surface accuracy at 10 mm/s feeding speed case is slightly better than the finished surface accuracy at 5 mm/s feeding speed case at 60 min tests. Furthermore, it can be clearly found that the initial hairlines of finished surface have almost completely been removed at 10 mm/s feeding speed condition through obtaining non-contact 3D measurement and SEM photographs. However, a few concave portions still exist on the finished surface at 10 mm/s feeding speed condition.

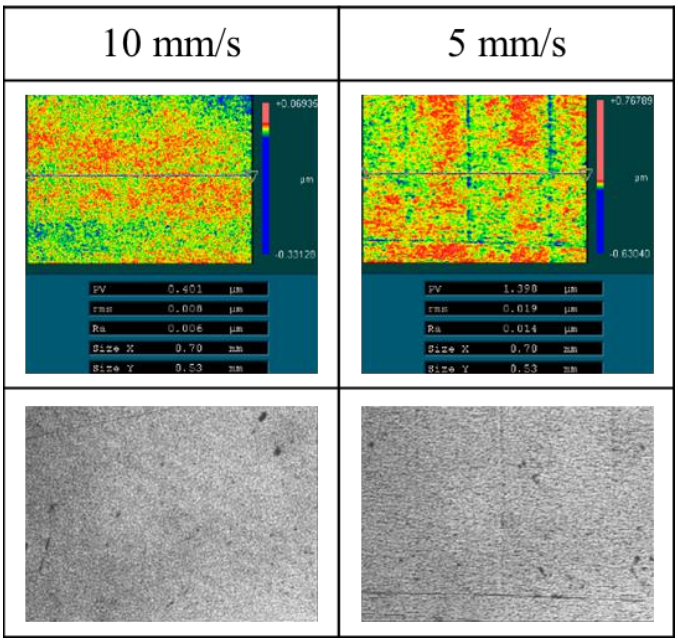

Fig. 4.2.1 Non-contact 3D measurement and SEM photographs of finished surface in various feeding speed of X-Y stage conditions after 60 min MAF process

In order to quantitatively compare and estimate the difference of surface roughness R_a and material removal weight M under different finishing times of traditional MAF process (per 10 min). The surface roughness R_a is estimated through using a contact optical profiling microscope. The change in material removal weight M is measured through a high-precision electronic scale. Figure 4.2.2 shows the change in surface roughness R_a and material removal weight M as a function of MAF processing time under different feeding speed conditions. The surface roughness R_a is an average surface roughness value of three

observed locations. Through quantitatively compare under different feeding speed conditions, it is noted that the change in surface roughness R_a at 10 mm/s feeding speed case is approximately same as the change in surface roughness R_a at 5 mm/s feeding speed case. Furthermore, the change in material removal weight M at 10 mm/s feeding speed case is also approximately same as the change in material removal weight M at 5 mm/s feeding speed stage case.

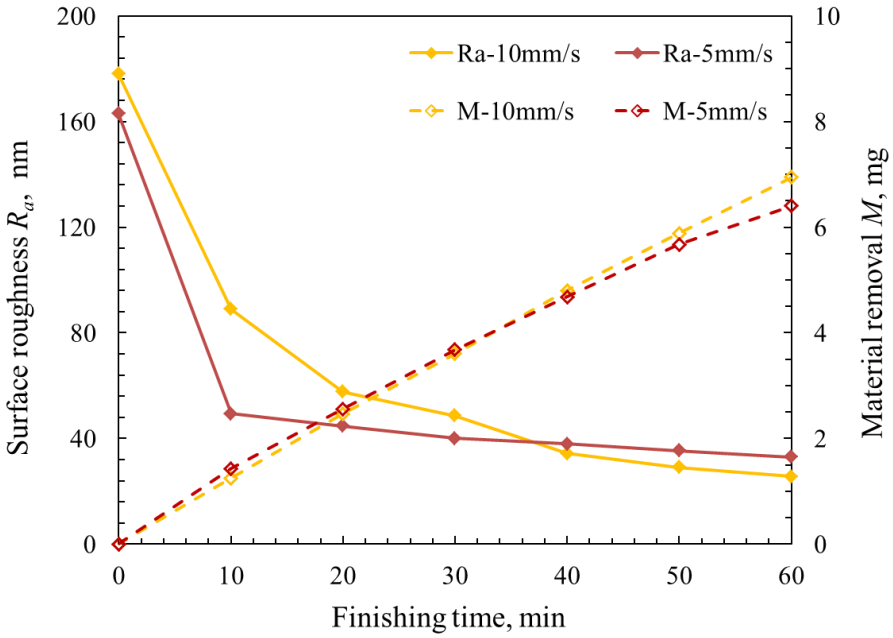

Fig. 4.2.2 Change in surface roughness R_a and material removal M as a function of MAF processing time under various feeding speed of X-Y stage conditions

4.3 Investigation of the rotational speed of compound machining tool

The amount of electrolytic iron powder is decided as 0.8 g, the amount of abrasive grains is decided as 0.2 g through the investigation of the amount of iron powder and WA abrasive grain. The feeding speed of X-Y stage is decided as 5 mm/s through the investigation of feeding speed of X-Y stage, because the effect of different feeding speed on the finished surface accuracy is almost same. Surface roughness of workpiece is measured at approximate 160 ~ 220 nm R_a as an original roughness before machining. The finishing time is selected as per 10 min (for six times) to measure and compare the finished surface differences. The working gap is adjusted to 1 mm. Then, the rotational speed of compound machining tool will be investigated for impacting on the finished surface accuracy. The detailed experimental conditions are shown in Table 4.3.1.

Table 4.3.1 Experimental condition for investigating the rotational speed of compound machining tool

Workpiece	SUS304 plane (100 × 100 × 1 mm)
Original surface roughness	160 ~ 220 nm
Compound magnetic abrasives	Electrolytic iron powder : 149 μm in mean diameter Abrasive grains: # 8000 Oily grinding fluid: 2 ml
Workinge gap	1 mm
Feeding speed	5 mm/s
Rotational speed	450 rpm & 230 rpm
MAF test time	60 min

Figure 4.3.1 shows the non-contact 3D measurement and SEM photographs of finished surface in various rotational speed conditions after 60 min MAF process obtained through a non-contact optical profiling microscope. Through comparing the finished surface profile in various rotational speed cases, it is recognized that the surface roughness R_a at 450 rpm

rotational speed of compound machining tool case is remarkably smaller than the surface roughness R_a at 230 rpm rotational speed of compound machining tool case at 60 min tests. Through comparing the SEM photographs of finished surface in various rotational speed of compound machining tool cases, it also can be recognized that the finished surface accuracy at 450 rpm rotational speed of compound machining tool case is obviously better than the finished surface accuracy at 230 rpm rotational speed of compound machining tool case at 60 min tests. Furthermore, it can be clearly found that the initial hairlines of finished surface have almost completely been removed at 450 rpm rotational speed of compound machining tool condition through obtaining non-contact 3D measurement and SEM photographs. However, a few concave portions still exist on the finished surface at 230 rpm rotational speed of compound machining tool condition.

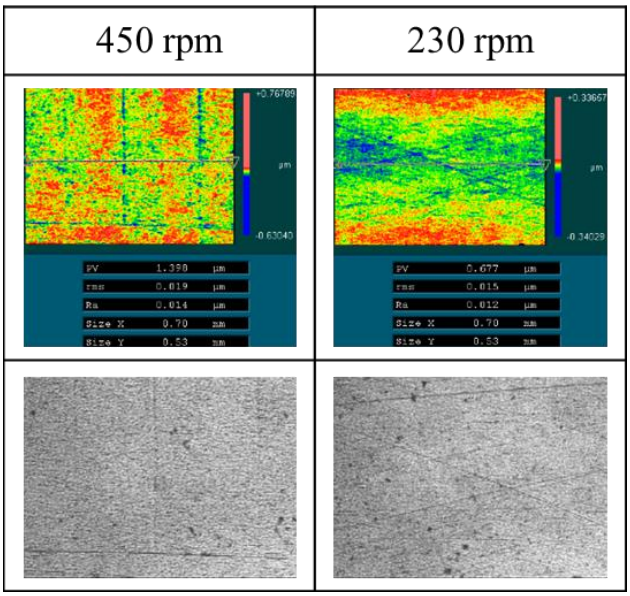

Fig. 4.3.1 Non-contact 3D measurement and SEM photographs of finished surface in various rotational speed of compound machining tool conditions after 60 min MAF process

In order to quantitatively compare and estimate the difference of surface roughness R_a and material removal weight M under different finishing times of traditional MAF process (per 10 min). The surface roughness R_a is estimated through using a contact optical profiling microscope. The change in material removal weight M is measured through a

high-precision electronic scale. Figure 4.3.2 shows the change in surface roughness R_a and material removal weight M as a function of MAF processing time under different rotational speed of compound machining tool conditions. The surface roughness R_a is an average surface roughness value of three observed locations. Through quantitatively compare under different rotational speed of compound machining tool conditions, it is noted that the surface roughness R_a at 450 rpm rotational speed of compound machining tool case is remarkably smaller than the surface roughness R_a at 230 rpm rotational speed of compound machining tool case. Furthermore, the change in material removal weight M at 450 rpm rotational speed of compound machining tool case is also much more than the change in material removal weight M at 230 rpm rotational speed case.

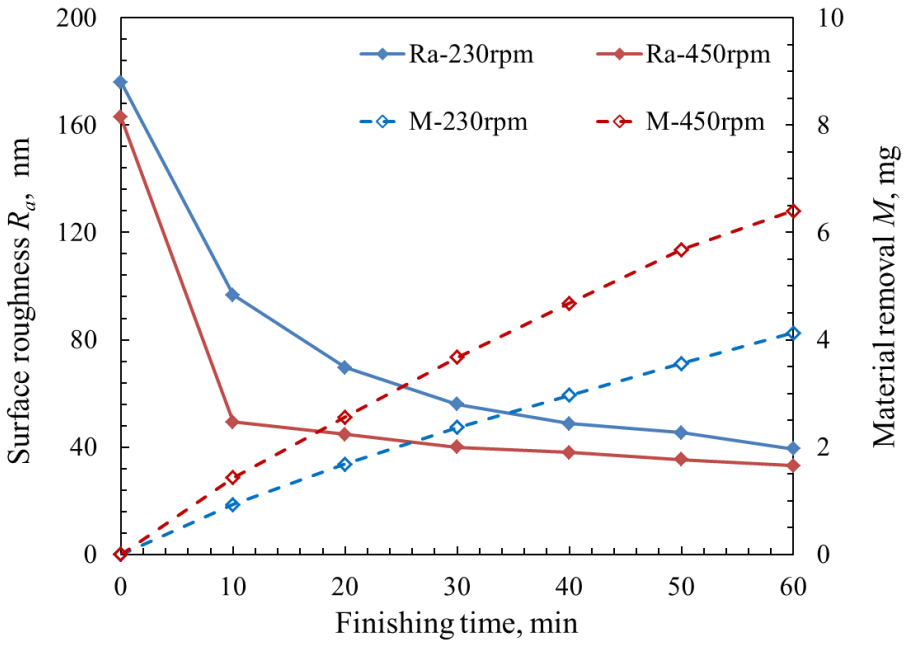

Fig. 4.3.2 Change in surface roughness R_a and material removal M as a function of MAF processing time under different rotational speed of compound machining tool conditions

4.4 Investigation of the working gap

Through investigating the rotational speed, the rotational speed is decided as 450 rpm. Surface roughness of workpiece is measured at approximate 160 ~ 220 nm R_a as an original roughness before machining. The finishing time is selected as per 10 min (for six times) to measure and compare the finished surface differences. The rotational speed of compound machining tool and feeding speed of X-Y stage are respectively adjusted to 450 rpm and 5 mm/s. Finally, we will investigate the working gap. The working gap is selected at 1 mm and 2 mm. Table 4.4.1 shows the detailed experimental condition for investigating the working gap.

Table 4.4.1 Experimental condition for investigating the working gap

Workpiece	SUS304 plane (100 × 100 × 1 mm)
Original surface roughness	160 ~ 220 nm
Compound magnetic abrasives	Electrolytic iron powder : 149 μm in mean diameter Abrasive grains: # 8000 Oily grinding fluid: 2 ml
Workinge gap	1 mm & 2 mm
Feeding speed	5 mm/s
Rotational speed	450 rpm
MAF test time	60 min

The non-contact 3D measurement and images of finished surface in various working gap conditions after 60 min MAF process obtained through a non-contact optical profiling microscope is shown in Figure 4.4.1. Through comparing the finished surface profile in various working gap cases, it is recognized that the surface roughness R_a at 1 mm working gap case is remarkably smaller than the surface roughness R_a at 2 mm working gap case at 60 min tests. Through comparing the images of finished surface in various working gap cases, it also can be recognized that the finished surface accuracy at 1 mm working gap

case is obviously better than the finished surface accuracy at 2 mm working gap case at 60 min tests. Furthermore, it can be clearly found that the initial hairlines of finished surface have almost completely been removed at 1 mm working gap condition through obtaining non-contact 3D measurement and SEM photographs. However, a lot of concave portions still exist on the finished surface at 2 mm working gap condition.

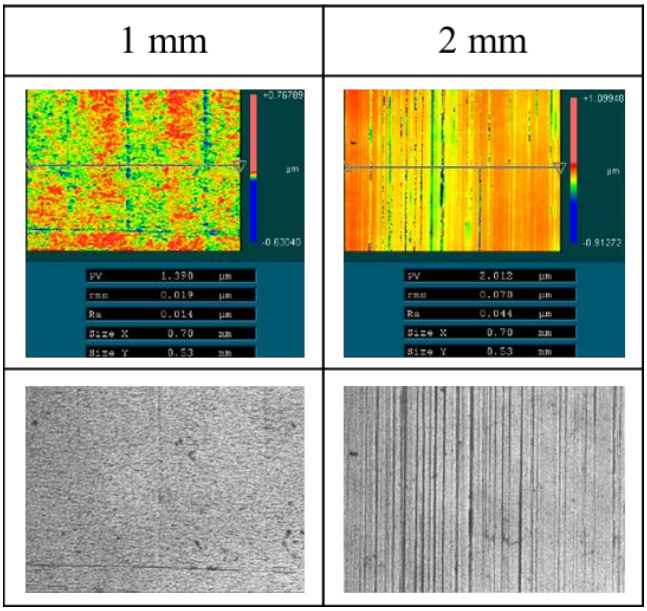

Fig. 4.4.1 Non-contact 3D measurement and SEM photographs of finished surface in various working gap conditions after 60 min MAF process

In order to quantitatively compare and estimate the difference of surface roughness R_a and material removal weight M under different finishing times of traditional MAF process (per 10 min). The surface roughness R_a is estimated through using a contact optical profiling microscope. The change in material removal weight M is measured through a high-precision electronic scale. Figure 4.4.2 shows the change in surface roughness R_a and material removal weight M as a function of MAF processing time under different working gap conditions. The surface roughness R_a is an average surface roughness value of three observed locations. Through quantitatively compare under different working gap conditions, it is noted that the surface roughness R_a at 1 mm working gap case is remarkably smaller than the surface roughness R_a at 2 mm working gap case. Furthermore,

the change in material removal weight M at 1 mm working gap case is also much more than the change in material removal weight M at 2 mm working gap case.

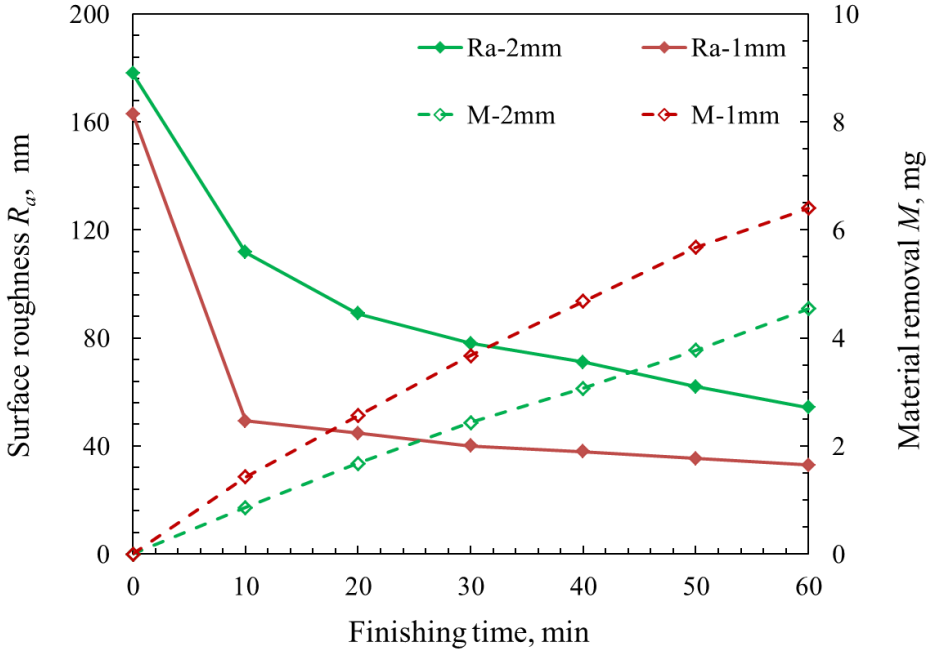

Fig. 4.4.2 Change in surface roughness R_a and material removal M as a function of MAF processing time under different working gap conditions

4.5 Investigation of the compound magnetic abrasives

Based on the above studies, most of machining parameters studies has been completed. Finally, we will investigate the effect of different sizes of electrolytic iron powder mixed with different sizes of abrasive grains.

Table 4.5.1 shows the detailed experimental condition for investigating the 75 μm in mean diameter of iron powder mixed with different sizes of abrasive grains. The 75 μm in mean diameter of iron powder respectively mixes with # 4000 abrasive grains, # 6000 abrasive grains, # 8000 abrasive grains and # 10000 abrasive grains. The amount of electrolytic iron powder is 0.8 g, the amount of WA abrasive grains is 0.2 g. The finishing time is selected as per 10 min (for six times) to measure and compare the finished surface differences. In order to ensure machining power to be adequate, the working gap is adjusted to 1 mm. For obtaining a higher surface accuracy and higher efficiency, the rotational speed of compound machining tool and feeding speed of X-Y stage are respectively adjusted to 450 rpm and 5 mm/s.

Table 4.5.1 Experimental condition for investigating the 75 μm in mean diameter of iron powder mixed with different sizes of abrasive grains

Workpiece	SUS304 plane (100 × 100 × 1 mm)
Original surface roughness	160 ~ 220 nm
Compound magnetic abrasives	Electrolytic iron powder : 75 μm in mean diameter Abrasive grains: # 4000, # 6000, # 8000, # 10000 Oily grinding fluid: 2 ml
Workinge gap	1 mm
Feeding speed	5 mm/s
Rotational speed	450 rpm
MAF test time	60 min

Figure 4.5.1 shows the non-contact 3D measurement of finished surface under the 75 μm in mean diameter of iron powder mixed with different sizes of abrasive grains conditions after 60 min MAF process obtained through a non-contact optical profiling microscope. Through comparing the finished surface profile under the 75 μm in mean diameter of iron powder mixed with different sizes of abrasive grains cases, it is recognized that the surface roughness R_a under 75 μm in mean diameter of iron powder mixed with # 10000 abrasive grains case is obviously smaller than the surface roughness R_a under 75 μm in mean diameter of iron powder mixed with # 6000 and # 8000 abrasive grains conditions. Moreover, the surface roughness R_a under 75 μm in mean diameter of iron powder mixed with # 10000 abrasive grains case is slightly smaller than the surface roughness R_a under 75 μm in mean diameter of iron powder mixed with # 4000 abrasive grains conditions. Through comparing the SEM photographs of finished surface under the 75 μm in mean diameter of iron powder mixed with different sizes of abrasive grains cases, it also can be recognized that the finished surface accuracy under 75 μm in mean diameter of iron powder mixed with # 4000 and # 10000 abrasive grains conditions is remarkably better than the finished surface accuracy under 75 μm in mean diameter of iron powder mixed with # 6000 and # 8000 abrasive grains conditions.

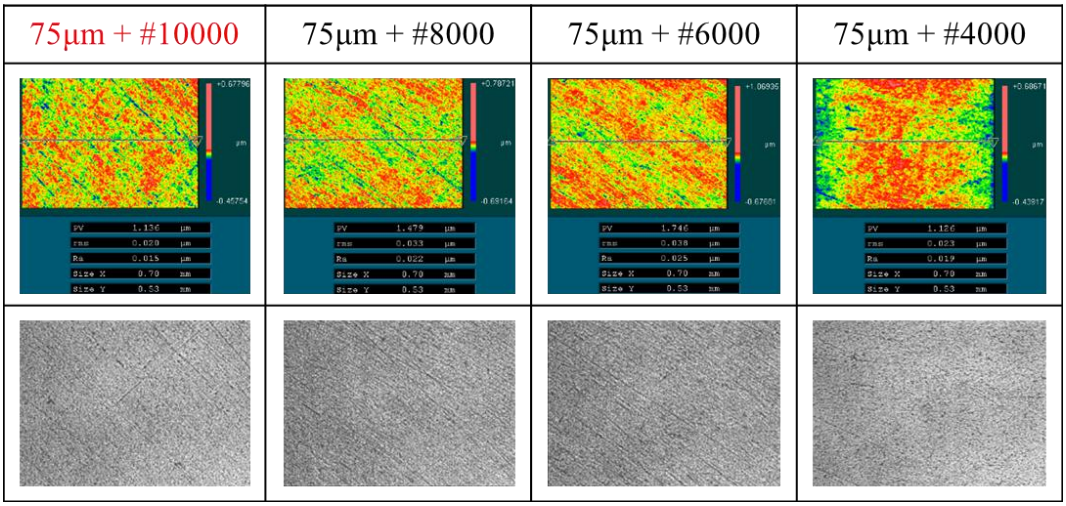

Fig. 4.5.1 Non-contact 3D measurement and SEM photographs of finished surface under the 75 μm in mean diameter of iron powder mixed with different sizes of abrasive grains conditions after 60 min MAF process

In order to quantitatively compare and estimate the difference of surface roughness R_a and material removal weight M under different finishing times of traditional MAF process (per 10 min). The surface roughness R_a is estimated through using a contact optical profiling microscope. The change in material removal weight M is measured through a high-precision electronic scale. Figure 4.5.2 shows the change in surface roughness R_a and material removal weight M as a function of MAF processing time under the 75 μm in mean diameter of iron powder mixed with different sizes of abrasive grains conditions. The surface roughness R_a is an average surface roughness value of three observed locations. Through quantitatively compare under the 75 μm in mean diameter of iron powder mixed with different sizes of abrasive grains conditions, it is noted that the surface roughness R_a under 75 μm in mean diameter of iron powder mixed with # 10000 abrasive grains conditions is remarkably smaller than the surface roughness R_a under 75 μm in mean diameter of iron powder mixed with other abrasive grains conditions.

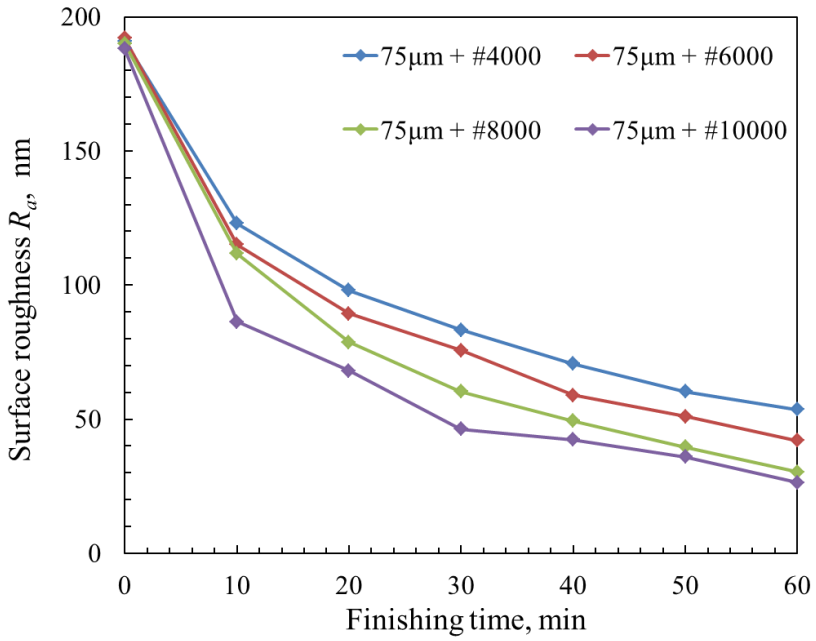

Fig. 4.5.2 Change in surface roughness R_a and material removal M as a function of MAF processing time under the 75 μm in mean diameter of iron powder mixed with different sizes of abrasive grains conditions

Table 4.5.2 shows the detailed experimental condition for investigating the 149 μm in mean diameter of iron powder mixed with different sizes of abrasive grains. The 149 μm in mean diameter of iron powder respectively mixes with # 4000 abrasive grains, # 6000 abrasive grains, # 8000 abrasive grains and # 10000 abrasive grains. The amount of electrolytic iron powder is 0.8 g, the amount of WA abrasive grains is 0.2 g. The finishing time is selected as per 10 min (for six times) to measure and compare the finished surface differences. In order to ensure machining power to be adequate, the working gap is adjusted to 1 mm. For obtaining a higher surface accuracy and higher efficiency, the rotational speed of compound machining tool and feeding speed of X-Y stage are respectively adjusted to 450 rpm and 5 mm/s.

Table 4.5.2 Experimental condition for investigating the 149 μm in mean diameter of iron powder mixed with different sizes of abrasive grains

Workpiece	SUS304 plane (100 × 100 × 1 mm)
Original surface roughness	160 ~ 220 nm
Compound magnetic abrasives	Electrolytic iron powder : 149 μm in mean diameter Abrasive grains: # 4000, # 6000, # 8000, # 10000 Oily grinding fluid: 2 ml
Workinge gap	1 mm
Feeding speed	5 mm/s
Rotational speed	450 rpm
MAF test time	60 min

Figure 4.5.3 shows the non-contact 3D measurement of finished surface under the 149 μm in mean diameter of iron powder mixed with different sizes of abrasive grains conditions after 60 min MAF process obtained through a non-contact optical profiling microscope. Through comparing the finished surface profile under the 149 μm in mean diameter of iron powder mixed with different sizes of abrasive grains cases, it is recognized that the surface roughness R_a under 149 μm in mean diameter of iron powder

mixed with # 8000 abrasive grains case is obviously smaller than the surface roughness R_a under 149 μm in mean diameter of iron powder mixed with # 4000 abrasive grains conditions. Moreover, the surface roughness R_a under 149 μm in mean diameter of iron powder mixed with # 8000 abrasive grains case is slightly smaller than the surface roughness R_a under 149 μm in mean diameter of iron powder mixed with # 10000 and # 6000 abrasive grains conditions. Through comparing the SEM photographs of finished surface under the 149 μm in mean diameter of iron powder mixed with different sizes of abrasive grains cases, it also can be recognized that the finished surface accuracy under 149 μm in mean diameter of iron powder mixed with # 10000 and # 8000 abrasive grains conditions is remarkably better than the finished surface accuracy under 149 μm in mean diameter of iron powder mixed with # 6000 and # 4000 abrasive grains conditions.

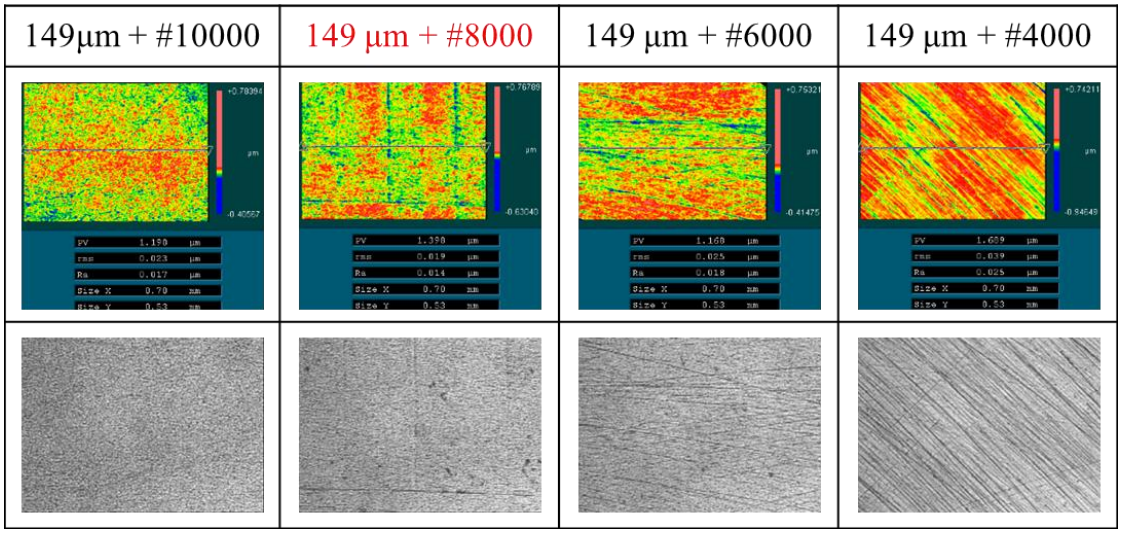

Fig. 4.5.3 Non-contact 3D measurement and SEM photographs of finished surface under the 149 μm in mean diameter of iron powder mixed with different sizes of abrasive grains conditions after 60 min MAF process

In order to quantitatively compare and estimate the difference of surface roughness R_a and material removal weight M under different finishing times of traditional MAF process (per 10 min). The surface roughness R_a is estimated through using a contact optical profiling microscope. The change in material removal weight M is measured through a

high-precision electronic scale. Figure 4.5.4 shows the change in surface roughness R_a and material removal weight M as a function of MAF processing time under the 149 μm in mean diameter of iron powder mixed with different sizes of abrasive grains conditions. The surface roughness R_a is an average surface roughness value of three observed locations. Through quantitatively compare under the 149 μm in mean diameter of iron powder mixed with different sizes of abrasive grains conditions, it is noted that the surface roughness R_a under 149 μm in mean diameter of iron powder mixed with # 8000 abrasive grains conditions is remarkably smaller than the surface roughness R_a under 149 μm in mean diameter of iron powder mixed with other abrasive grains conditions.

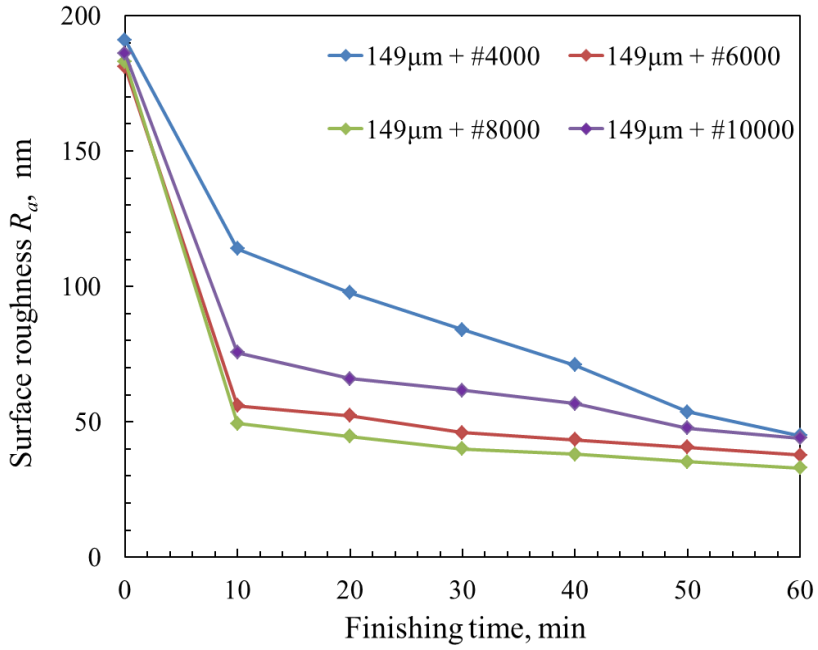

Fig. 4.5.4 Change in surface roughness R_a and material removal M as a function of MAF processing time under the 149 μm in mean diameter of iron powder mixed with different sizes of abrasive grains conditions

Table 4.5.3 shows the detailed experimental condition for investigating the 330 μm in mean diameter of iron powder mixed with different sizes of abrasive grains. The 330 μm in mean diameter of iron powder respectively mixes with # 4000 abrasive grains, # 6000 abrasive grains, # 8000 abrasive grains and # 10000 abrasive grains. The amount of

electrolytic iron powder is 0.8 g, the amount of WA abrasive grains is 0.2 g. The finishing time is selected as per 10 min (for six times) to measure and compare the finished surface differences. In order to ensure machining power to be adequate, the working gap is adjusted to 1 mm. For obtaining a higher surface accuracy and higher efficiency, the rotational speed of compound machining tool and feeding speed of X-Y stage are respectively adjusted to 450 rpm and 5 mm/s.

Table 4.5.3 Experimental condition for investigating the 330 μm in mean diameter of iron powder mixed with different abrasive grains

Workpiece	SUS304 plane (100 × 100 × 1 mm)
Original surface roughness	160 ~ 220 nm
Compound magnetic abrasives	Electrolytic iron powder : 330 μm in mean diameter Abrasive grains: # 4000, # 6000, # 8000, # 10000 Oily grinding fluid: 2 ml
Workinge gap	1 mm
Feeding speed	5 mm/s
Rotational speed	450 rpm
MAF test time	60 min

Figure 4.5.5 shows the non-contact 3D measurement of finished surface under the 330 μm in mean diameter of iron powder mixed with different sizes of abrasive grains conditions after 60 min MAF process obtained through a non-contact optical profiling microscope. Through comparing the finished surface profile under the 330 μm in mean diameter of iron powder mixed with different sizes of abrasive grains cases, it is recognized that the surface roughness R_a under 330 μm in mean diameter of iron powder mixed with # 4000 abrasive grains case is obviously smaller than the surface roughness R_a under 330 μm in mean diameter of iron powder mixed with other abrasive grains conditions. Through comparing the SEM photographs of finished surface under the 330 μm in mean diameter of iron powder mixed with different sizes of abrasive grains cases, it also

can be recognized that the finished surface accuracy under 330 μm in mean diameter of iron powder mixed with # 4000 and # 10000 abrasive grains conditions is remarkably better than the finished surface accuracy under 330 μm in mean diameter of iron powder mixed with # 6000 and # 8000 abrasive grains conditions.

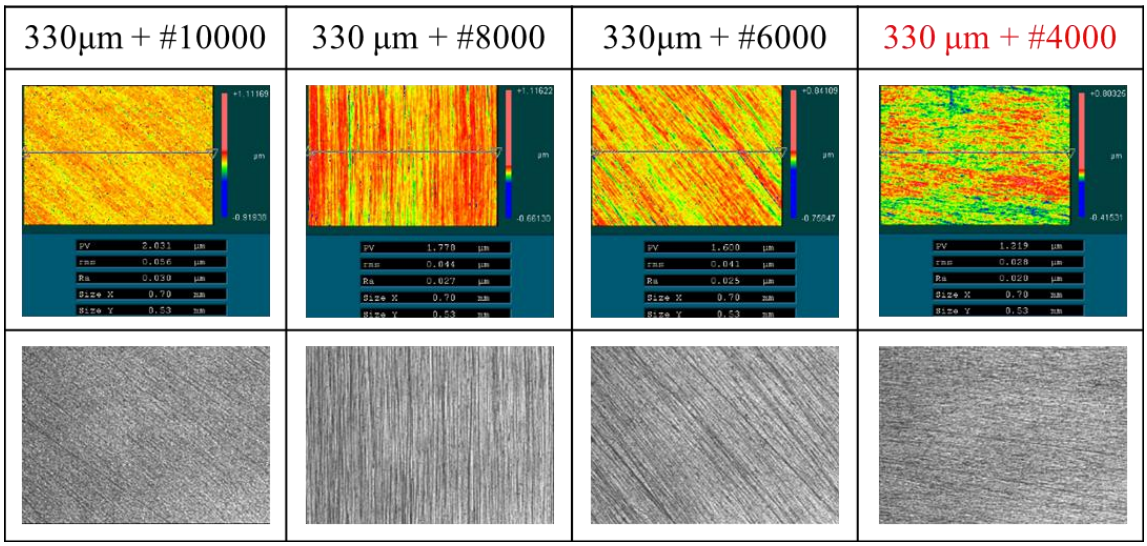

Fig. 4.5.5 Non-contact 3D measurement and SEM photographs of finished surface under the 330 μm in mean diameter of iron powder mixed with different sizes of abrasive grains conditions after 60 min MAF process

In order to quantitatively compare and estimate the difference of surface roughness R_a and material removal weight M under different finishing times of traditional MAF process (per 10 min). The surface roughness R_a is estimated through using a contact optical profiling microscope. The change in material removal weight M is measured through a high-precision electronic scale. Figure 4.5.6 shows the change in surface roughness R_a and material removal weight M as a function of MAF processing time under the 330 μm in mean diameter of iron powder mixed with different sizes of abrasive grains conditions. The surface roughness R_a is an average surface roughness value of three observed locations. Through quantitatively compare under the 330 μm in mean diameter of iron powder mixed with different sizes of abrasive grains conditions, it is noted that the surface roughness R_a under 330 μm in mean diameter of iron powder mixed with # 4000 abrasive grains

conditions is remarkably smaller than the surface roughness R_a under 330 μm in mean diameter of iron powder mixed with other abrasive grains conditions.

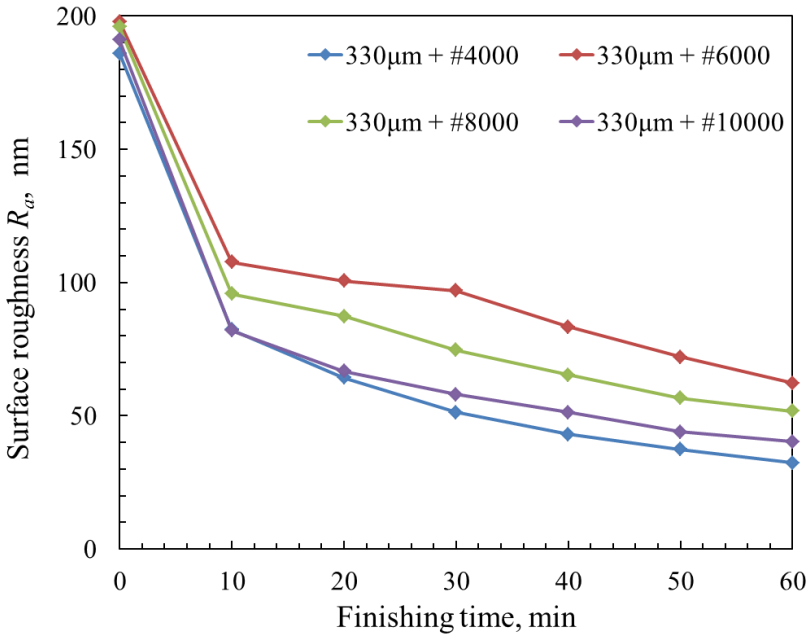

Fig. 4.5.6 Change in surface roughness R_a and material removal M as a function of MAF processing time under the 330 μm in mean diameter of iron powder mixed with different sizes of abrasive grains conditions

Finally, we choose the best experimental results from each of above experimental results to compare surface profile shown in Figure 4.5.7. Through comparing the finished surface profile, it is recognized that the surface roughness R_a under 149 μm in mean diameter of iron powder mixed with # 8000 abrasive grains case is obviously smaller than the surface roughness R_a under the other two conditions. The surface roughness R_a under 75 μm in mean diameter of iron powder mixed with # 10000 abrasive grains case is slightly smaller than the surface roughness R_a under 330 μm in mean diameter of iron powder mixed with # 4000 abrasive grains case. Through comparing the SEM photographs of finished surface, it also can be recognized that the finished surface accuracy under 149 μm in mean diameter of iron powder mixed with # 8000 abrasive grains case is remarkably better than the finished surface accuracy under the other two conditions. The finished surface accuracy

under 75 μm in mean diameter of iron powder mixed with # 10000 abrasive grains case is a little better than the finished surface accuracy under 330 μm in mean diameter of iron powder mixed with # 4000 abrasive grains case.

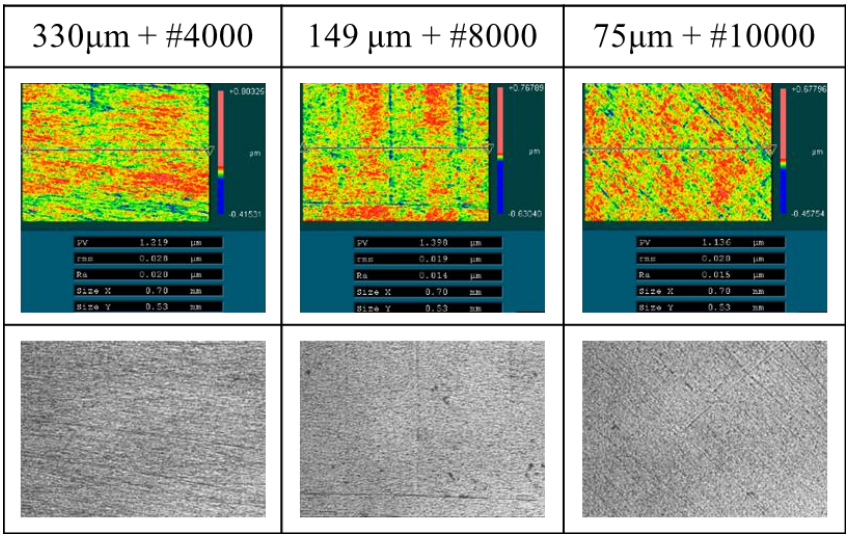

Fig. 4.5.7 Non-contact 3D measurement and SEM photographs of finished surface in various compound magnetic abrasives conditions after 60 min MAF process

Figure 4.5.8 shows the change in surface roughness R_a and material removal M as a function of MAF processing time under different compound magnetic abrasives conditions. Through comparing the experimental results, it is noted that the surface roughness R_a under 149 μm in mean diameter of iron powder mixed with # 8000 abrasive grains case is obviously smaller than the surface roughness R_a under the other two conditions before 50 min finishing time. The surface roughness R_a under 75 μm in mean diameter of iron powder mixed with # 10000 abrasive grains case is smaller than the surface roughness R_a under the other two conditions after 50 min finishing time. Moreover, the change in material removal weight M is almost same under the three kinds of conditions before 40 min finishing time. The change in material removal weight M under 75 μm in mean diameter of iron powder mixed with # 10000 abrasive grains case is much more than the change in material removal weight M under the other two conditions after 40 min finishing time.

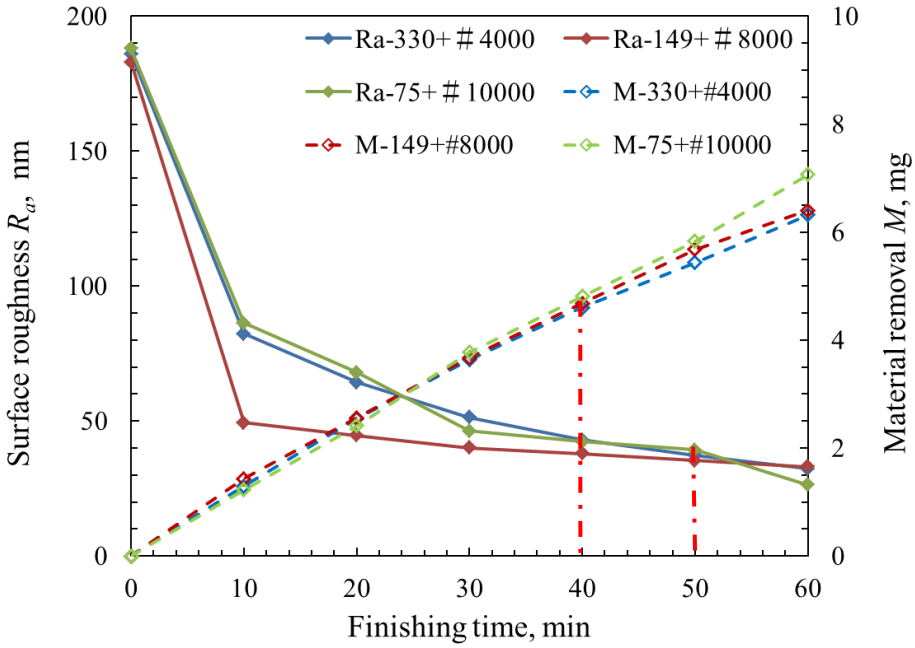

Fig. 4.5.8 Change in surface roughness R_a and material removal M as a function of MAF processing time under different compound magnetic abrasives conditions

4.6 Multi-stage magnetic abrasive finishing

Based on the abovementioned studies of processing parameters, the working gap is set at 1 mm, the feeding speed of X-Y stage is adjusted to 5 mm/s and the rotational speed of compound machining tool is adjusted to 450 rpm. Table 4.6.1 shows the experimental conditions for investigating the multi-stage magnetic abrasive finishing. Surface roughness of workpiece is measured at approximate 160 ~ 220 nm R_a as an original roughness before machining. The finishing time is selected as per 10 min (for six times) to measure and compare the finished surface differences. The electrolytic iron powder is selected at 30 μm, 75 μm, 149 μm, 330 μm in mean diameter, the abrasive grains is selected at # 4000, # 6000, # 8000, # 10000. The amount ratio of electrolytic iron powder and abrasive grains is 4:1. The amount of electrolytic iron powder is respectively 0.8 g and the amount of WA abrasive grains is 0.2 g.

Table 4.6.1 Experimental condition for investigating the multi-stage magnetic abrasive finishing

Workpiece	SUS304 plane (100 × 100 × 1 mm)
Original surface roughness	160 ~ 220 nm
Compound magnetic abrasives	Electrolytic iron powder : 30 μm,75 μm, 149 μm, 330 μm in mean diameter Abrasive grains: # 4000, # 6000, # 8000, # 10000 Oily grinding fluid: 2 ml
Workinge gap	1 mm
Feeding speed	5 mm/s
Rotational speed	450 rpm
MAF test time	60 min

We mainly investigate combination of electrolytic iron powder and abrasive grains during the multi-stage magnetic abrasive finishing. There are four kinds of combinations of

electrolytic iron powder and abrasive grains to investigate multi-stage magnetic abrasive finishing. The detailed combinations of electrolytic iron powder and abrasive grains are shown in Table 4.6.2. In the No. 1, 330 μm electrolytic iron powder and #4000 abrasive grains are used in the first step (first 10 finishing time); 330 μm electrolytic iron powder and #4000 abrasive grains are used in the second step (second 10 finishing time); 149 μm electrolytic iron powder and #8000 abrasive grains are used in the third step (third 10 finishing time); 149 μm electrolytic iron powder and #8000 abrasive grains are used in the fourth step (fourth 10 finishing time); 75 μm electrolytic iron powder and #10000 abrasive grains are used in the fifth step (fifth 10 finishing time); 75 μm electrolytic iron powder and #10000 abrasive grains are used in the sixth step (sixth 10 finishing time). In the No. 2, 330 μm electrolytic iron powder and #4000 abrasive grains are used in the first step (first 10 finishing time); 149 μm electrolytic iron powder and #8000 abrasive grains are used in the second step (second 10 finishing time); 149 μm electrolytic iron powder and #8000 abrasive grains are used in the third step (third 10 finishing time); 75 μm electrolytic iron powder and #10000 abrasive grains are used in the fourth step (fourth 10 finishing time); 75 μm electrolytic iron powder and #10000 abrasive grains are used in the fifth step (fifth 10 finishing time); 30 μm electrolytic iron powder and #20000 abrasive grains are used in the sixth step (sixth 10 finishing time). In the No. 3, 149 μm electrolytic iron powder and #8000 abrasive grains are used in the first step (first 10 finishing time); 149 μm electrolytic iron powder and #8000 abrasive grains are used in the second step (second 10 finishing time); 75 μm electrolytic iron powder and #10000 abrasive grains are used in the third step (third 10 finishing time); 75 μm electrolytic iron powder and #10000 abrasive grains are used in the fourth step (fourth 10 finishing time); 30 μm electrolytic iron powder and #20000 abrasive grains are used in the fifth step (fifth 10 finishing time); 30 μm electrolytic iron powder and #20000 abrasive grains are used in the sixth step (sixth 10 finishing time). In the No. 4, 330 μm electrolytic iron powder and #4000 abrasive grains are used in the first step (first 10 finishing time); 149 μm electrolytic iron powder and #8000 abrasive grains are used in the second step (second 10 finishing time); 75 μm

electrolytic iron powder and #10000 abrasive grains are used in the third step (third 10 finishing time); 75 μm electrolytic iron powder and #10000 abrasive grains are used in the fourth step (fourth 10 finishing time); 30 μm electrolytic iron powder and #20000 abrasive grains are used in the fifth step (fifth 10 finishing time); 30 μm electrolytic iron powder and #20000 abrasive grains are used in the sixth step (sixth 10 finishing time).

Table. 6.2 Combinations of electrolytic iron powder and abrasive grains

	First step	Second step	Third step	Fourth step	Fifth step	Sixth step
No. 1	330 μm+ #4000	330 μm+ #4000	149 μm+ #8000	149 μm+ #8000	75 μm+ #10000	75 μm+ #10000
No. 2	330 μm+ #4000	149 μm+ #8000	149 μm+ #8000	75 μm+ #10000	75 μm+ #10000	30 μm+ #20000
No. 3	149 μm+ #8000	149 μm+ #8000	75 μm+ #10000	75 μm+ #10000	30 μm+ #20000	30 μm+ #20000
No. 4	330 μm+ #4000	149 μm+ #8000	75 μm+ #10000	75 μm+ #10000	30 μm+ #20000	30 μm+ #20000

Figure 4.6.1 shows the non-contact 3D measurement and SEM photographs of finished surface in multi-stage magnetic abrasive finishing after 60 min MAF process. Compared with the finished surface profile of original workpiece, it is recognized that the surface roughness R_a during No. 1 and No. 2 multi-stage magnetic abrasive finishing is obviously smaller than the surface roughness R_a during No. 3 and No. 4 multi-stage magnetic abrasive finishing. Moreover, the surface roughness R_a during No. 1 multi-stage magnetic abrasive finishing is slightly smaller than the surface roughness R_a during No. 2 multi-stage magnetic abrasive finishing. Through comparing the SEM photographs of finished surface, it also can be recognized that the finished surface accuracy during No. 1 and No. 2 multi-stage magnetic abrasive finishing is remarkably better than the finished surface accuracy during No. 3 and No. 4 multi-stage magnetic abrasive finishing.

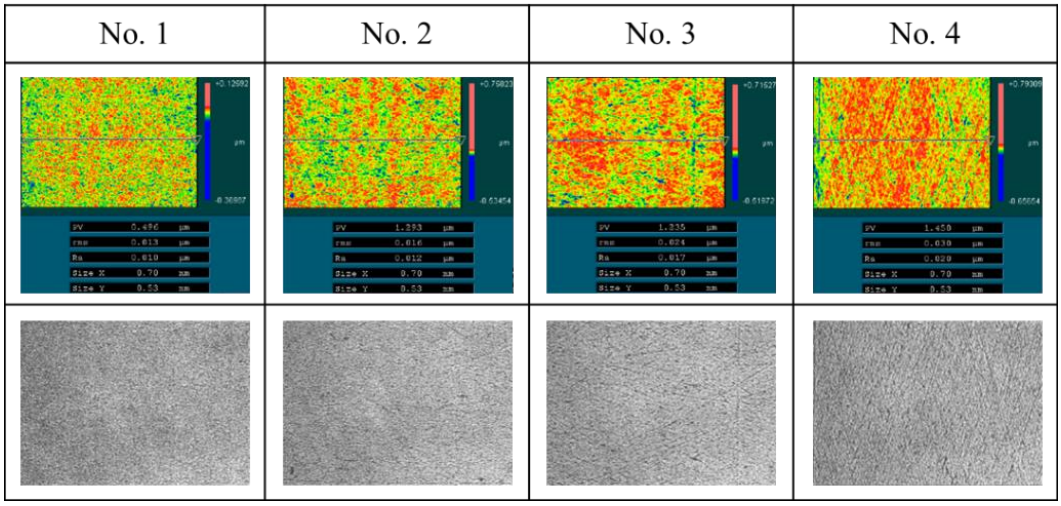

Fig. 4.6.1 Non-contact 3D measurement and SEM photographs of finished surface in multi-stage magnetic abrasive finishing after 60 min MAF process

Figure 4.6.2 shows the change in surface roughness R_a as a function of MAF processing time in multi-stage magnetic abrasive finishing. Through comparing four kinds of multi-stage magnetic abrasive finishing, it is noted that the surface roughness R_a during No. 1 multi-stage magnetic abrasive finishing is obviously smaller than the surface roughness R_a during the other three conditions. The surface roughness R_a during No. 2 multi-stage magnetic abrasive finishing is approximately same as the surface roughness R_a during No. 4 multi-stage magnetic abrasive finishing. The surface roughness R_a during No. 3 multi-stage magnetic abrasive finishing is biggest during the four kinds of multi-stage magnetic abrasive finishing.

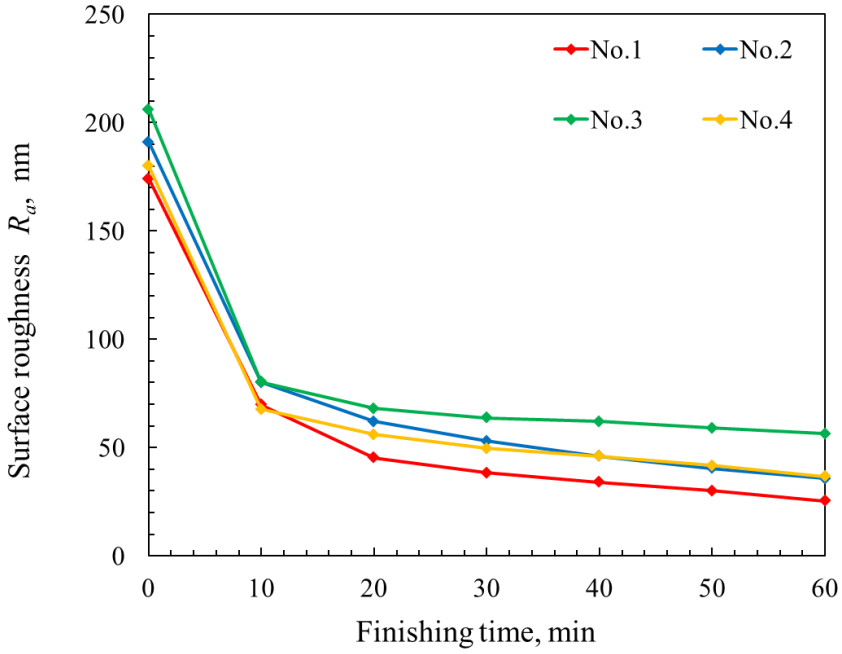

Fig. 4.6.2 Change in surface roughness R_a as a function of MAF processing time in multi-stage magnetic abrasive finishing

4.7 Conclusions

In this chapter, the mechanical finishing characteristics of MAF process were firstly investigated in order to explore the optimal mechanical finishing conditions of the electrolytic magnetic compound machining tool. The main conclusions were shown as follows:

(1) Through quantitatively compare under different amount of iron powder and WA abrasive grain conditions, it is noted that 1 g mixed magnetic abrasives is the most suitable amount.

(2) It can be approximately regarded that the different feeding speed conditions have little effect on both the change in surface roughness R_a and material removal M through measured results and observed images.

(3) Through quantitatively compare under different rotational speed of compound machining tool conditions, it can be recognized that the higher surface accuracy can be obtained at relatively higher rotational speed (450 rpm) condition.

(4) Through quantitatively compare under different working gap conditions, it can be recognized that the higher surface accuracy can be obtained at relatively smaller working gap (1 mm) condition.

(5) The combination of 149 μm iron powder mixed with #8000 WA particles can be considered as the optimal mixed magnetic abrasive through the experimental results.

(6) Through comparing four kinds of multi-stage magnetic abrasive finishing, it is noted that the surface roughness R_a in the condition of No. 1 multi-stage magnetic abrasive finishing is obviously smaller than the surface roughness R_a during the other three conditions.

Chapter 5 Study on finishing stainless steel SUS304 plane workpiece finishing by using electrolytic magnetic compound machining tool in electrolytic process

Through the foregoing narrative, it is easy to see that electrolytic process plays an extremely important role in EMAF process. The main role of electrolytic process is rapidly decreasing surface hardness through the formed passive films, and the initial hairline of surface can be reduced to achieve finitely planarization [1, 2]. Hence, the investigations of electrolytic process were also necessarily carried out before researching EMAF process. The working voltage, electrolyte concentration, working gap, rotational speed of tool and feeding speed of X-Y stage were emphatically investigated [3]. Due to the unstable contact between carbon brush and copper ring when the spindle rotates with a high speed, resulting in the electrolytic current instability. In order to solve this problem, from this chapter, the electrodes connected to the negative of DC constant voltage power through a thin copper sheet with elasticity instead of the previously mentioned carbon brush.

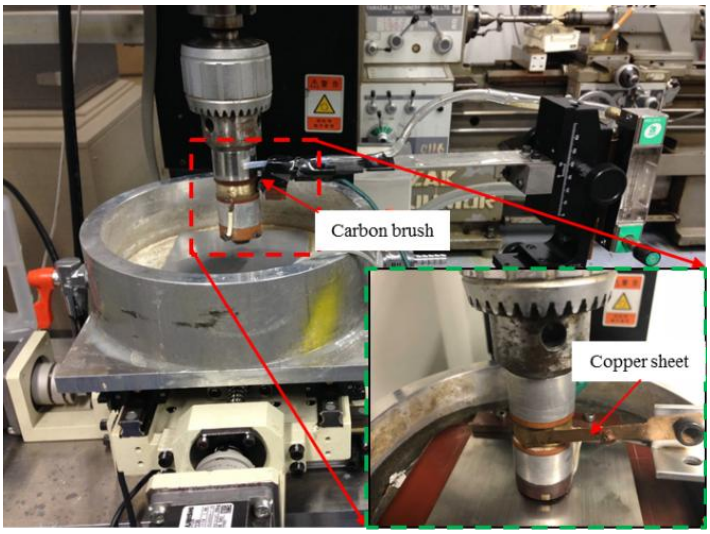

Fig. 5 Improved experimental setup

Chapter 5 Study on finishing stainless steel SUS304 plane workpiece finishing by using electrolytic magnetic compound machining tool in electrolytic process

5.1 Investigation of electrolytic process characteristics of voltage

Fristly, we focused on investigating the effect of working voltage on change in surface roughness and hardness. Table 5.1 shows experimental condition for investigating electrolytic process characteristics of different voltage. The surface roughness R_a of workpiece is measured at approximate 0.16 ~ 0.2 μm as an original roughness. The working gap is adjusted to 1 mm, the rotational speed of machining tool is selected at 450 rpm, the feeding speed of X-Y stage is adjusted to 5 mm/s, and the electrolyte concentration is respectively selected as 20 wt%. The working voltage is respectively selected at 8 V, 10 V and 12 V. The finishing time of electrolytic process is respectively selected at 2 min, 4 min, 6 min, 8 min and 10 min.

Table 5.1 Experimental condition for investigating electrolytic process characteristics of working voltage

Workpiece	SUS304 plane (100 × 100 × 1 mm)
Original surface roughness	160 ~ 200 nm
Working voltage	8 V, 10 V, 12 V
Electrolyte concentration	20 wt%
Workinge gap	1 mm
Feeding speed	5 mm/s
Rotational speed	450 rpm
MAF test time	2, 4, 6, 8, 10 min

Figure 5.1.1 shows the change in surface roughness R_a and material removal M as a function of electrolytic processing time under various voltage conditions. Through

quantitatively compare change in surface roughness R_a and material removal M under various voltage conditions, it is noted that the surface roughness R_a at 12 V voltage case is obviously smaller than the surface roughness R_a under other voltage cases. Moreover, the material removal M at 12 V voltage case is also remarkably more than the material removal M under other voltage cases.

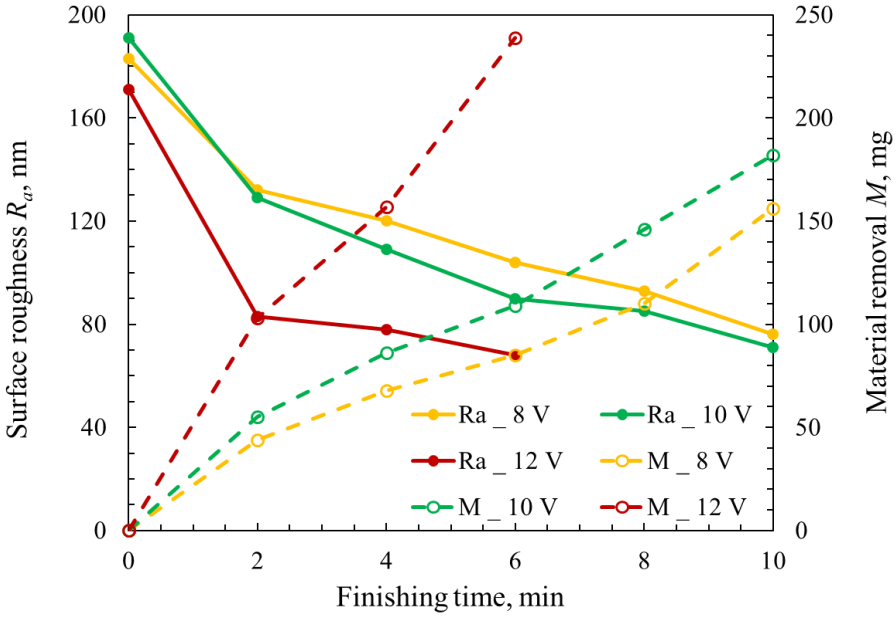

Fig. 5.1.1 Change in surface roughness R_a and material removal M as a function of electrolytic processing time under various voltage conditions

Although the surface roughness can be obtained below 100 nm in electrolytic process, it can be found that the intensity of finished surface is not good since the passive films formed on the finished surface through the exterior photo of finished surface shown in Figure 5.1.2.

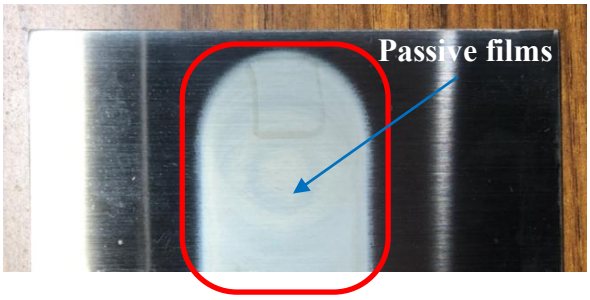

Fig. 5.1.2 Exterior photo of finished surface in electrolytic process

The non-contact 3D measurement and images of finished surface after various electrolytic processing time at 8, 10, 12 V voltage cases obtained through a non-contact optical profiling microscope are respectively shown from Figure 5.1.3 ~ 5.1.5. Through comparing the 3D measurement and images of finished surface under various voltage conditions, it is recognized that the finished surface accuracy at 10 min 8 V voltage condition is better than the finished surface accuracy at other finishing time 8 V voltage conditions; the finished surface accuracy at 10 min 10 V voltage condition is better than the finished surface accuracy at other finishing time 10 V voltage conditions; the finished surface accuracy at 6 min 12 V voltage condition is better than the finished surface accuracy at other finishing time 12 V voltage conditions.

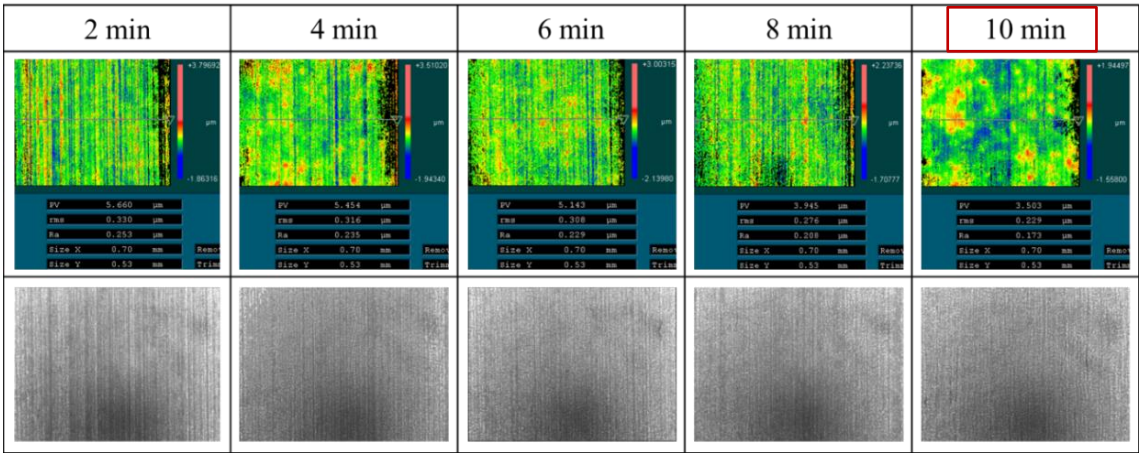

Fig. 5.1.3 Non-contact 3D measurement and images of finished surface after various electrolytic processing time at 8 V voltage case

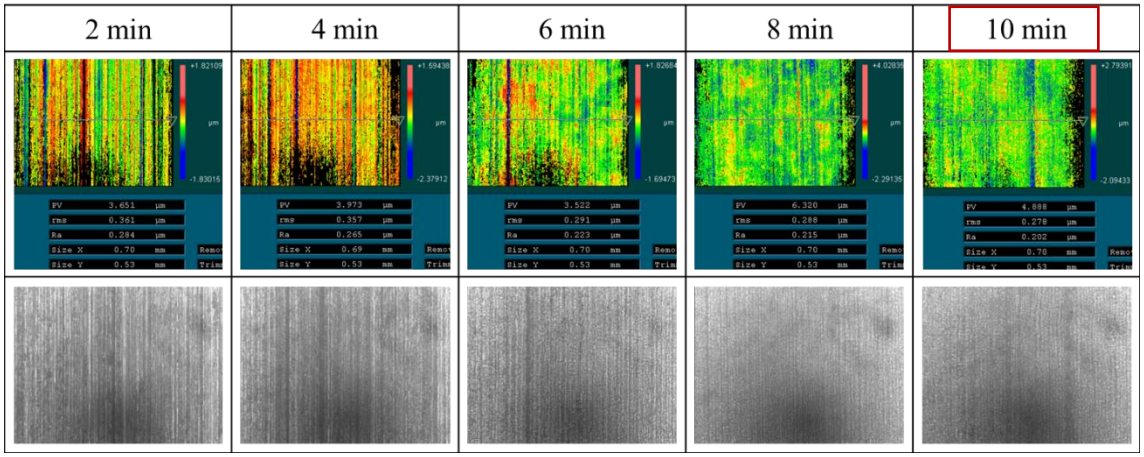

Fig. 5.1.4 Non-contact 3D measurement and images of finished surface after various electrolytic processing time at 10 V voltage case

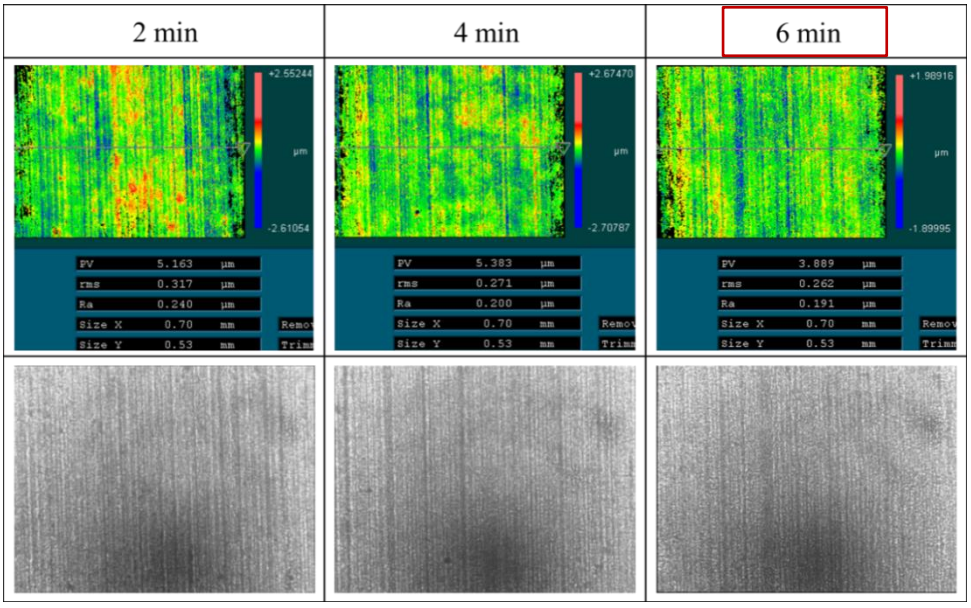

Fig. 5.1.5 Non-contact 3D measurement and images of finished surface after various electrolytic processing time at 12 V voltage case

Figure 5.1.6 shows the change in hardness HV of finished surface after various electrolytic processing time under various voltage cases. Through comparing the change in hardness HV of finished surface after various electrolytic processing time under various

voltage conditions, it can be clearly found that the hardness HV of finished surface decreases with machining time increases under same working voltage; the hardness HV of finished surface decreases with voltage increases at same machining time. Moreover, it is also regarded that the hardness of finished surface can be maximally reduced by 15% under 12 V voltage at 6 min machining time condition. Thence, it can be considered slightly better electrolytic process characteristics of working voltage can be obtained at 12 V voltage case.

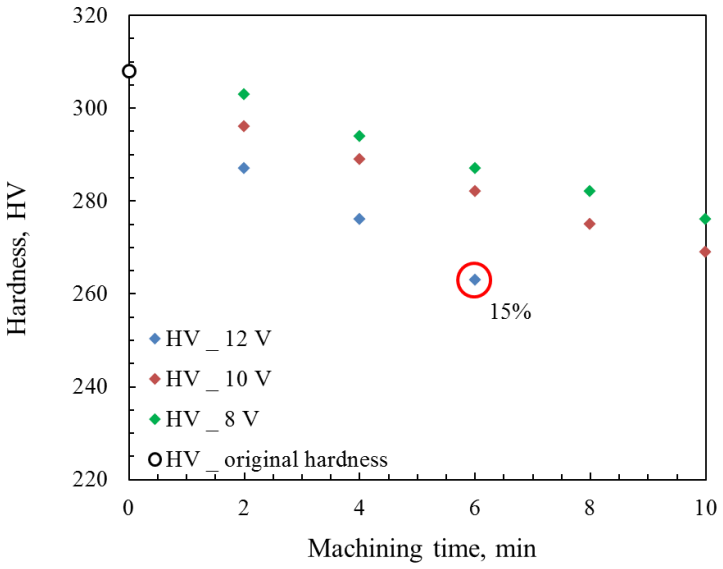

Fig. 5.1.6 Change in hardness HV of finished surface after various electrolytic processing time under various voltage cases

5.2 Investigation of electrolytic process characteristics of electrolyte concentration

Then, we focused on investigating the effect of electrolyte concentration on change in surface roughness and hardness. Table 5.2 shows experimental condition for investigating electrolytic process characteristics of different electrolyte concentration. The surface roughness R_a of workpiece is measured at approximate 0.16 ~ 0.2 μm as an original roughness. The working gap is adjusted to 1 mm, the rotational speed of machining tool is selected at 450 rpm, the feeding speed of X-Y stage is adjusted to 5 mm/s, and the working voltage is selected at 10 V. The electrolyte concentration is respectively selected as 10 wt%, 20 wt% and 30 wt%. The finishing time of electrolytic process is selected at 6 min.

Table 5.2 Experimental condition for investigating electrolytic process characteristics of electrolyte concentration

Workpiece	SUS304 plane (100 × 100 × 1 mm)
Original surface roughness	160 ~ 200 nm
Working voltage	10 V
Electrolyte concentration	10 wt%, 20 wt%, 30 wt%
Workinge gap	1 mm
Feeding speed	5 mm/s
Rotational speed	450 rpm
MAF test time	6 min

Figure 5.2.1 shows the change in surface roughness R_a and material removal M as a function of electrolytic processing time under various electrolyte concentration conditions. Through quantitatively compare change in surface roughness R_a and material removal M

under various electrolyte concentration conditions, it is noted that the surface roughness R_a at 20wt% and 30wt% cases is obviously smaller than the surface roughness R_a under 10wt% case. Moreover, the material removal M at 30wt% case is also remarkably more than the material removal M under other electrolyte concentration cases.

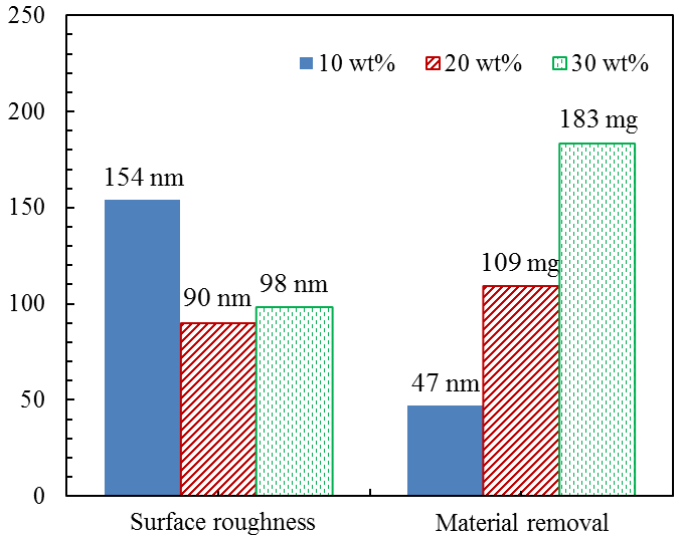

Fig. 5.2.1 Change in surface roughness R_a and material removal M under various electrolyte concentration conditions at 6 min finishing time and 10 V voltage case

The non-contact 3D measurement and images of finished surface under various electrolyte concentration conditions at 6 min finishing time and 10 V voltage case obtained through a non-contact optical profiling microscope is shown in Figure 5.2.2. Through comparing the 3D measurement and images of finished surface under various electrolyte concentration conditions, it is recognized that the finished surface accuracy under 20wt% and 30wt% conditions is obviously better than the finished surface accuracy under 10wt% condition. Moreover, the finished surface accuracy under 30wt% condition is slightly better than the finished surface accuracy under 20wt% condition.

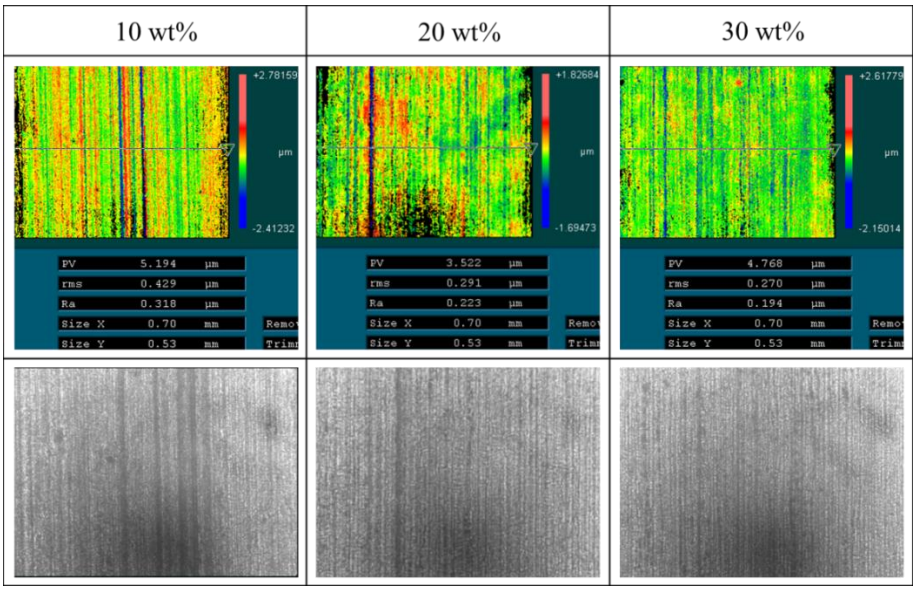

Fig. 5.2.2 Non-contact 3D measurement and images of finished surface under various electrolyte concentration conditions at 6 min finishing time and 10 V voltage case

The change in hardness HV of finished surface with different electrolyte concentration conditions at 6 min finishing time and 10 V voltage case is shown in Figure 5.2.3. Through comparing the change in hardness HV of finished surface under various electrolyte concentration conditions, it is recognized that the hardness HV of finished surface under 30wt% electrolyte concentration condition is smaller than the hardness HV of finished surface under 20wt% and 10wt% electrolyte concentration conditions. Therefore, it can be regarded that the hardness HV decreases with the electrolyte concentration increases through experimental result. In other words, it can be considered slightly better electrolytic process characteristics of electrolyte concentration can be obtained under 20wt% or 30wt% electrolyte concentration case.

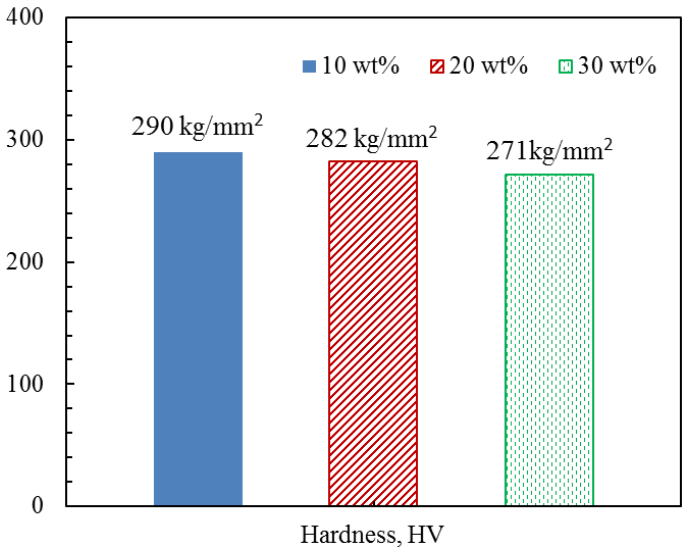

Fig. 5.2.3 Change in hardness of finished surface under various electrolyte concentration conditions at 6 min finishing time and 10 V voltage case

5.3 Investigation of electrolytic process characteristics of working gap

After that, we focused on investigating the effect of working gap on change in surface roughness and hardness. Table 5.3 shows experimental condition for investigating electrolytic process characteristics of different working gap. The surface roughness R_a of workpiece is measured at approximate 0.16 ~ 0.2 μm as an original roughness. The rotational speed of machining tool is selected at 450 rpm, the feeding speed of X-Y stage is adjusted to 5 mm/s, the electrolyte concentration is selected as 20 wt%, and the working voltage is selected at 10 V. The working gap is respectively adjusted to 1 mm, 1.5 mm and 2 mm. The finishing time of electrolytic process is selected at 6 min.

Table 5.3 Experimental condition for investigating electrolytic process characteristics of electrolyte concentration

Workpiece	SUS304 plane (100 × 100 × 1 mm)
Original surface roughness	160 ~ 220 nm
Working voltage	10 V
Electrolyte concentration	20 wt%
Workinge gap	1 mm, 1.5 mm, 2 mm
Feeding speed	5 mm/s
Rotational speed	450 rpm
MAF test time	6 min

Figure 5.3.1 shows the change in surface roughness R_a and material removal M as a function of electrolytic processing time under various working gap conditions. Through quantitatively compare change in surface roughness R_a and material removal M under

various working gap conditions, it is noted that the surface roughness R_a at 1 mm working gap case is obviously smaller than the surface roughness R_a under other two cases. Moreover, the material removal M at 1 mm working gap case is also remarkably more than the material removal M under other working gap cases.

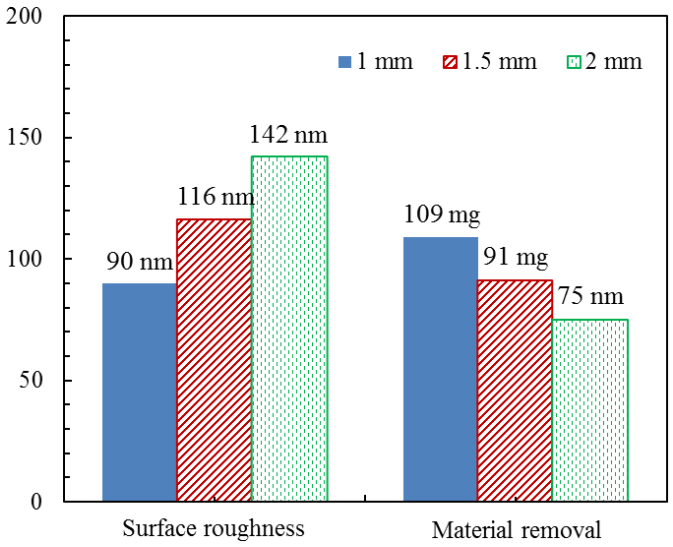

Fig. 5.3.1 Change in surface roughness R_a and material removal M under various working gap conditions at 6 min finishing time and 10 V voltage case

The non-contact 3D measurement and images of finished surface under various working gap conditions at 6 min finishing time and 10 V voltage case obtained through a non-contact optical profiling microscope is shown in Figure 5.3.2. Through comparing the 3D measurement and images of finished surface under various working gap conditions, it is recognized that the finished surface accuracy under 1 mm working gap condition is slightly better than the finished surface accuracy under 1.5 mm and 2 mm working gap conditions.

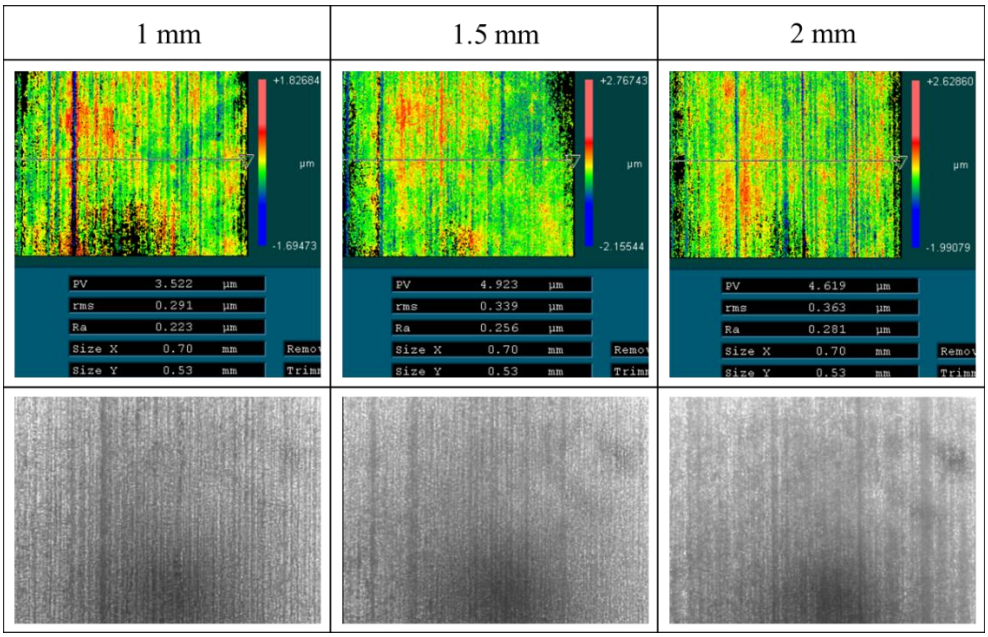

Fig. 5.3.2 Non-contact 3D measurement and images of finished surface under various working gap conditions at 6 min finishing time and 10 V voltage case

The change in hardness HV of finished surface with different working gap conditions at 6 min finishing time and 10 V voltage case is shown in Figure 5.3.3. Through comparing the change in hardness HV of finished surface under various working gap conditions, it is recognized that the hardness HV of finished surface under 1 mm working gap condition is smaller than the hardness HV of finished surface under 1.5 mm and 2 mm working gap conditions. Hence, it can be regarded that the hardness HV decreases with the working gap decreases. In other words, it can be considered slightly better electrolytic process characteristics of working gap can be obtained at 1 mm working gap case.

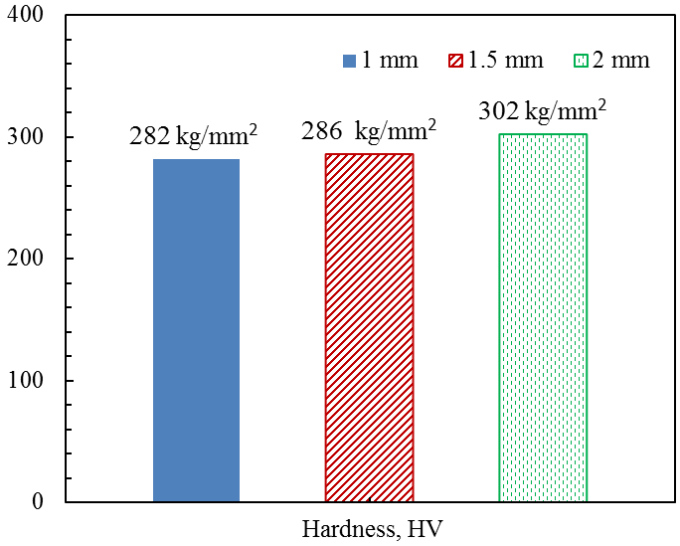

Fig. 5.3.3 Change in hardness of finished surface under various working gap conditions at 6 min finishing time and 10 V voltage case

5.4 Investigation of electrolytic process characteristics of rotational speed

After that, we focused on investigating the effect of rotational speed on change in surface roughness and hardness. Table 5.4 shows experimental condition for investigating electrolytic process characteristics of different rotational speed. The surface roughness R_a of workpiece is measured at approximate 0.16 ~ 0.2 μm as an original roughness. The feeding speed of X-Y stage is adjusted to 5 mm/s, the electrolyte concentration is selected as 20 wt%, the working gap is adjusted to 1 mm, and the working voltage is selected at 10 V. The rotational speed of machining tool is respectively selected at 230 rpm and 450 rpm. The finishing time of electrolytic process is selected at 6 min.

Table 5.4 Experimental condition for investigating electrolytic process characteristics of electrolyte concentration

Workpiece	SUS304 plane (100 × 100 × 1 mm)
Original surface roughness	160 ~ 220 nm
Working voltage	10 V
Electrolyte concentration	20 wt%
Workinge gap	1 mm
Feeding speed	5 mm/s
Rotational speed	230 rpm, 450 rpm
MAF test time	6 min

Figure 5.4.1 shows the change in surface roughness R_a and material removal M under various rotational speed conditions at 6 min finishing time and 10 V voltage case. Through quantitatively compare change in surface roughness R_a and material removal M under

various rotational speed conditions, it is noted that the surface roughness R_a at 450 rpm case is obviously smaller than the surface roughness R_a at 230 rpm case. Moreover, the material removal M at 450 rpm case is also remarkably more than the material removal M at 230 rpm case.

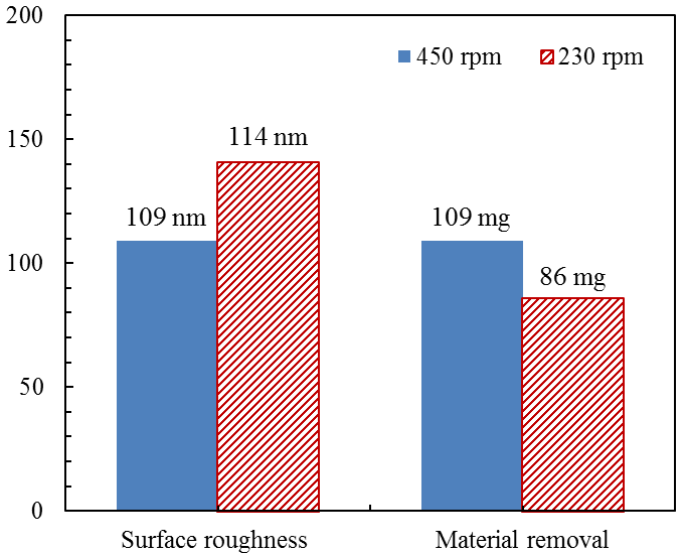

Fig. 5.4.1 Change in surface roughness R_a and material removal M under various rotational speed conditions at 6 min finishing time and 10 V voltage case

The non-contact 3D measurement and images of finished surface under various rotational speed conditions at 6 min finishing time and 10 V voltage case obtained through a non-contact optical profiling microscope is shown in Figure 5.4.2. Through comparing the 3D measurement and images of finished surface under various rotational speed conditions, it is recognized that the finished surface accuracy under 450 rpm rotational speed condition is approximately same as the finished surface accuracy under 230 rpm rotational speed condition.

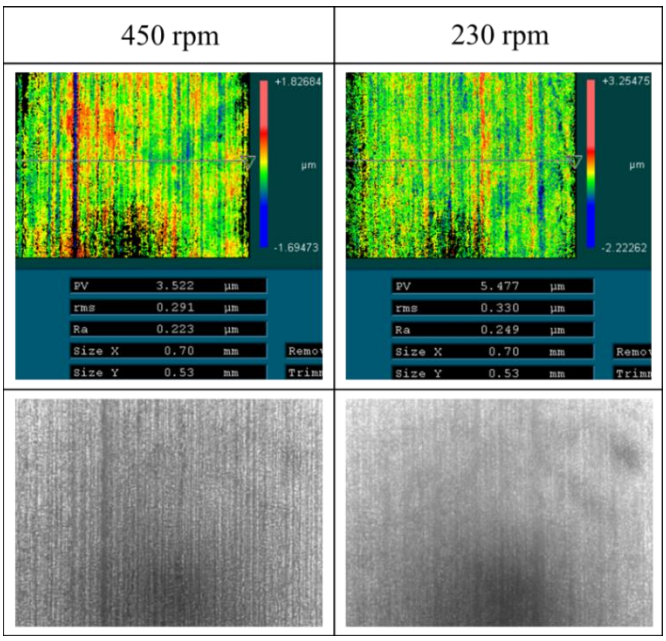

Fig. 5.4.2 Non-contact 3D measurement and images of finished surface under various rotational speed conditions at 6 min finishing time and 10 V voltage case

The change in hardness HV of finished surface with different rotational speed conditions at 6 min finishing time and 10 V voltage case is shown in Figure 5.4.3. Through comparing the change in hardness HV of finished surface under various rotational speed conditions, it is recognized that the hardness HV of finished surface under 450 rpm rotational speed condition is smaller than the hardness HV of finished surface under 230 rpm rotational speed condition. The experimental result indicated that the hardness HV decreases with the rotational speed increases. So, it can be regarded slightly better electrolytic process characteristics of rotational speed can be obtained at 450 rpm rotational speed case.

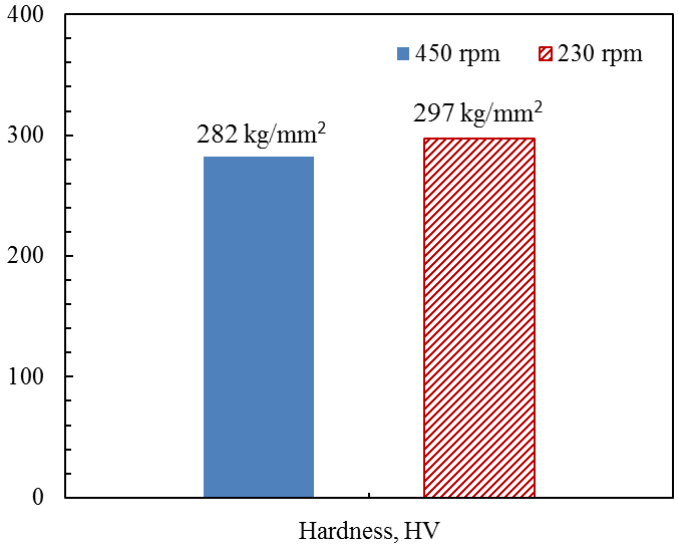

Fig. 5.4.3 Change in hardness of finished surface under various rotational speed conditions at 6 min finishing time and 10 V voltage case

5.5 Investigation of electrolytic process characteristics of feeding speed

Finally, we focused on investigating the effect of feeding speed on change in surface roughness and hardness. Table 5.5 shows experimental condition for investigating electrolytic process characteristics of different feeding speed. The surface roughness R_a of workpiece is measured at approximate 0.16 ~ 0.2 μm as an original roughness. The rotational speed of machining tool is selected at 450 rpm, working gap is adjusted to 1 mm, the electrolyte concentration is selected as 20 wt%, and the working voltage is selected at 10 V. The feeding speed of X-Y stage is respectively adjusted to 5 mm/s and 10 mm/s. The finishing time of electrolytic process is selected at 6 min.

Table 5.5 Experimental condition for investigating electrolytic process characteristics of electrolyte concentration

Workpiece	SUS304 plane (100 × 100 × 1 mm)
Original surface roughness	160 ~ 220 nm
Working voltage	10 V
Electrolyte concentration	20 wt%
Workinge gap	1 mm
Feeding speed	5 mm/s, 10 mm/s
Rotational speed	450 rpm
MAF test time	6 min

Figure 5.5.1 shows the change in surface roughness R_a and material removal M under various feeding speed conditions at 6 min finishing time and 10 V voltage case. Through quantitatively compare change in surface roughness R_a and material removal M under

various feeding speed conditions, it is noted that the surface roughness R_a at 5 mm/s case is a little smaller than the surface roughness R_a at 10 mm/s case. Moreover, the material removal M at 5 mm/s case is also a little more than the material removal M at 10 mm/s case.

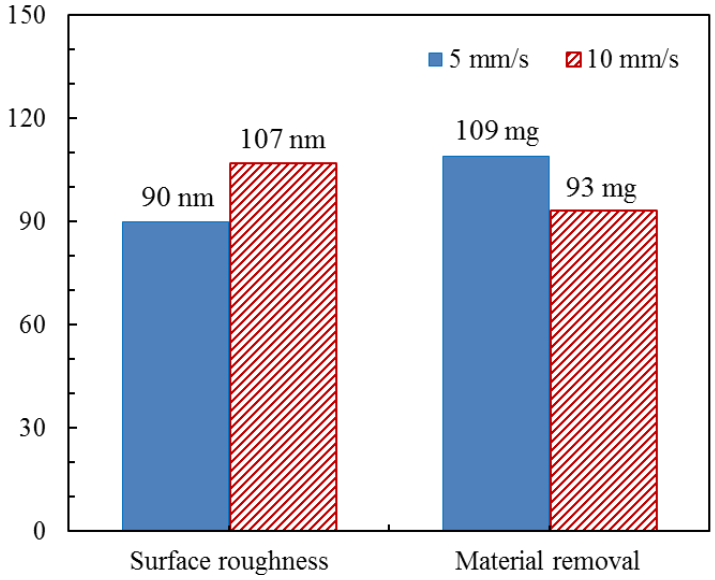

Fig. 5.5.1 Change in surface roughness R_a and material removal M under various feeding speed conditions at 6 min finishing time and 10 V voltage case

The non-contact 3D measurement and images of finished surface under various feeding speed conditions at 6 min finishing time and 10 V voltage case obtained through a non-contact optical profiling microscope is shown in Figure 5.5.2. Through comparing the 3D measurement and images of finished surface under various feeding speed conditions, it is recognized that the finished surface accuracy under 5 mm/s feeding speed condition is approximately same as the finished surface accuracy under 10 mm/s feeding speed condition.

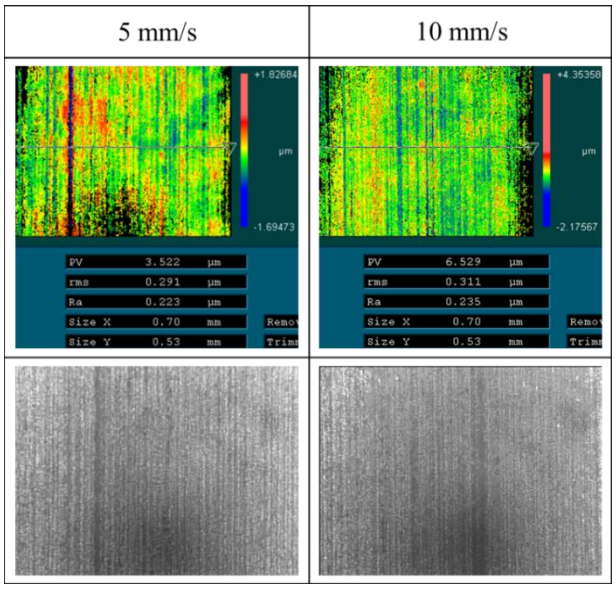

Fig. 5.5.2 Non-contact 3D measurement and images of finished surface under various feeding speed conditions at 6 min finishing time and 10 V voltage case

The change in hardness HV of finished surface with different feeding speed conditions at 6 min finishing time and 10 V voltage case is shown in Figure 5.5.3. Through comparing the change in hardness HV of finished surface under various feeding speed conditions, it is recognized that the hardness HV of finished surface under 5 mm/s feeding speed condition is almost same as the hardness HV of finished surface under 10 mm/s feeding speed condition. Therefore, it can be regarded that the effect of feeding speed on hardness HV of finished surface can be almost neglected.

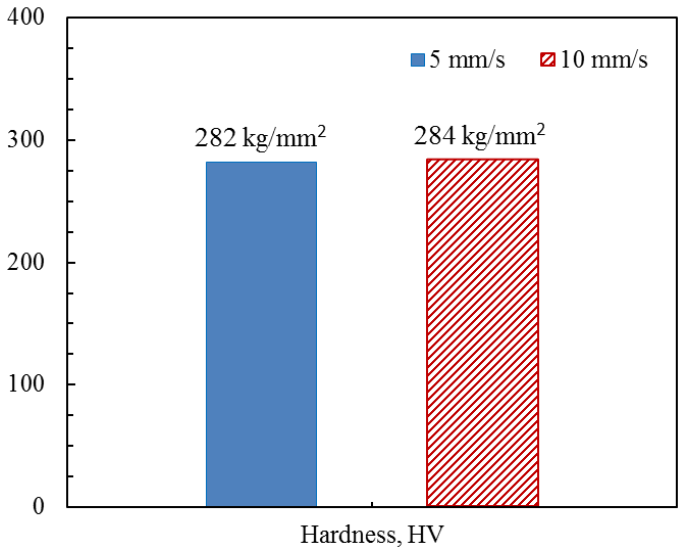

Fig. 5.5.3 Change in hardness of finished surface under various feeding speed conditions at 6 min finishing time and 10 V voltage case

5.6 EDX analysis of surface composition and SEM analysis of surface morphology

The homogeneity of finished surface materials as an important parameter is investigated by Energy Dispersive X-Ray Spectroscopy (HITACHI S 4500 & HITACHI TM 3030 Plus) to evaluate the change in elemental composition in different finishing processes. Since the main metal composition of stainless steel SUS304 is iron element (70%) and chromium element (18%), the change in iron and chromium elements will be emphatically measured [3]. Figure 5.6.1 shows the change in content of iron (Fe), chromium (Cr), oxygen (O) elements after electrolytic process and EMAF process by EDX analysis. The composition of original surface is shown in Figure 5.6.1 (a). It can be confirmed that the major composition of SUS304 is constituted by Fe, Cr, Ni and other elements through Figure 5.6.1 (a). Figure 5.6.1 (b), (c) respectively shows that composition of finished surface after electrolytic process and EMAF process. Compared with the composition of original surface, it can be found that the composition of finished surface after electrolytic process is significantly different from the composition of original surface. As previously mentioned, a large amount of metal ions have been dissolved out on the surface of workpiece under the action of electrolytic process. It is the main reason for that the content of Fe, Cr etc. metal elements after electrolytic process is less than the content of original surface composition. Additionally, the content of O element is a little more than the content of original surface composition since passive films formed on the workpiece surface under electrolytic action. Through comparing Figure 5.6.1 (a) and Figure 5.6.1 (c), it can be revealed that the content of Fe, Cr etc. metal elements and the content of O element after EMAF process are almost same as original surface. It is because the formed passive films have been almost completely removed after EMAF process, and the original material exposed on the surface.

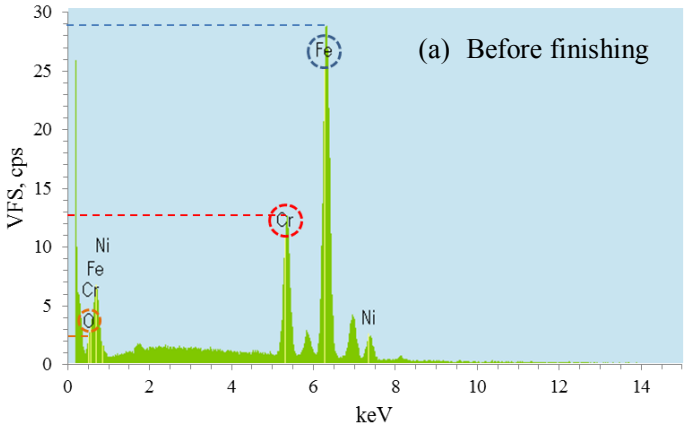

(a) EDX analysis of original surface

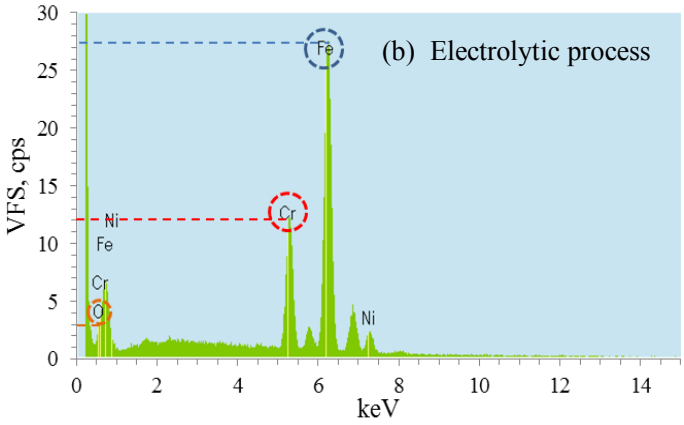

(b) EDX analysis of finished surface after electrolytic process

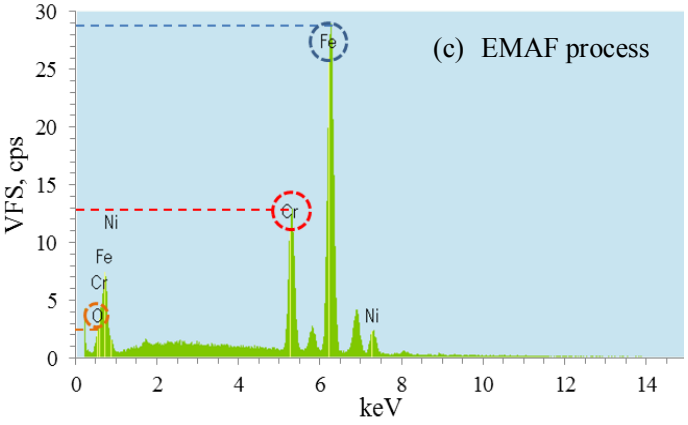

(c) EDX analysis of finished surface after EMAF process

Fig. 5.6.1 Change in content of iron (Fe), chromium (Cr), oxygen (O) elements after electrolytic process and EMAF process by EDX analysis

Obviously, it can be confirmed that the electrolytic process is a main reason for leading to change in the content of finished surface composition. Since the major composition of SUS304 material is constituted by Fe, Cr, Ni elements, Figure 5.6.2 depicts some representative images of Fe, Cr and Ni elements along with the local elemental distribution mapping. The main compositions of original surface before electrolytic process are shown in Figure 5.6.2 (a); the change in main compositions of the finished surface after electrolytic process is shown in Figure 5.6.2 (b). By comparing the analysis results, it can be revealed that a lot of large black dots which cannot be identified substance shown in white circle inner generates on the finished surface, and the content of each element significantly decreases during electrolytic process. The results also completely conforms that electrochemical reactions occur during the electrolytic process. In addition, the local elemental mapping indicates that the distribution of Fe, Cr and Ni elements becomes non-uniform after electrolytic process.

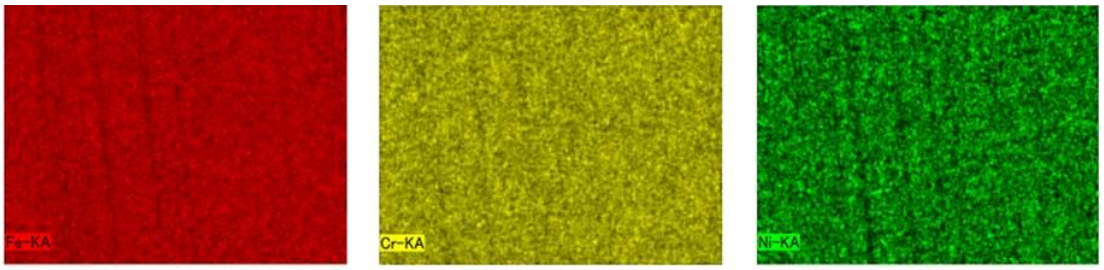

(a) Main compositions of the original surface

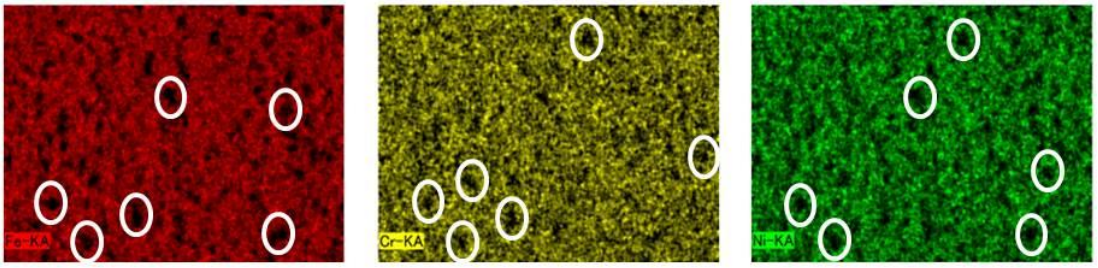

(b) After ECM process, change in main compositions of the finished surface

Figure 5.6.2 Representative SEM images and elemental mapping of Fe, Cr and Ni element

While measuring elemental composition, the surface morphology also is obtained by a

scanning electron microscope (SEM) shown in Figure 5.6.3. It can be seen that the numbers of micro-porous increase with electrolytic process time increases under same working voltage case; the depth of micro-porous also become deepen with electrolytic process time increases under same working voltage case. In addition, it also can be noted that the numbers of micro-porous increase with working voltage increases at the same electrolytic process time case; the depth of micro-porous also become deepen with working voltage increases at the same electrolytic process time case. In particular, the change in surface morphology is especially significant at 12 V voltage condition.

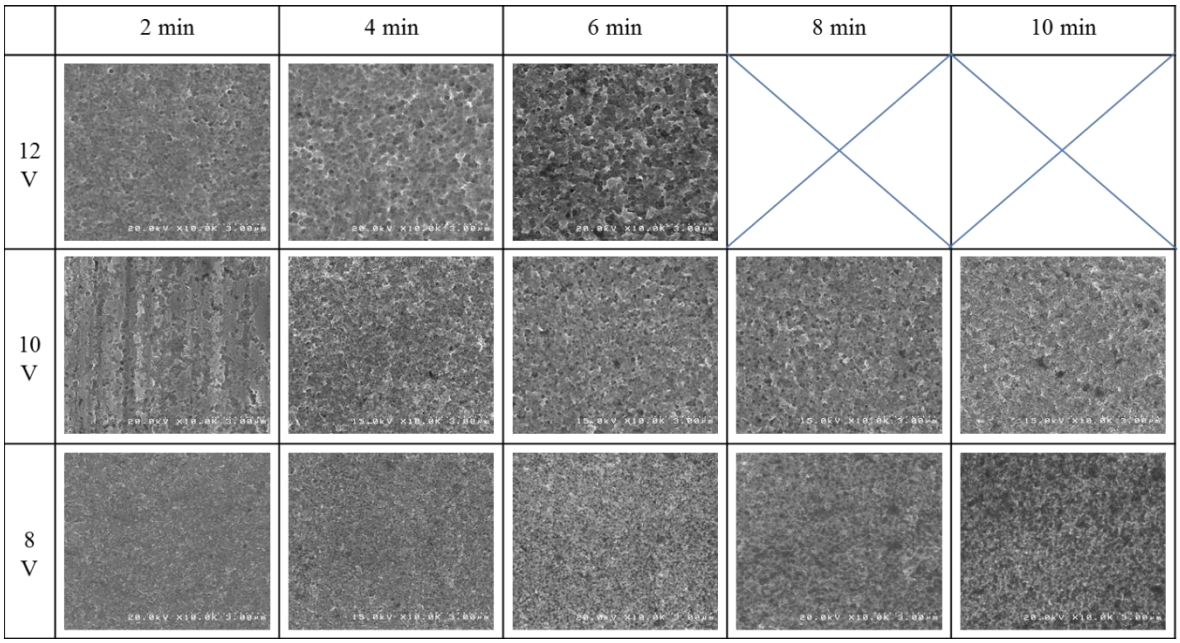

Figure 5.6.3 SEM images under different electrolytic process time and different working voltage conditions

5.7 Conclusions

In the chapter 5, the electrolytic action of electrolytic process was firstly investigated in order to explore the optimal electrolytic machining conditions of the electrolytic magnetic compound machining tool. The main conclusions were shown as follows:

(1) Through quantitatively compare change in surface roughness R_a and material removal M under various voltage conditions, it is noted that the relatively smaller surface roughness R_a and relatively more material removal M can be obtained at 12 V voltage condition. Additionally, it also can be clearly found that the hardness HV of finished surface decreases with machining time increases under same working voltage; the hardness HV of finished surface decreases with voltage increases at same machining time. Moreover, it is also regarded that the hardness of finished surface can be maximally reduced by 15% under 12 V voltage at 6 min machining time condition.

(2) Through quantitatively compare change in surface roughness R_a and material removal M under various electrolyte concentration conditions, it is noted that the surface roughness R_a at 20wt% and 30wt% cases is obviously smaller than the surface roughness R_a under 10wt% case. The material removal M at 30wt% case is also remarkably more than the material removal M under other electrolyte concentration cases. Moreover, it also can be considered that the hardness HV decreases with the electrolyte concentration increases through experimental result.

(3) Through quantitatively compare change in surface roughness R_a and material removal M under various working gap conditions, it is noted that the surface roughness R_a at 1 mm working gap case is obviously smaller than the surface roughness R_a under other two cases. The material removal M at 1 mm working gap case is also remarkably more than the

material removal M under other working gap cases. Furthermore, it can be regarded that the hardness HV decreases with the working gap decreases.

(4) Through quantitatively compare change in surface roughness R_a and material removal M under various rotational speed conditions, it is noted that the surface roughness R_a at 450 rpm case is obviously smaller than the surface roughness R_a at 230 rpm case. The material removal M at 450 rpm case is also remarkably more than the material removal M at 230 rpm case. In addition, the experimental result indicated that the hardness HV decreases with the rotational speed increases.

(5) Through quantitatively compare change in surface roughness R_a and material removal M under various feeding speed conditions, it is noted that the surface roughness R_a at 5 mm/s case is a little smaller than the surface roughness R_a at 10 mm/s case. The material removal M at 5 mm/s case is also a little more than the material removal M at 10 mm/s case. Moreover, it can be regarded that the effect of feeding speed on hardness HV of finished surface can be almost neglected.

(6) The generation of passive films, EDX analysis of surface composition and SEM analysis of surface morphology has been completed at the end of this chapter.

Chapter 6 Study on finishing stainless steel SUS304 plane workpiece by using electrolytic magnetic compound machining tool in electrolytic magnetic abrasive finishing

The focus of this study is to develop a new method of plane magnetic abrasive finishing combined with electrolytic process to solve the problem of low efficiency when polishing hard metal materials by traditional magnetic abrasive finishing. The EMAF process includes two finishing steps which are respectively the 1st finishing step (EMAF step) and the 2nd finishing step (MAF step). In EMAF step, protruding portions are preferentially leveled, material remove rapidly increases and passive films form on the surface of workpiece under electrolytic action. Simultaneously, the magnetic abrasive particles of magnetic brush are used to exert friction on the surface of workpiece. Compared to stainless steel SUS304 material, the passive films can be more easily removed. By the way, the hardness of passive films is smaller than the hardness of SUS304 stainless material [1]. Thus, the efficient of precision machining can be basically achieved in EMAF step. However, generated speed of passive films is far faster than removed speed of passive films. Since a few passive films still exists on the finished surface after EMAF step, the residual passive films will affect the surface accuracy. Hence, MAF step as a final process after EMAF step is used to completely remove residual passive films on workpiece surface in order to improve surface accuracy of workpiece. In this chapter, we focused on researching the combinations of EMAF step time and MAF step time for EMAF process. The combination of two different finishing steps time plays a vital role for improving polishing efficient in EMAF process.

Chapter 6 Study on finishing stainless steel SUS304 plane workpiece by using electrolytic magnetic compound machining tool in electrolytic magnetic abrasive finishing

6.1 First finishing step (EMAF step)

Firstly, the experiments of compound finishing step (EMAF step) were conducted under different working voltage conditions and different finishing time conditions. Table 6.1 shows experimental condition of EMAF step. The surface roughness R_a of workpiece is measured at approximate 0.16 ~ 0.2 μm as an original roughness. The rotational speed of machining tool is selected at 450 rpm, working gap is adjusted to 1 mm, the feeding speed of X-Y stage is adjusted to 5 mm/s, and the electrolyte concentration is selected as 20 wt%. The working voltage is respectively selected at 8 V, 10 V and 12 V. The finishing time of electrolytic process is respectively selected at 2 min, 4 min, 6 min, 8 min and 10 min.

Table 6.1 Experimental condition of EMAF step under different working voltage and different finishing time conditions

Workpiece	SUS304 plane (100×100×1 mm)
Original roughness R_a	0.16 ~ 0.2 μm
Mixed magnetic abrasive	Electrolytic iron powder: 149 μm
	WA particles: #8000
	Oily grinding fluid
Working gap	1 mm
Feeding speed of stage	5 mm/s
Rotational speed of tool	450 rpm
Working voltage	8 V, 10 V, 12 V
Electrolyte concentration	20 wt%
Finishing time	2 min, 4 min, 6 min, 8 min, 10 min

Figure 6.1 shows the change in surface roughness R_a and material removal M as a function in EMAF step under different working voltage and different finishing time conditions. It can be seen that surface roughness R_a decreases with finishing time increases, material removal M also increases with finishing time increases at 8 V and 10 V working

voltage conditions. The surface roughness R_a at 10 V working voltage condition is smaller than the surface roughness R_a at 8 V working voltage condition, the material removal M at 10 V working voltage condition is slightly more than the material removal M at 8 V working voltage condition. However, the mix surface roughness occurred at 4 min under the condition of 12 V working voltage. Then the surface roughness slightly increased after 4 min under the condition of 12 V working voltage. The material removal rate before 4 min under the condition of 12 V working voltage is remarkably more than the material removal rate after 4 min under the condition of 12 V working voltage.

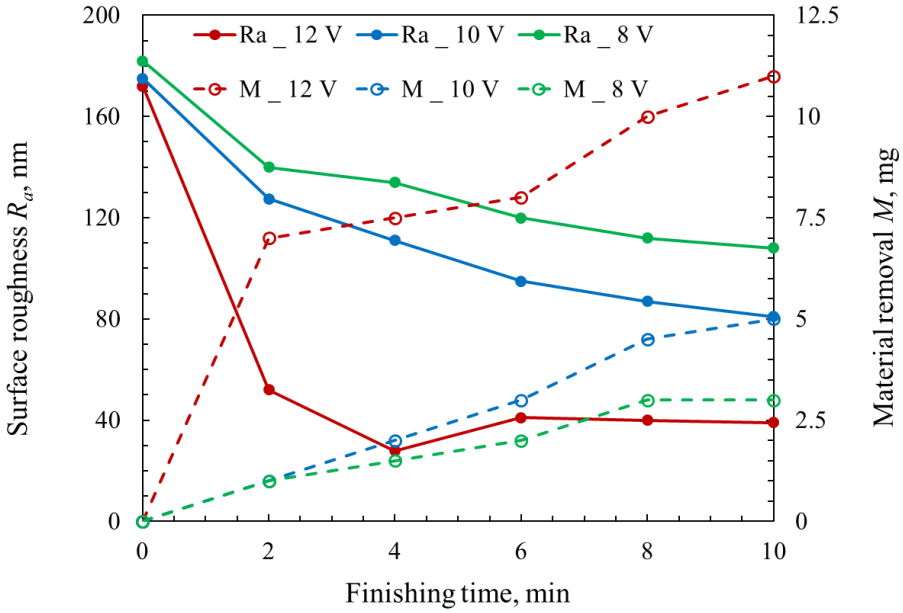

Figure 6.1 Change in surface roughness R_a and material removal M as a function under different working voltage and different finishing time conditions

6.2 EMAF process

Compared with metal material removal in traditional MAF process, the essence of EMAF process is using magnetic brush to remove formed passive films form electrolytic process. There are three kinds of matching relations between electrolytic action and mechanical action in EMAF step. When the formed rate of passive films is faster than removed rate of passive films in EMAF step as shown in Figure 6.2.1 (a), passive films can't be completely removed in EMAF step. When the formed rate of passive films is slower than removed rate of passive films in EMAF step as shown in Figure 6.2.1 (b), the removed objects of magnetic brush can be considered as metal material. When the formed rate of passive films is as same as removed rate of passive films in EMAF step as shown in Figure 6.2.1 (c), it can be considered that the passive films can be completely removed in this optimal case in EMAF step.

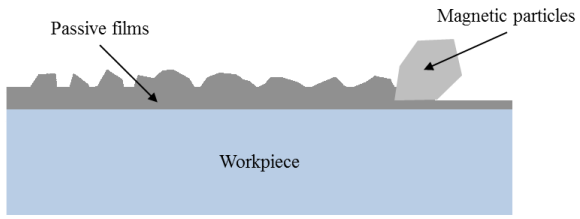

(a) Electrolytic action is stronger than mechanical action

(b) Mechanical action is stronger than electrolytic action

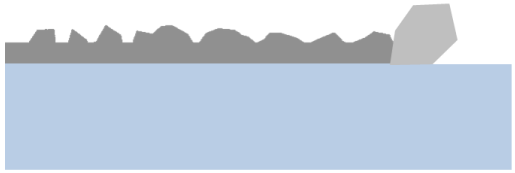

(c) Electrolytic action is consistent with mechanical action

Figure 6.2.1 Matching relations between electrolytic action and mechanical action

Chapter 6 Study on finishing stainless steel SUS304 plane workpiece by using electrolytic magnetic compound machining tool in electrolytic magnetic abrasive finishing

Through investigating the machining characteristics of traditional MAF process and single electrolytic process, it is recognized that the effect of rotational speed and working gap on machining characteristics are very obvious in MAF process, the effect of feeding speed on machining characteristics is almost insignificant. In electrolytic process, the machining characteristics under 12 V voltage condition are obviously better than the machining characteristics under 10 V and 8 V voltage condition; the machining characteristics under 20 wt% or 30 wt% electrolyte concentration conditions are better than the machining characteristics under 10 wt% electrolyte concentration condition. Based on the experimental investigation of machining characteristics for single MAF process and single electrolytic process, the detailed experimental conditions of EMAF process under different combinations of EMAF step time and MAF step time conditions are decided and shown in Table 6.2. The surface roughness R_a of workpiece is measured at approximate 0.16 ~ 0.2 μm as an original roughness. The mixed magnetic abrasive consists of quantitative electrolytic iron powder with 149 μm in mean diameter and quantitative #8000 WA particles. The working gap is adjusted to 1 mm, the rotational speed of complex machining tool is selected at 450 rpm, and the feeding speed of X-Y stage is adjusted to 5 mm/s. The working voltage is selected at 12 V. The electrolyte concentration is selected as 20 wt%. According to matching relations between electrolytic action and mechanical action shown in Figure 6.2.1, it can be seen the combination of EMAF step time and MAF step time is extremely important for achieving high-efficiency polishing. The total finishing time of EMAF process is selected at 30 min. We will focus on investigating the combination of the first finishing step time and second finishing step time for EMAF process. The combination of total finishing time is respectively 2 min (EMAF step) + 28 min (MAF step), 4 min (EMAF step) + 26 min (MAF step), 6 min (EMAF step) + 24 min

(MAF step), 8 min (EMAF step) + 22 min (MAF step) and 10 min (EMAF step) + 20 min (MAF step). The finished surface is respectively measured and observed after EMAF step, each 10 min MAF step and remaining time of MAF step.

Table 6.2 Experimental condition of EMAF process under different combinations of EMAF step time and MAF step time conditions

Workpiece	SUS304 plane (100×100×1 mm)
Original roughness R_a	0.16 ~ 0.2 μm
Mixed magnetic abrasive	Electrolytic iron powder: 149 μm
	WA particles: #8000
	Oily grinding fluid
Working gap	1 mm
Feeding speed of stage	5 mm/s
Rotational speed of tool	450 rpm
Working voltage	12 V
Electrolyte concentration	20 wt%
Finishing time (30 min)	2 min (EMAF step) + 28 min (MAF step) 4 min (EMAF step) + 26 min (MAF step) 6 min (EMAF step) + 24 min (MAF step) 8 min (EMAF step) + 22 min (MAF step) 10 min (EMAF step) + 20 min (MAF step)

Figure 6.2.2 shows the change in roughness R_a and material removal M as a function under different combinations of EMAF step time and MAF step time conditions. Through comparing the experimental results of EMAF process under different combinations of EMAF step time and MAF step time, it can be noted that the surface roughness R_a drastically decreases in EMAF step, the material removal M in EMAF step is obviously more than the material removal M in MAF step. The material removal M is approximately 7 ~ 10 g in EMAF step; the material removal M is approximately 4 ~ 6 g in MAF step. In other words, the material removal rate in EMAF step is nearly 8 times than that in MAF

step. Furthermore, the optimal experimental result of EMAF process shows that the surface roughness R_a can be reduced to less than 30 nm at 4 min EMAF step, the surface roughness R_a can be reduced to 20 nm at 10 min MAF step, and the surface roughness R_a almost don't change after 10 min MAF step. In other words, the optimal surface accuracy can be obtained at 14 min EMAF process under combination of 4 min EMAF step and 26 min MAF step condition. Since the electrolytic action is not enough in 2 min EMAF step, and the electrolytic action excessive in 6 min, 8 min, 10 min EMAF step. Therefore, 4 min EMAF step is considered as the optimal finishing time for EMAF process. Generated passive films from electrolytic process can be maximally removed in 4 min EMAF step.

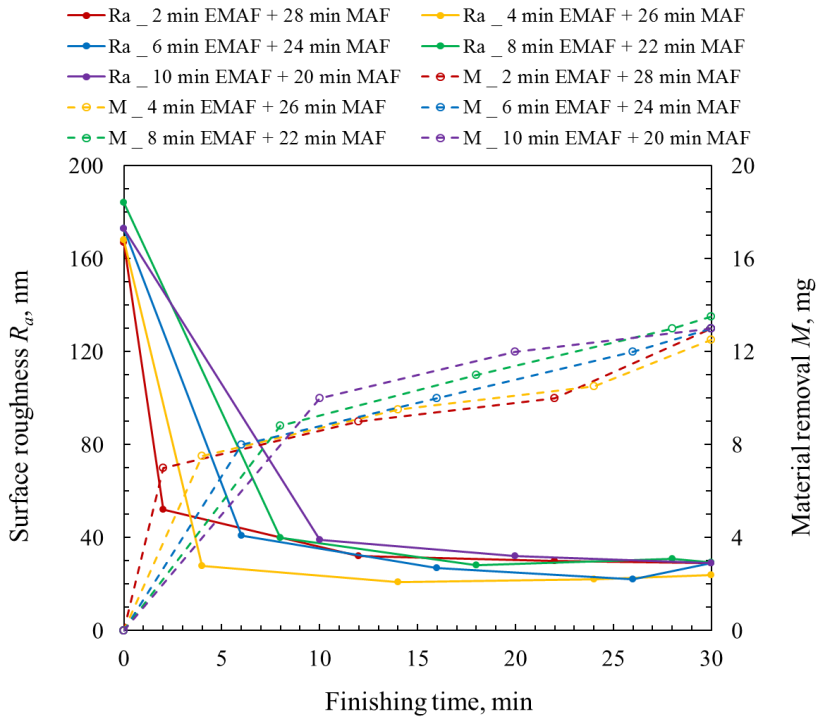

Figure 6.2.2 Change in surface roughness R_a and material removal M as a function under different combinations of EMAF step time and MAF step time condition

Figure 6.2.3 shows the obtained surface maps under different combinations of EMAF step time and MAF step time condition. At the same time, the intensity maps under different combinations of EMAF step time and MAF step time condition are also obtained

shown in Figure 6.2.4. The Figures on the left show the macroscopic confocal surface maps and intensity maps of finished surface after 2 min, 4 min, 6 min, 8 min and 10 min EMAF step. It can be seen that the protruding part of original surface has be rapidly removed after EMAF step. However, several deep concave hairlines still retain on the finished surface after EMAF step. The Figures on the right show the macroscopic confocal surface maps and intensity maps of finished surface after 30 min EMAF process under different combinations of EMAF step time and MAF step time condition. It can be regarded that the depth of residual concave hairlines obviously become shallow, the number of residual concave hairlines also greatly reduces after MAF step.

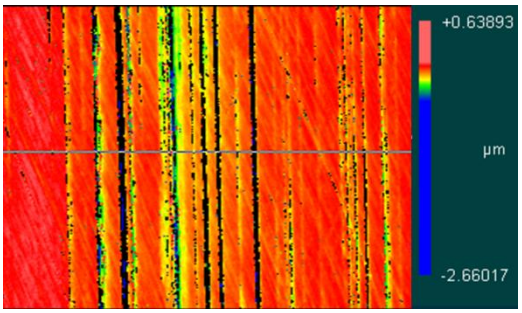

(a) After 2 min EMAF step

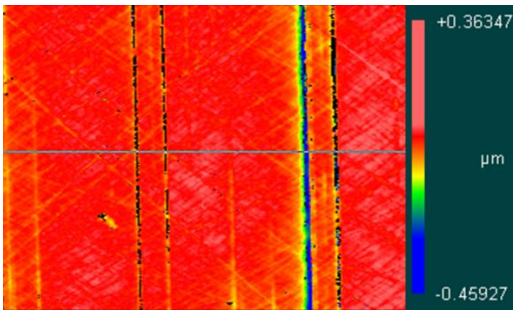

(a1) After 2 min EMAF step and 28 min MAF step

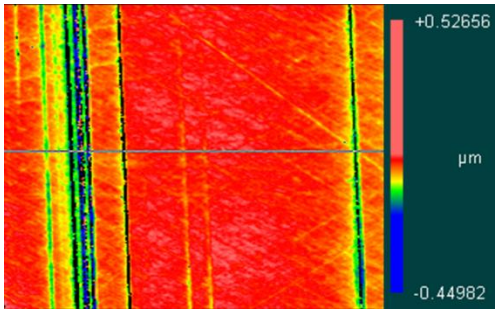

(b) After 4 min EMAF step

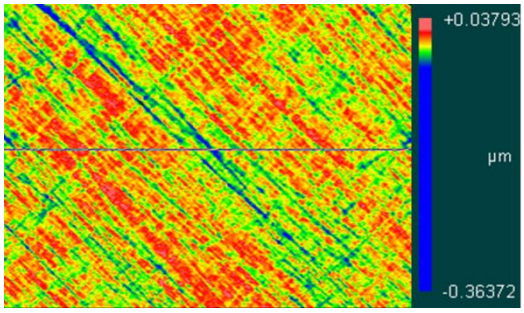

(b1) After 4 min EMAF step and 26 min MAF step

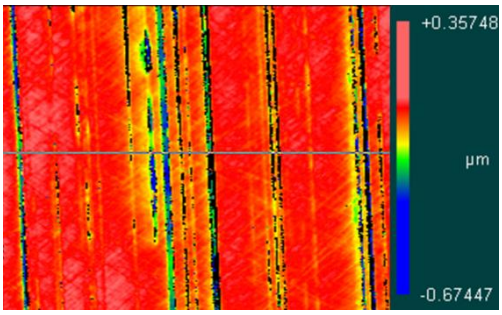

(c) After 6 min EMAF step

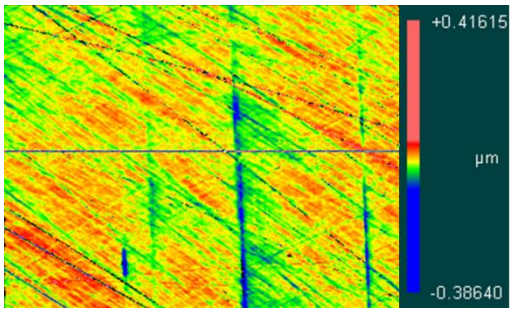

(c1) After 6 min EMAF step and 24 min MAF step

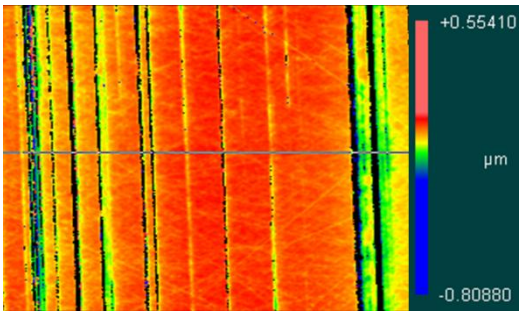

(d) After 8 min EMAF step

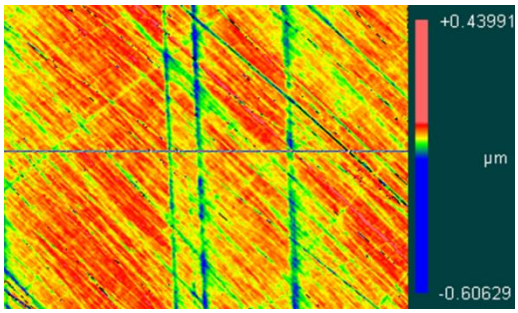

(d1) After 8 min EMAF step and 22 min MAF step

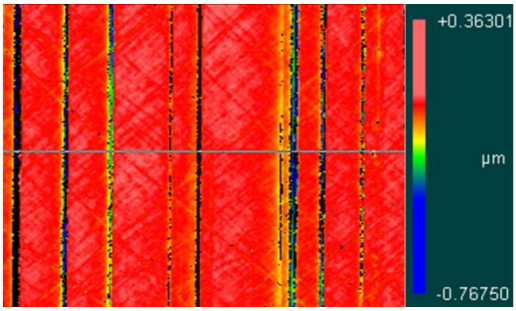

(e) After 10 min EMAF step

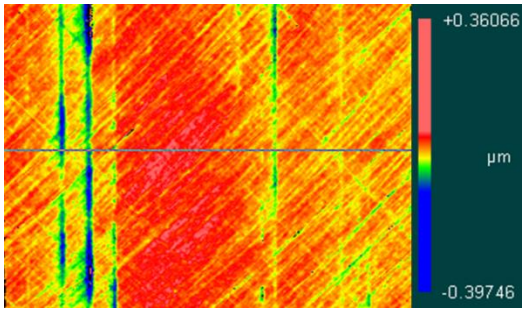

(e1) After 10 min EMAF step and 20 min MAF step

Figure 6.2.3 Obtained surface maps under different combinations of EMAF step time and MAF step time condition

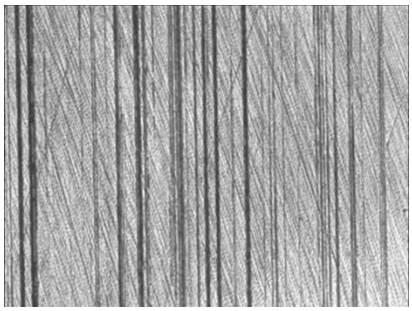

(a) After 2 min EMAF step

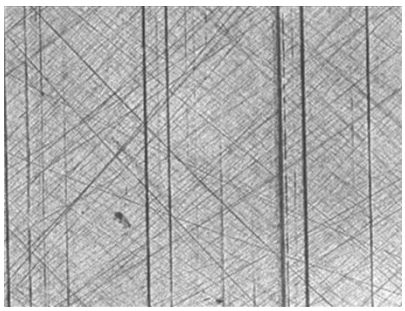

(a1) After 2 min EMAF step and 28 min MAF step

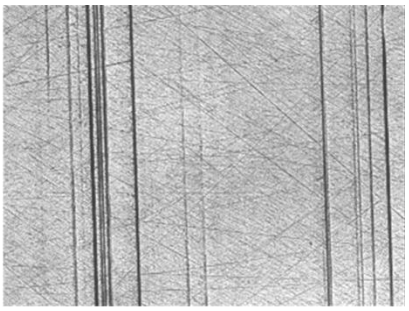

(b) After 4 min EMAF step

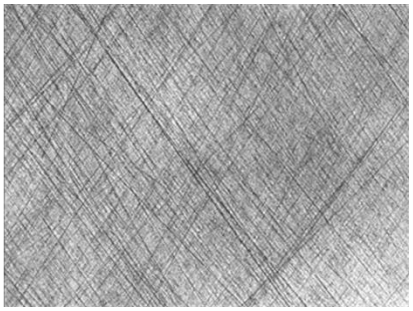

(b1) After 4 min EMAF step and 26 min MAF step

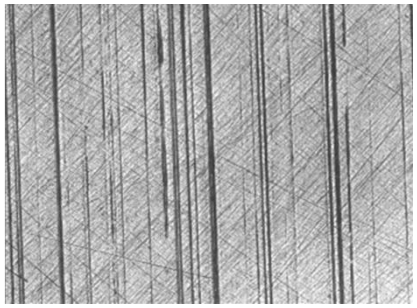

(c) After 6 min EMAF step

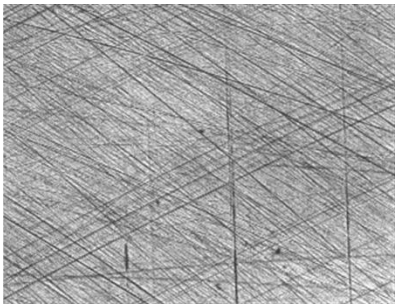

(c1) After 6 min EMAF step and 24 min MAF step

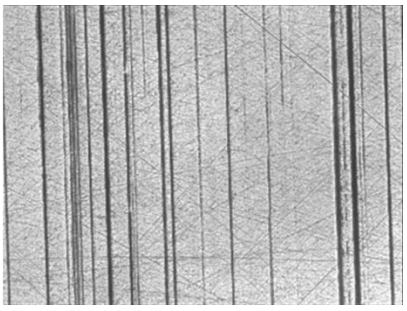

(d) After 8 min EMAF step

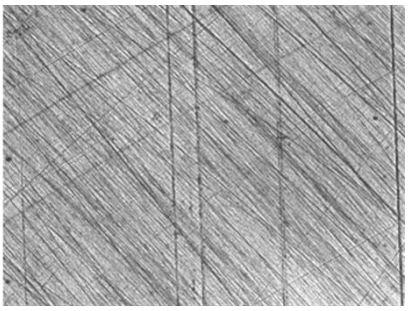

(d1) After 8 min EMAF step and 22 min MAF step

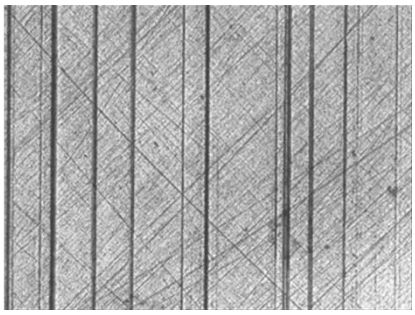

(e) After 10 min EMAF step

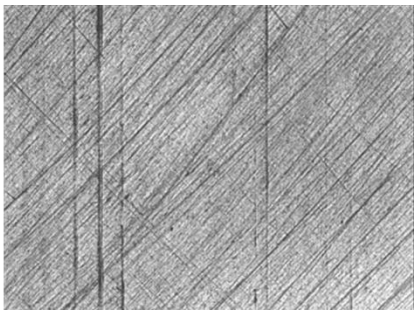

(e1) After 10 min EMAF step and 20 min MAF step

Figure 6.2.4 Obtained intensity maps under different combinations of EMAF step time and MAF step time condition

6.3 Discussions

Figure 6.3.1 shows macroscopic confocal images of unfinished surface and finished surface under the combination of 4 min EMAF step and 26 min MAF step condition. The SEM photograph of original surface before EMAF process is shown in Figure 6.3.1 (a). The initial hairline of unfinished surface can be clearly seen through the SEM photograph. Figure 6.3.1 (b) shows the SEM photograph of finished surface after 4 min EMAF step. It can be found that a small amount of micro-porous still exists on the finished surface. Moreover, it also indicates that the action of MAF process can not completely remove the generated passive films from electrolytic process. The SEM photograph of finished surface after 26 min MAF step is shown in Figure 6.3.1 (c). Compared with the original surface of workpiece, it can be clearly found that the initial hairline of surface has been almost completely removed. Furthermore, it also can be confirmed that MAF step plays an essential role to achieve precision machining during the EMAF process.

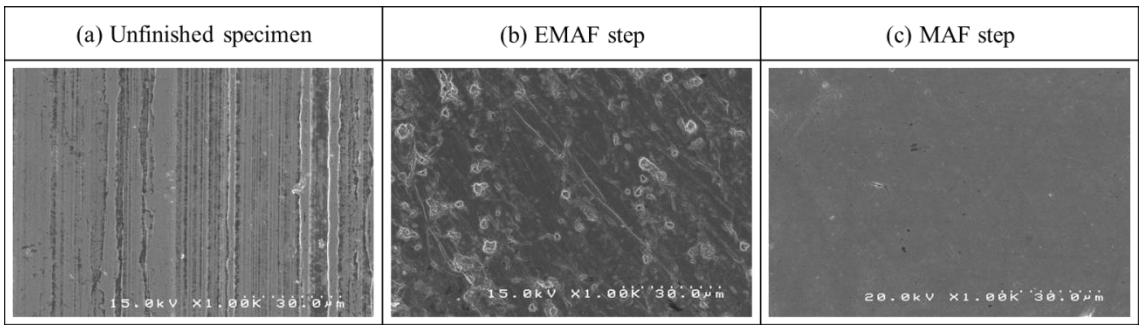

Figure 6.3.1 Macroscopic confocal images of unfinished surface and finished surface under the combination of 4 min EMAF step and 26 min MAF step condition

Figure 6.3.1 shows the SEM images of change in mixed magnetic abrasive under different EMAF step time and different voltage conditions. It can be considered that the size of mixed magnetic abrasive drastically decreases with EMAF step time increases at

the same voltage case; the size of mixed magnetic abrasive slightly decreases with working voltage increases at the same EMAF step time case. Combined with SEM images in electrolytic process from chapter 5 and change in size of mixed magnetic abrasive in EMAF step from this chapter, it is easy to understand why the optimal surface accuracy can be obtained under combination of 4 min EMAF step and 26 min MAF step condition. Since the electrolytic action is not enough in 2 min EMAF step and the size of mixed magnetic abrasive drastically decreases in 6 min, 8 min, 10 min EMAF step (iron powder polishing capacity is almost ignored after 6 min EMAF step), the polishing efficiency is low in 2 min and 6 min, 8 min, 10 min EMAF step. Thus, 4 min EMAF step is considered as the optimal finishing time for EMAF process. Generated passive films from electrolytic process can be maximally removed in 4 min EMAF step.

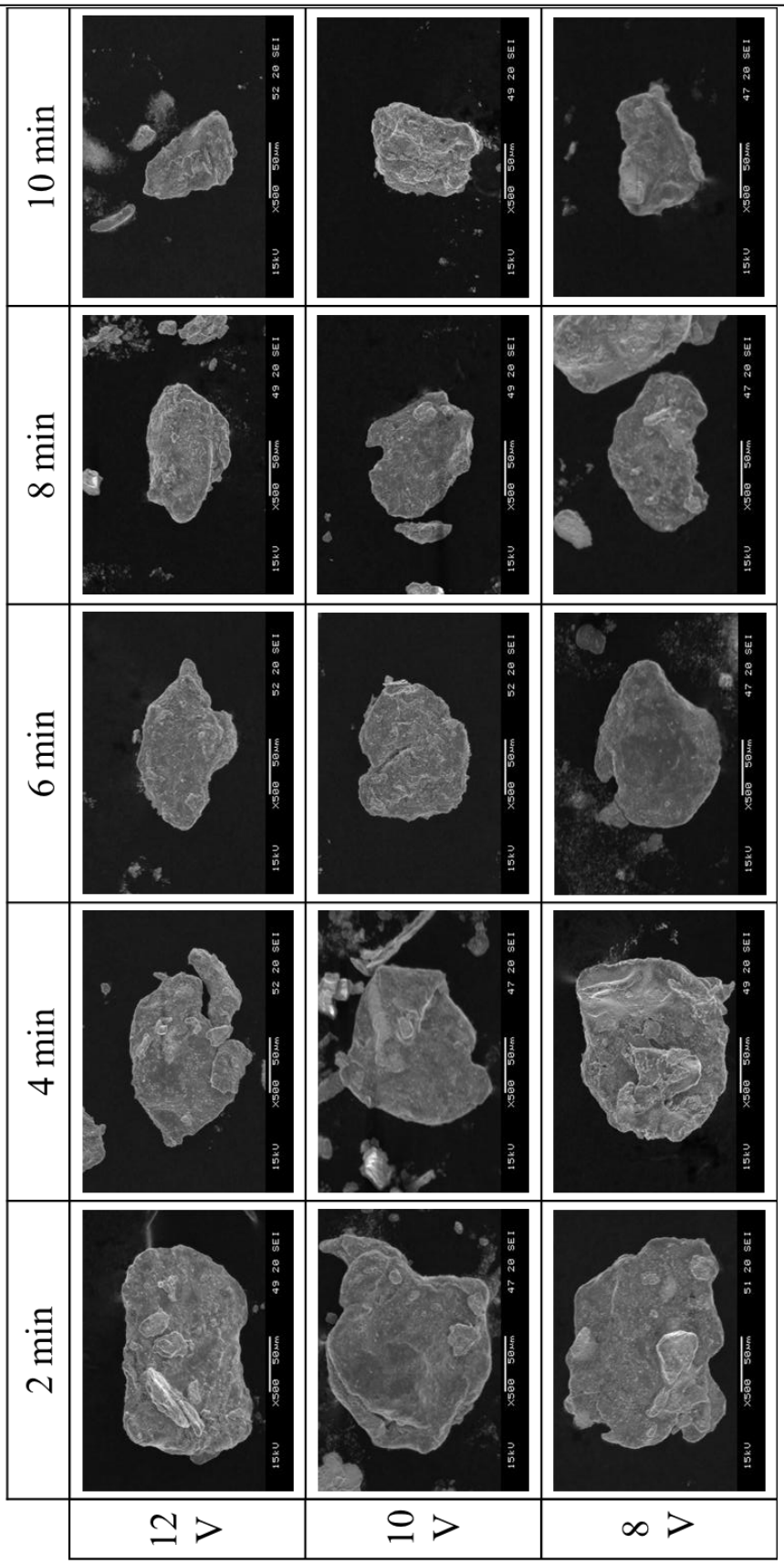

Figure 6.3.2 SEM images of change in mixed magnetic abrasive under different EMAF step time at and different voltage conditions

According to the SEM images of change in mixed magnetic abrasive, we quantitatively measured change in size of mixed magnetic abrasive under different EMAF step time at and different voltage conditions shown in Figure 6.3.3. It can be seen the significant change in size of mixed magnetic abrasive through quantitative measurement. The consumption of mixed magnetic abrasive is approximately 10% in 2 min EMAF step; the consumption of mixed magnetic abrasive is approximately 25% in 4 min EMAF step; the consumption of mixed magnetic abrasive is approximately 35% in 6 min EMAF step; the consumption of mixed magnetic abrasive is approximately less than 50% in 8 min EMAF step; the consumption of mixed magnetic abrasive is approximately more than 50% in 10 min EMAF step. Therefore, it can be considered that the mixed magnetic abrasive is invalid after 6 min EMAF step.

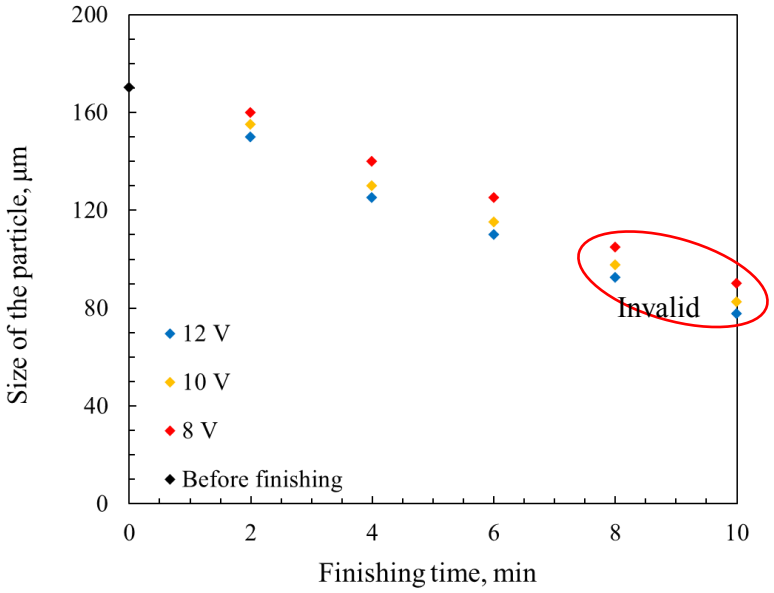

Figure 6.3.3 change in size of mixed magnetic abrasive under different EMAF step time at and different voltage conditions

6.4 Comparison of MAF process, electrolytic process, and EMAF process

In order to quantitatively compare the polishing effects in traditional MAF process and EMAF process, the optimal polishing effects in traditional MAF process and EMAF process are compared in 30 min finishing time. Figure 6.4.1 shows the comparison of EMAF process and traditional MAF process for surface roughness R_a and material removal M. It is recognized that the material removal efficiency of EMAF process is remarkably higher than that of traditional MAF process, and the surface quality of EMAF process is also better than that of MAF process. The material removal in EMAF process is nearly 3.5 times than that in traditional MAF process. The surface roughness in 4 min EMAF step of EMAF process is a little better than that in 30 min traditional MAF process. The polishing efficiency by using EMAF process can be improved approximate 90%.

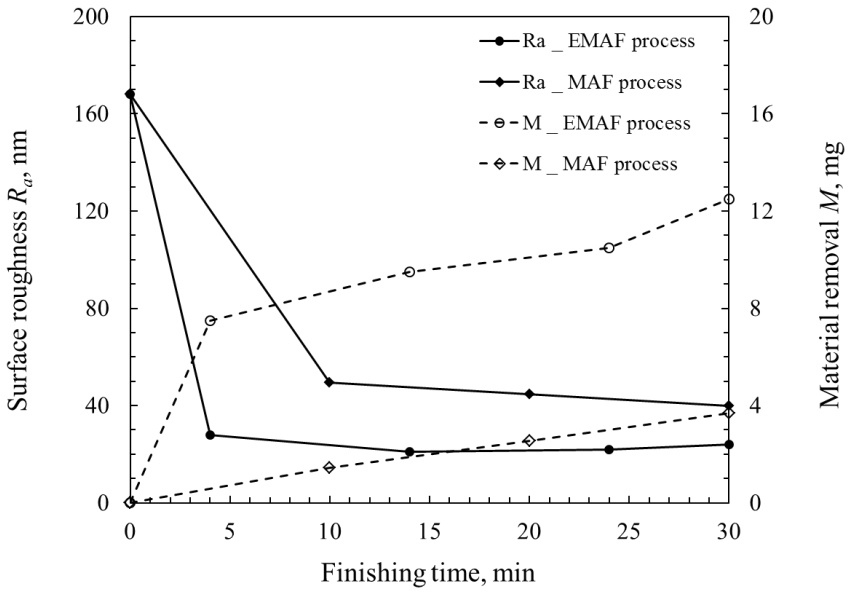

Figure 6.4.1 Comparison of EMAF process and traditional MAF process for surface roughness R_a and material removal M

Figure 6.4.2 shows the comparing polishing effects of MAF process, electrolytic process,

and EMAF process. It can be seen that 68 nm surface roughness can be obtained in 6 min electrolytic process; 20 nm surface roughness can be obtained in 14 min EMAF process; 26 nm surface roughness can be obtained in 60 min MAF process. Through comparing the three different finishing methods, it can be regarded that the polishing accuracy of EMAF process is obviously higher than that of single electrolytic process; the polishing efficiency of EMAF process is remarkably higher than that of traditional MAF process.

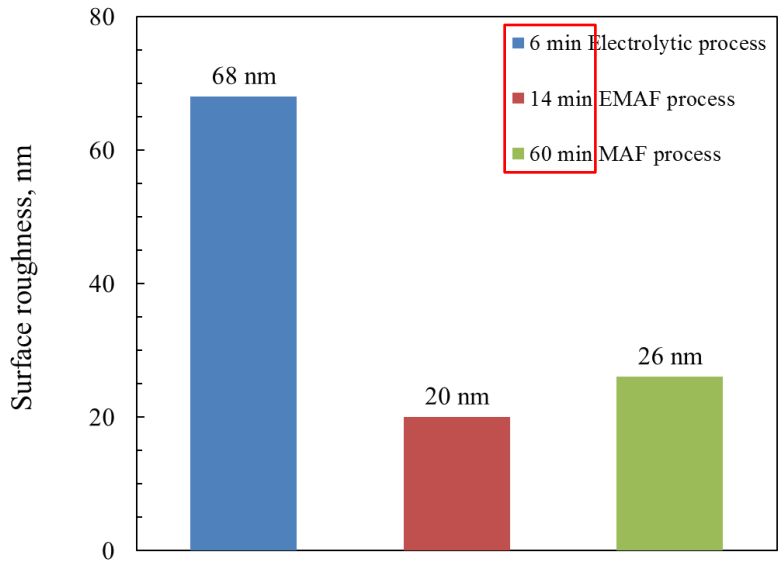

Figure 6.4.2 Comparing the polishing effects of three different finishing methods

Figure 6.4.3 shows the photographs of the unfinished surface and the finished surface by three different finishing methods of traditional MAF process, electrolytic process and EMAF process. It can be seen that the intensity of finished surface by electrolytic process is not good. Although the surface roughness can rapidly reach to below 100 nm in electrolytic process, the intensity of finished surface is not good since the passive films formed on the finished surface. Additionally, it can be regarded that the mirror polishing can be achieved by both traditional MAF process and EMAF process.

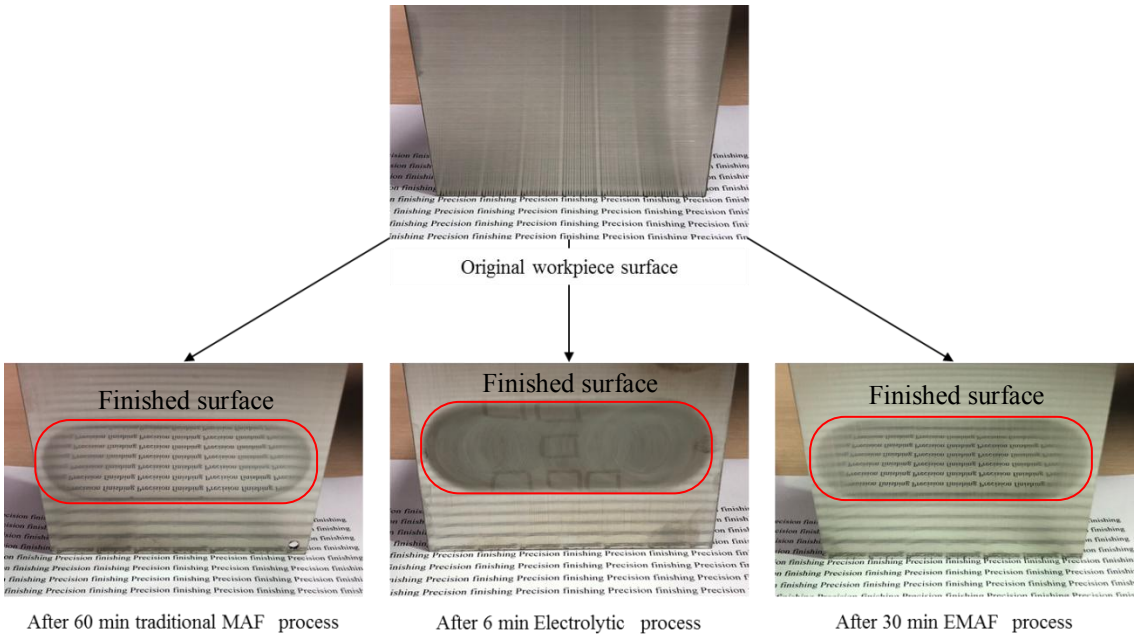

Figure 6.4.3 Photographs of the unfinished surface and the finished surface by three different finishing methods of traditional MAF process, electrolytic process and EMAF process

6.5 Conclusions

In this chapter, based on the optimal mechanical finishing conditions and electrolytic machining conditions in single MAF process and single electrolytic process, the electrolytic magnetic abrasive finishing (EMAF) process was conducted. The main conclusions were shown as follows:

(1) It can be recognized that the optimal working voltage is 12 V for the EMAF step through investigating the different working voltage.

(2) Through investigating the combination of the first finishing step time and second finishing step time, it can be regarded that the combination of 4 min EMAF step and 26 min MAF step is the optimal finishing time for EMAF process. It also can be considered that the generated passive films from electrolytic process can be maximally removed in 4 min EMAF step.

(3) It can be proven that a few passive films still existed on the finished surface after the EMAF step through observing the SEM images after each finishing step.

(4) Through observing the SEM images of change in mixed magnetic abrasive under different EMAF step time and different voltage conditions, it can be found that the size of mixed magnetic abrasive drastically decreases with EMAF step time increases at the same voltage case; the size of mixed magnetic abrasive slightly decreases with working voltage increases at the same EMAF step time case.

(5) Compared with the traditional MAF process, it can be recognized that the surface roughness in 4 min EMAF step of EMAF process is a little better than that in 30 min traditional MAF process. The polishing efficiency by using EMAF process can be

improved approximate 90%.

(6) Although the surface roughness can rapidly reach to below 100 nm in electrolytic process, the intensity of finished surface is not good since the passive films formed on the finished surface. Additionally, it can be regarded that the mirror polishing can be achieved by both traditional MAF process and EMAF process.

Chapter 7 Conclusions

In order to solve the problem of low efficiency when polishing hard metal materials by traditional magnetic abrasive finishing (MAF), a novel method of plane magnetic abrasive finishing combined with electrolytic process (EMAF) was proposed in this research. In addition, the corresponding compound machining tool and experimental equipment were also developed. In this study, experiments of traditional plane MAF process, electrolytic process and EMAF process were performed to explored mechanism of EMAF process. The feasibility and high-efficiency of EMAF process was also proven by experimental results. Moreover, we analyzed the finishing mechanism of EMAF process, investigated the finishing characteristics of EMAF process and discussed the applicability in industry. The main research contents and summary of each chapter are as follows:

In chapter 1, the background and objective of this research were introduced in detail. Firstly, the properties and applications of stainless steel SUS304 material were reported through literature survey. Then, developed history and current status of traditional magnetic abrasive finishing were inducted. After that, the necessity and aim of this study were clarified. Finally, based on the reference materials reviewed and the actual conditions of the study, system model of EMAF process was described by a summary graph.

In chapter 2, machining principles of traditional plane MAF and electrolytic process were firstly introduced. Then, machining principles of EMAF process were emphatically explained in this chapter. In this research, EMAF process includes two finishing steps which are respectively the 1st finishing step (EMAF step) and the 2nd finishing step (MAF

step). The protruding portions will be preferentially leveled and the passive films will form on the surface of workpiece by electrolytic process. Simultaneously, the magnetic abrasive particles of magnetic brush is used to exert friction on the surface of workpiece, the passive films can be effectively removed. By the way, the hardness of passive films is smaller than the hardness of SUS304 stainless material. Thus, the efficiency of precision machining can be improved in EMAF step through MAF process combines with electrolytic process. However, a few passive films generally still exist on the finished surface after EMAF step. The residual passive films will affect the surface accuracy. Hence, the MAF step as a final process after EMAF step is used to completely remove passive films from in order to improve surface accuracy of workpiece. In addition, the design and structure of electrolytic magnetic compound machining tool were firstly described in detail through three-dimensional images, external views, CAD design drawings and CAD assembly drawing. Then, experimental setup and experimental procedure were introduced in detail. Finally, all of the measuring instruments (surface roughness measurement, material removal measurement, surface profile measurement and surface composition measurement) and instructions were also explained in this chapter.

In chapter 3, we firstly preformed a series of comparative experiments about MAF process, electrolytic process and EMAF process in order to verify the feasibility of EMAF process. The experimental results of three kinds of polishing methods were respectively reported in this chapter. In addition, the comparison of experimental results of MAF process and EMAF process was also reported. Through contrasting with traditional MAF process, it is confirmed that EMAF process can obtain a little higher quality surface, and machining efficiency is improved by about 50%. Hence, the feasibility of electrolytic

magnetic abrasive finishing (EMAF process) can be preliminarily proven.

In chapter 4, a series of comparing experiments about traditional plane MAF process were conducted and reported. On the one hand, mechanical finishing characteristics of the electrolytic magnetic compound machining tool can be explored through comparing experiments. On the other hand, the optimal mechanical finishing conditions can be determined for EMAF process. This chapter focused on investigated amount of iron powder and WA abrasive grain, combinations of mixed magnetic abrasive, feeding speed of X-Y stage, rotational speed of compound machining tool and working gap etc. finishing parameters. Experimental results showed the smaller surface roughness R_a and more material removal M can be obtained at relatively higher rotational speed (450 rpm), relatively smaller working gap (1 mm) conditions and combination of 149 μm in mean diameter of iron powder and # 8000 abrasive grains conditions through a series of comparative experiments. The surface roughness can reached to 30 nm at 60 min MAF process.

In chapter 5, it was reported the effect of electrolytic process on surface roughness, material removal and surface hardness under different machining conditions was reported. On the one hand, electrolytic machining characteristics of the electrolytic magnetic compound machining tool can be explored through experiments of single electrolytic process. On the other hand, the optimal electrolytic machining conditions can be determined for EMAF process. Experimental results showed the smaller surface roughness R_a, more material removal and smaller surface hardness be obtained at relatively higher working voltage (12 V), relatively higher electrolyte concentration (20 wt% or 30 wt%), relatively smaller working gap (1 mm) and relatively higher rotational speed (450 rpm).

Chapter 7 Conclusions

The surface roughness can reach to below 70 nm, material removal can reach to 240 mg, and surface hardness maximally reduced by 15% under the optimal electrolytic machining conditions. Although the surface roughness can rapidly reach to below 100 nm in electrolytic process, the intensity of finished surface is not good since the passive films formed on the finished surface. Moreover, machining mechanism of electrolytic process was understood by EDX analysis and SEM analysis.

In chapter 6, experiments and finishing mechanism of EMAF process is emphatically explained. Based on experimental results of traditional MAF process and electrolytic process in chapter 4 and chapter 5, the experimental conditions of EMAF process were basically determined. This chapter focused on investigated the combinations of first finishing step (EMAF step) time and second finishing step (MAF step) time. The total finishing time of EMAF process is selected at 30 min. The combination of total finishing time is respectively 2 min (EMAF step) + 28 min (MAF step), 4 min (EMAF step) + 26 min (MAF step), 6 min (EMAF step) + 24 min (MAF step), 8 min (EMAF step) + 22 min (MAF step) and 10 min (EMAF step) + 20 min (MAF step). Experimental results showed the surface roughness R_a drastically decreases in EMAF step, the material removal M in EMAF step is remarkably more than the material removal M in MAF step. Furthermore, the optimal experimental results of EMAF process shows that the surface roughness R_a can be reduced to less than 30 nm at 4 min EMAF step. Then, the surface roughness R_a can be reduced to 20 nm at 10 min MAF step. In other words, the surface roughness R_a can reach to 20 nm from 178 nm original surface roughness R_a at 14 min EMAF process.

It can be proven that a small amount of passive films still remained on the surface after EMAF step by obtained SEM images. Since iron powder of magnetic brush can be

considered as anode in EMAF step, iron powder would be rapidly consumed. It can be regarded that the polishing action of iron powder was invalid after 6 min EMAF step through observing the change in mixed magnetic abrasive. Hence, finishing time of EMAF step should not be too long. In short, it can be proven in this chapter that the polishing efficiency of traditional plane MAF can be significantly improved by EMAF process, and surface quality is also slightly better than the surface quality by traditional MAF process. The application of MEAF process technology in industry is worth looking forward to.

In chapter 7, we made the summary for this Ph. D thesis.

Reference

Chapter 1

1. M. Tanino, S. Suzuki, Science of Iron and Steel Materials: Technology Enriched in Iron. 3rd Edition, Uchida Old Crane Field <Materials Series>, (2013), ISBN 978-4-7536-5615-8. (in Japanese)
2. M. Tokuda, K. Yamada, N. Katagiri, Science of Metals. Initial Edition, Natsume Inc. <Illustrated Triumph Series> (2005), ISBN 4-8163-4040-8. (in Japanese)
3. R. Tanaka, Revised edition of How to choose and use stainless steel, Japan Standard Association <JIS usage series> (2005), ISBN 978-4-542-30422-2. (in Japanese)
4. M. Tanino, S. Suzuki, Science of Iron and Steel Materials: Technology Enriched in Iron, 3rd Edition, Uchida Old Crane Field <Materials Series> (2013), ISBN 978-4-7536-5615-8. (in Japanese)
5. Manabu TANAKA, Ryuichi KATO, Tadashi FUJITA and Rika YODA. Microstructures of Cutting Chips of SUS430 and SUS304 Steels, and NCF 750 and 6061-T6 Alloys. ISIJ International, Vol. 51 (2011), No. 7, pp. 1142–1150.
6. Lijun XU, Wen WANG, Cheng YANG, Review of Magnetic Abrasive Finishing (Application to plane finishing), China Academic Journal Electronic Publish House 1001– 2265(2003) 01–0041–03.
7. T. Shinmura, T. Aizawa, Development of plane magnetic abrasive finishing apparatus and its finishing performance (2nd Report, Finishing apparatus using a stationary type electromagnet), J. Jpn. Soc. Prec. Eng. 54 (5) (1988) 928–933. (in Japanese)

8. T. Shinmura, K. Takazawa, E. Hatano, Study on magnetic abrasive process (Application to plane finishing), Bull. of the JSPE 19 (4) (1985) 289–294.

9. T. Shinmura, Study on free-form surface finishing by magnetic abrasive finishing process (1st Report, Fundamental experiments), Trans. Jpn. Soc. Mech. Eng. 53 (485C) (1986) 202–208, (in Japanese).

10. Shinmura T, Takazawa K, Hatano E, Matsunaga M. Study on magnetic abrasive finishing. Ann CIRP 1990;39(l):325-8.

11. T. Shinmura, Study on plane magnetic abrasive finishing (3rd Report on the finishing characteristics of non-ferromagnetic substance), J. Jpn. Soc. Prec. Eng. 55 (7) (1989) 1271–1276, (in Japanese).

12. T. Shinmura, K. Takazawa, E. Hatano, Study on magnetic abrasive process (Process principles and finishing possibility), Bull. Jan. Soc. Precis. Eng. 19 (1) (1985) 54-55.

13. T. Shinmura, K. Takazawa, E. Hatano, Study on magnetic abrasive process (1st Report)- Process principles and finishing possibility, Precision Engineering 52, 5 (1986),851, (in Japanese).

14. M. Anzai, T. Sudo, K. Masaki, H. Otaki, T. Nakagawa, Magnetic Finishing of 3-dimensional Mold Surface. Bull. Jpn. Soc. Precis.Eng. 57 (12), (1991), 2209. (in Japanese)

15. H. Yamaguchi and T. Shinmura, Study of the surface modification resulting from an internal magnetic abrasive finishing process, Wear, vol. 225–229 (1999) 246–255.

16. H. Yamaguchi and T. Shinmura, Study of an internal magnetic abrasive finishing using a pole rotation system. Discussion of the characteristic abrasive behavior, Precision

Engineering, 24, (2000), 237–244.

17. H. Yamaguchi and T. Shinmura, Internal finishing process for alumina ceramic components by a magnetic field assisted finishing process. Precision Engineering, 28 (2) (2004) 135-142.

18. K. Suzuki, K. Takeuchi, T. Uematsu, T. Makizaki, A New Dressing Method for Superabrasive Wheels Utilizing Magnetic Abrasive Polishing. International Journal of the Japan Society for Precision Engineering, 33 (1), (1999), 27-31.

19. J.D. Kim, M.S. Choi, Study on Magnetic Polishing of Free-from Surface. International Journal of machine tools & manufacture, 37 (8), (1997), 1179 – 1187.

20. V.K. Jain, P. Kumar, P.K. Behera, S.C. Jayswal, Effect of working gap and circumferential speed on the performance of magnetic abrasive finishing process. Wear, 250(1-12), (2001), 384-390.

21. D.K. Singh, V.K. Jain, V. Raghuram, Parametric study of magnetic abrasive finishing process. Journal of Materials Processing Technology 149 (2004), 22-29.

22. A.A. Ponnanna, S.M. Joshi, S. Bhat, P. Shetty, Evaluation of the polished surface characteristic of cobalt-chrome castings subsequent to various finishing and polishing techniques. Indian J Dent Res, (2001), 12(4): 222-228.

23. S. Yin, T. Shinmura, A comparative study: polishing characteristics and its mechanisms of three vibration modes in vibration-assisted magnetic abrasive polishing, Int. J. Mach. Tool Manuf. 44 (2004), 383-390.

24. S. Yin, T. Shinmura, Vertical vibration-assisted magnetic abrasive finishing and deburring for magnesium alloy. Int. J. Mach. Tool Manuf. 44 (2004), 1297-1303.

25. S. Yin, T. Shinmura, Study of Magnetic Abrasive Finishing Process Using Pulsed Finishing Pressure and Its Processing Characteristics. Proceeding of the 10th International Conference on Precision Engineering, (2001), 506-510.

26. R.S. Mulik, P.M. Pandey, Mechanism of surface finishing in ultrasonic-assisted magnetic abrasive finishing process. Journal of Material Manufacture Process, 25 (12), (2010), 1418-1427.

27. R.S. Mulik, P.M. Pandey, Ultrasonic-assisted magnetic abrasive finishing of hardened AISI 52100 steel using unbounded SiC abrasives. Int. J. Refract. Met. Mater., 29 (2011), 68-77.

28. Y.H. Zou, T. Shinmura, Development of Magnetic Field Assisted Machining Process Using Magnetic Machining Jig. Trans. Japan Soc. Mech. Eng. Ser. 68 (669), (2002), 1575-1581. (in Japanese)

29. Y.H. Zou, T. Shinmura, Study on a new plane magnetic abrasive finishing process by application of a constant-pressure magnetic brush. J. Jpn. Soc. Abras. Technol, 53 , (2009), 31-34. (in Japanese)

30. Y.H. Zou, T. Shinmura, F. Wang, Study on a Magnetic deburring method by the application of the plane magnetic abrasive machining process. Ad. Mater. Res. 76 (2009), 276-281.

31. M.M. Ridha, Y.H. Zou, H. Sugiyama, Development of a new internal finishing of tube by magnetic abrasive finishing process combined with electrochemical machining, International Journal of Mechanical Engineering and Applications, 1 (3), (2015), 22-29.

32. X. Sun, Y.H. Zou (2017) Development of magnetic abrasive finishing combined with electrolytic process for finishing SUS304 stainless steel plane. Int. J. Adv. Manuf.

Technol. 92: 3373-3384.

33. Xu SUN, Yanhua ZOU; Study on plane magnetic abrasive finishing combined with electrolytic process. 2014 JSPE Spring Meeting.

34. Z.W. Du, Y. Chen, K. Zhou, C. Li, Research on the electrolytic-magnetic abrasive finishing of nickel-based superalloy GH4169. Int. J. Adv. Manuf. Technol. 81: 897-903.

35. N. Sihag, P. Kala, P.M. Pandey, Chemo Assisted Magnetic Abrasive Finishing: Experimental Investigations. Procedia CIRP 2015, 26, (2015) 539 -543.

36. G.Y. Liu, Z.N. Guo, S.Z. Jiang, N.S. Qu, Y.B. Li, A study of processing Al 6061 with electrochemical magnetic abrasive finishing. Procedia CIRP 2014, 14, (2014) 234-238.

37. G.Y. Liu, Z.N. Guo, Y.B. Li, J.W. Liu, Composite Tools Design for Electrolytic Magnetic Abrasive Finishing Process with FEM. Advanced Material Research, 325, (2011), 536-541.

38. K. Yasuo, Ultra-precision machining by electrolytic complex method. Tokyo:aipishi (1994), 111–116.

Reference

Chapter 2

1. T. Shinmura, K. Takazawa, E. Hatano, Development of Plane Magnetic Abrasive Finishing Apparatus and Its Finishing Performance (2nd Report) – Finishing Apparatus Using a Stationary Type Electromagnet. Bull. Jan. Soc. Precis. Eng. 54 (5), (1988), 928. (In Japanese)
2. T. Shinmura, T. Aizawa, Study on magnetic abrasive finishing process (Development of plane finishing apparatus a stationary type electromagnet). Bull. Jan. Soc. Precis. Eng. 23 (3) (1989), 236-239. (In Japanese)
3. M. Natsume, T. Shinmura, Study on mechanism of plane magnetic abrasive finishing process (Elucidation of normal force characteristics). Trans. Jpn. Soc. Mech. Eng., 74 (737), (2008), 212-218. (In Japanese)
4. K. Yasuo, Ultra-precision machining by electrolytic complex method. Tokyo: aipishi (1994), 111–116.
5. T.R. Lin, C.R. Su, Experimental study of lapping and electropolishing of tungsten carbides. Int. J. Adv. Manuf. Technol., (2008), 36 (7-8): 715-723.
6. E.S. Lee, Machining characteristics of the electropolishing of stainless steel (STS316L). Int. J. Adv. Manuf. Technol., (2000), 16 (8): 591–599.
7. G.Y. Liu, Z.N. Guo, Y.B. Li, J.W. Liu, Composite Tools Design for Electrolytic Magnetic Abrasive Finishing Process with FEM. Advanced Material Research, 325, (2011), 536-541.
8. Z.W. Du, Y. Chen, K. Zhou, C. Li, Research on the electrolytic-magnetic abrasive finishing of nickel-based superalloy GH4169. Int. J. Adv. Manuf. Technol. 81:

897-903.

9. N. Sihag, P. Kala, P.M. Pandey, Chemo Assisted Magnetic Abrasive Finishing: Experimental Investigations. Procedia CIRP 2015, 26, (2015) 539 -543.
10. G.Y. Liu, Z.N. Guo, Y.B. Li, J.W. Liu, Composite Tools Design for Electrolytic Magnetic Abrasive Finishing Process with FEM. Advanced Material Research, 325, (2011), 536-541.
11. Xu Sun, Yanhua Zou (2018.6) Study on Electrolytic Magnetic Abrasive Finishing Stainless Steel SUS304 Plane with a Special Compound Machining Tool. International Journal of Manufacturing and Materials Processing, 2: 41–53.

Chapter 3

1. Shinmura T (1989) Study on plane magnetic abrasive finishing (3rd report on the finishing characteristics of non-ferromagnetic substance). J Jpn Soc Prec Eng 55(7):1271–1276 (in Japanese).
2. T. Shinmura, K. Takazawa, E. Hatano (1985) Study on magnetic abrasive process-finishing characteristics. Vol. 19, No.1 54.

Chapter 4

1. T. Shinmura, Study on plane magnetic abrasive finishing (3rd Report on the finishing characteristics of non-ferromagnetic substance), J. Jpn. Soc. Prec. Eng. 55 (7) (1989) 1271–1276, (in Japanese).

2. X. Sun, Y.H. Zou (2017) Development of magnetic abrasive finishing combined with electrolytic process for finishing SUS304 stainless steel plane. Int. J. Adv. Manuf. Technol. 92: 3373-3384.

Chapter 5

1. X. Sun, Y.H. Zou (2017) Development of magnetic abrasive finishing combined with electrolytic process for finishing SUS304 stainless steel plane. Int. J. Adv. Manuf. Technol. 92: 3373-3384.
2. N. Sihag, P. Kala, P.M. Pandey, Chemo Assisted Magnetic Abrasive Finishing: Experimental Investigations. Procedia CIRP 2015, 26, (2015) 539 -543.
3. Yasuo, K. Ultra-precision machining by electrolytic complex method. Tokyo:aipishi, 1994.

Chapter 6

1. Yasuo, K. Ultra-precision machining by electrolytic complex method. Tokyo: aipishi 1994, 111-116.

Acknowledgements

The 4.5 years life in Utsunomiya university of Japan has enriched and deeply impressed for me forever. Countless benevolent people must be gratefully thanked in my course of the pursuit of doctoral degree. Without their kindhearted help and full-hearted supports, the work couldn't be completed.

First of all, thanks must go to my advisor, Associate Prof. Yanhua Zou. Associate Prof. Zou is not only an excellent supervisor but also a best guider for me in the scientific world. I am fortunate to have such a precious opportunity to study under her guidance. Her erudition on the field of magnetic abrasive finishing has left an everlasting impression on me. Her prudent and rigorous attitude towards scientific research will definitely spur me to carry on researching with meticulous attitude throughout the rest of my scientific career.

Then, I am also very grateful to all of the commentary committee members, Professor Hitoshi Sugiyama, Professor Yoshimasa Takayama, Professor Kazutaka Yokota and Professor Katsutoshi Yoshida etc. for their invaluable advices and suggestions on my research.

I also must express special thanks to the Rotary Yoneyama Memorial Foundation of Japan and my counselor Mr. Jisoji for my economic aid to provide the scholarship, so I can do my best to research. The gratitude is also extended to some supports from Creative Department for Innovation (CDI) of Utsunomiya University and mechanical processing factories of Utsunomiya University for this research. I must also express special thanks to all members of Zou laboratory, especially graduate Mr. Longjian

Acknowledgements

Piao made some contributions for the initial work of this study and graduate Mr. Takumi Kojo made some contributions for the auxiliary work of this study.

Finally, I am deeply indebted to my parents, wife, son and friends. Without the financial and emotional support from them, I can't complete the doctoral course smoothly in Japan. Hereby, I have to thank my wife (Ms. Yuan Xue) again. She not only supported and encouraged my studies, but also gave birth to a baby for me in the last year on Feb. 15th.

Thank you very much! Wish you all the best in the future!

Contributed papers related to this study

[1] Articles

Xu Sun, Yanhua Zou. (2017.4) Development of magnetic abrasive finishing combined with electrolytic process for finishing SUS304 stainless steel plane. International Journal of Advanced Manufacturing Technology 92: 3373–3384.

Xu Sun, Yanhua Zou (2018.6) Study on Electrolytic Magnetic Abrasive Finishing Stainless Steel SUS304 Plane with a Special Compound Machining Tool. International Journal of Manufacturing and Materials Processing, 2: 41–53.

[2] International conference

Xu SUN, Yanhua ZOU and Hitoshi SUGIYAMA. Study on processing thesurface of SUS304 plate with electrochemical magnetic abrasive finishing. The 8th International Conference on Leading Edge Manufacturing in 21st Century (LEM21_2015), 1005,1-6(2015), Oct. 2015, Kyoto.

Xu SUN, Yanhua ZOU. Experimental investigations for plane magnetic abrasive finishing combined with electrolytic process. The 13th China-Japan International Conference on Ultra-Precision Machining Process (CJUMP 2017) Shanghai, China, November 19 - 21, 2017.

Xu SUN, Yanhua ZOU. Study on magnetic abrasive finishing combined with electrolytic process. The 21st International Symposium on Advances in Abrasive Technology (ISAAT 2018)， Ryerson University, Toronto, Canada, Oct. 14 - 17, 2018.

[3] Domestic conference

Xu Sun, Yanhua Zou. Study on plane magnetic abrasive finishing combined with electrolytic process. 2018 Japan Society for Precision Engineering Spring Meeting, Chuo University, Tokyo, March 15-17, 2018.